Design and control of combined chemical processes for the production of pure enantiomers

Dissertation
zur Erlangung des akademischen Grades

Doktoringenieur
(Dr.-Ing.)

von M.S. Subramanian Swernath

geb. am 10-10-1983 in Chennai, India

genehmigt durch die Fakultät für Elektrotechnik und Informationstechnik

der Otto-von-Guericke Universität Magdeburg

Gutachter:
Prof. Dr.-Ing. Achim Kienle
Prof. Dr.-Ing. Malte Kaspereit

Promotionskolloquium am 10-01-2013

Acknowledgements

This thesis evolved from the research which was performed during my PhD at the Max Planck Institute for Dynamics of Complex Technical Systems, Magdeburg, Germany.

I am deeply indebted to Prof. Achim Kienle for providing me this opportunity to work at the MPI as a part of the IMPRS. He has been patient and encouraging during the entire course of the work. He has enlightened me with his wide knowledge of the process dynamics and control. I am also extremely thankful to Prof. Malte Kaspereit who has helped me personally and professionally during my stay at the institute.

I would like to express my gratitude to all of my group members for their kind cooperation. Here, Michael Mangold needs to be mentioned explicitly for his immediate support in sorting out the issues in DIVA. Among other group members, I want to thank Carolyn Mangold for proof-reading the thesis.

I would like to thank the IMPRS coordinator Dr. Barbara Witter and Dr. Juergen Koch for all the necessary support during my stay in Magdeburg. Without their constant cooperation, my stay in Magdeburg would not have been very pleasant. A special thanks to the group secretary Carolyn for her help. I would also like to express my gratitude to IT staff members as well as MPI administration for always sorting out my problems efficiently and quickly.

I would like to thank all the Indian colleagues in MPI with whom we had intense scientific and non-scientific discussion during the regular cofee breaks. I would also like to thank Praveen for clearing some of the mathematical doubts over skype. Finally, I want to thank my parents for providing me the necessary love and motivation during the entire four years.

To my parents

Contents

Acknowledgements ii

Dedication iii

List of Figures vii

List of Tables x

Notation xi

German Abstract xiv

Abstract xvi

Chapter

1. Introduction 1

1.1 Introduction 1
1.2 State-of-the-art and Objectives 4
1.2.1 SMB-crystallization 4
1.2.2 SMB-racemization 5
1.2.3 Advanced optimization approaches 6
1.2.4 Process dynamics and control 7
1.3 Outline of the thesis 9

2. Optimal design methodology 10

2.1 Mathematical formulation 10
2.2 Model system 1: PDE (Simple system) 16
2.2.1 SMB-crystallization 17
2.2.2 SMB-racemization 18
2.2.3 SMB-racemization-crystallization 19

2.2.4 SMB-crystallization-crystallization 21
2.3 Model system 2: 2',6'-Pipecoloxylidide (PPX) 22
2.3.1 Design of fixed process structures (NLP optimization) 24
2.3.2 Simultaneous design of the process structure and operating conditions (MINLP optimization) 30
2.4 Summary 33

3. Dynamics and control of SMB-crystallization processes . . . 36

3.1 Open loop dynamics 36
3.1.1 Robust design 36
3.1.2 Extract configuration 37
3.1.3 Raffinate configurations 43
3.2 Feedback control 48
3.3 Summary 53

4. Dynamics and control of SMB-racemization processes 54

4.1 Slow reaction kinetics and moderate purities 54
4.1.1 Static controllability analysis 55
4.1.2 Open loop and closed loop process dynamics 57
4.2 Fast reaction kinetics and high purities 62
4.2.1 Static controllability analysis 62
4.2.2 Open and closed loop dynamics 64
4.3 Summary 68

5. Conclusions 69

Appendices 72

A. Physico-chemical parameters 73

B. MINLP optimization of SMB processes and process combinations with variable number of stages 75

B.1 Model formulation 75
B.2 Results 79
B.2.1 Simple cost function 79
B.2.2 Super structure based optimization for process combinations 85
B.2.3 SMB design using TMB parameters 86

C. Dynamic crystallizer model 89

Bibliography 93

List of Figures

Figure

1.1 Enantiomer forms of Lactic acid. Non-super imposable mirror images of each other. Dashed lines represent a hypothetical mirror 2
1.2 Schematic of an SMB process 2
1.3 Different possible SMB based process combinations to produce pure enantiomers (a) stand-alone SMB process, (b) SMB-crystallization, (c) SMB-racemization, (d) SMB-crystallization-racemization 3
2.1 Figure illustrating the nomenclature for the solvent removal unit before the crystallizer 12
2.2 SLE on a rectangular diagram 13
2.3 Figure illustrating the nomenclature around the the crystallizer and the solvent makeup 14
2.4 Figure illustrating the nomenclature around the the reactor and the solvent removal before the reactor 15
2.5 Decision tree based on simple qualitative criteria for the selection of a suitable combined or integrated process concept for the production of a pure enantiomer 23
2.6 Costs as a function of production rate of a stand-alone SMB as in Figure 1.3(a) (dashed line), compared to an SMB process coupled with a racemizer as in Figure 1.3(c) (solid line) for two different feed cost scenarios. 26
2.7 Maximum production rates and coupling purity as a function of the total number of theoretical stages of a stand-alone SMB (dashed line) compared to an SMB process with a crystallizer at the raffinate. . . 28
2.8 Maximum production rates and coupling purity as a function of the total number of theoretical stages of a stand-alone SMB (dashed line) compared to an SMB process with a crystallizer at the extract. . . . 28
2.9 Maximum production rates and coupling purity as a function of the total number of theoretical stages of a stand-alone SMB (dashed line) compared to an SMB process with a crystallizer at the raffinate and a crystallizer at the extract. 29
2.10 Superstructure for MINLP optimization 32

3.1 Optimal and robust operating points obtained from a steady state optimization . . . 38
3.2 Schematic diagram for an SMB-crystallization with a crystallizer at the extract . . . 39
3.3 Effect of step disturbances of the external feed concentration for a crystallizer at the extract . . . 41
3.4 Effect of step disturbances of the external feed flow rate for a crystallizer at the extract . . . 42
3.5 Effect of step disturbances of the external feed concentration for a crystallizer at the raffinate (configuration 1) . . . 44
3.6 Effect of step disturbances of the external feed flow rate for a crystallizer at the raffinate (configuration 1) . . . 45
3.7 Schematic diagram for the alternative raffinate configuration (configuration 2) . . . 46
3.8 Effect of step disturbances of the external feed flow rate for a crystallizer at the raffinate (configuration 2) . . . 47
3.9 Comparison of open loop and closed loop process behavior for a step disturbance of +10.0% of the external feed concentration for a crystallizer at the extract . . . 50
3.10 Comparison of open loop and closed loop process behavior for a step disturbance of +17.5% of the external feed concentration for a crystallizer at the extract . . . 51
3.11 Comparison of open loop and closed loop process behavior for a step disturbance of -33% of the external feed flow rate for a crystallizer at the extract . . . 52
4.1 Schematic diagram for an SMB-racemization process . . . 55
4.2 Comparison of steady state parameter continuation profiles when subjected to step disturbances of ± 5% of the external feed concentration for slow kinetics . . . 56
4.3 Comparison of steady state parameter continuation profiles when subjected to step disturbances of ± 5% of the external feed flow rate for slow kinetics . . . 56
4.4 Comparison of an open loop and closed loop process for ± 5% disturbance of the external feed concentration for slow kinetics . . . 58
4.5 Comparison of an open loop and closed loop process for ± 5% disturbance of the external feed flow rate for slow kinetics . . . 59
4.6 Comparison of steady state parameter continuation profiles when subjected to step disturbances of 7.5% disturbance of the external feed concentration for slow kinetics . . . 60
4.7 Comparison of an open loop and closed loop process for ± 7.5% disturbance of the external feed concentration for slow kinetics . . . 61
4.8 Comparison of steady state parameter continuation profiles for nominal, 5%, -5% disturbance of the external feed concentration for the fast kinetics . . . 63

4.9 Comparison of steady state parameter continuation profiles for nominal, 5%, -5% disturbance of the external feed flow rate for fast kinetics 63
4.10 Comparison of possible control options for 5% disturbance of the external feed concentration through steady state parameter continuation for fast kinetics 65
4.11 Comparison of an open loop and closed loop process for ± 5 % disturbance of the external feed concentration for fast kinetics 66
4.12 Comparison of an open loop and closed loop process for ± 5% disturbance of the external feed flow rate for fast kinetics 67
B.1 Schematic models for stage number optimization for SMB processes and process combinations 76
B.2 Enumeration approach for understanding the effect of stage number for PDE enantiomer 80
B.3 Effect of purity and feed flow rate on the number of stages 83
B.4 Effect of separation factor on the number of stages 84
C.1 Open loop dynamics for a step disturbance of +17.5% of the external feed concentration for a crystallizer at the extract with finite dynamics with a capacity of 0.1 (red), 1 (blue) and 10 (black) volume units. Meaning of thick and thin lines in diagrams (a) and (d) is as in Figure 3.3. 91
C.2 Closed loop dynamics for a step disturbance of +17.5% of the external feed concentration for a crystallizer at the extract with finite dynamics with a capacity of 0.1 (red), 1 (blue) and 10 (black) volume units. Meaning of thick and thin lines in diagrams (a) and (d) is as in Figure 3.3. 92

List of Tables

Table

2.1	Optimal design for an SMB-crys	18
2.2	Optimal design for an SMB-extr.rac	19
2.3	Optimal design for an SMB-raff.rac	19
2.4	Optimal design for an SMB-extr.rac and raff.cryst	20
2.5	Optimal design for an SMB-raff.rac and extr.cryst	20
2.6	Optimal design for an SMB-crys-crys	21
2.7	NLP calculations for PPX	30
2.8	MINLP calculations for PPX	35
3.1	Robust design for an SMB-crys	37
3.2	Controller parameters for an SMB-extr.crys	49
4.1	Controller parameters for an SMB-racemization for slow kinetics	57
4.2	Robust design for an SMB-Extr.rac for slow kinetics	60
4.3	Robust design for an SMB-Extr.rac for fast kinetics	64
4.4	Controller parameters for an SMB-racemization for fast kinetics	64
A.1	Parameters for the model system: PDE	73
A.2	Parameter values for the model system: PPX	73
B.1	Comparison of CPU time for the two methods to perform stage number optimization. Computations were performed on a linux 2GHz, AMD Athlon single core processer	82
B.2	Minimum number of stages for the different process schemes	82
B.3	Minimum number of stages for unequal stage number for stand alone SMB	85
B.4	Comparison of different processes with translation to SMB	88
B.5	Comparison of different processes with translation to SMB for case 1 in Table B.4	88
C.1	Controller parameters for an SMB-crystallization with dynamic model	90

Notation

Abbreviations

Symbols	Meaning
Crys	MSMPR crystallizer
GAMS	General Algebraic Modelling System
MINLP	Mixed-Integer Non-Linear Programming
MSMPR	Mixed Suspension Mixed Product Removal
NLP	Non-Linear-Programming
PDE	Pharmaceutical Intermediate Compound
PPX	2', 6'-Pipecoloxylidide
Rac	Racemization reactor (CSTR)
SLE	Solid-Liquid-Equilibrium
SMB	Simulated Moving Bed
SM	Solvent Makeup
SR	Solvent Removal unit
TMB	True Moving Bed

Arabic Symbols

Symbols	Meaning	SI Units
a	Adsorption isotherm parameter	
A_c	Area of column	[m2]
b	Adsorption isotherm parameter	[l/g]
$c_{i,k}$	Liquid phase concentration of the component i on the stage k	[g/l]
$c_{i,F0}$	Liquid phase feed concentration of the component i in feed	[g/l]
$c^{reac}_{i,recycle}$	Liquid phase concentration of the component i in reactor	[g/l]
$c^{reac}_{i,evap}$	Liquid phase concentration of the component i leaving SR	[g/l]
$c^{cryst}_{i,evap}$	Liquid phase concentration of the component i leaving SR	[g/l]
$c^{cryst}_{i,recycle}$	Liquid phase concentration of the component i in cryst recycle	[g/l]
$c^{cryst}_{i,evap,feed}$	Liquid phase concentration of the component i entering SR	[g/l]
$c^{reac}_{i,evap,feed}$	Liquid phase concentration of the component i entering SR	[g/l]
C_f	Feed material cost	[USD/hr]
C_{op}	Operation cost	[USD/hr]
C_{inv}	Investment material cost	[USD/hr]
D_c	Length of column	[m2]
$HETP$	Height equivalent to theoretical plate	
i	Components/enantiomer	
I_E	Binary variable for extract of TMB	
I_R	Binary variable for raffinate of TMB	
I_D	Binary variable for desorbent of TMB	
I_L	Binary variable for last stage of TMB	
k	Stage number in the SMB	
K_c	Controller gain	[min/ml]
L_c	Length of column	[m]
M_{rac}	Mass of racemic feed	[kg/hr]
M_{prod}	Mass of product	[kg/hr]
$NTPCOL$	Number of theoretical plates in a column	
$k_{forward}$	Reaction rate constant	[1/s]
$q_{i,k}$	Solid phase concentration of the component i on the stage k	[g/l]
Pu_{min}	Minimum purity requirement	[-]
$\dot{Q}_{ml}$	Mother liquor flow rate from the crystallizer	[ml/min]
Q_k	Real SMB flow rate in Appendix B	[ml/min]
$\dot{Q}_{F0}$	External feed flow rate	[ml/min]
$\dot{Q}_{i,crystal}$	Crystal flow rate of the component i from the crystallizer	[ml/min]
$\dot{Q}_{Diluent}$	Diluent flow rate to the mother liquor	[ml/min]
$\dot{Q}^{cryst}_{recycle}$	Recycle flow rate from the crystallizer	[ml/min]
$\dot{Q}^{reac}_{recycle}$	Recycle flow rate from the reactor	[ml/min]
$\dot{Q}_{solid}$	Solid flow rate within the SMB	[ml/min]
$\dot{Q}_k$	Liquid flow rate on the stage k of the TMB	[ml/min]
$\dot{Q}_{external}$	Liquid flow rate of the stream from/to the TMB	[ml/min]

Arabic Symbols - Continued ...,

Symbols	Meaning	SI Units
$\dot{Q}_{SR}^{cryst}$	Liquid flow rate of the stream leaving the SR before cryst	[ml/min]
$\dot{Q}_{SR}^{reac}$	Liquid flow rate of the stream leaving the SR before reac	[ml/min]
$\dot{Q}_{evap}^{cryst}$	Liquid flow rate of the stream leaving the SR to cryst	[ml/min]
$\dot{Q}_{evap}^{reac}$	Liquid flow rate of the stream leaving the SR to reac	[ml/min]
$\dot{Q}_{evap,feed}^{cryst}$	Liquid flow rate of the stream entering the SR before cryst	[ml/min]
$\dot{Q}_{evap,feed}^{reac}$	Liquid flow rate of the stream entering the SR before reac	[ml/min]
t_{switch}	Switch time of an SMB	[s]
$ULIN$	Linear velocity	
V	Volume of each stage of the SMB unit	[ml]
V_c	Volume of an SMB column	[ml]
V_{reac}	Volume of the reactor	[ml]
V_{cryst}	Volume of the crystallizer	[ml]
W_f	Feed material cost	[USD/kg]
W_{op}	Operation cost	[USD/hr]
W_{inv}	Investment material cost	[USD/kg]
$x_{i,evap}$	Mass fraction of the component i leaving SR	
y	Binary decision variables	
Y	Yield of racemization	

Greek Symbols

Symbols	Meaning
ϵ	Void fraction of liquid phase in SMB
ν_i	Stoichiometric coefficient
ψ	Void fraction of the crystallizer
δ	Fraction of crystals of the enantiomer 1
ρ	Density of liquid
τ_I	Integral time in controller

German Abstract

Enatiomere sind Stereoisomere mit spiegelsymmetrischer Struktur. Sie spielen eine wichtige Rolle in der pharmazeutischen Industrie. Typischerweise haben sie identische physikalisch-chemische Eigenschaften in einer achiralen Umgebung, können aber verschiedene physiologische Effekte haben. Dies macht die Herstellung von enatiomerenreinen Medikamenten notwendig. Solche Produktionprozesse basieren oft auf einer nicht-selektiven chemischen Synthese. Diese führt auf eine 50:50 Mischung der beiden Enantiomere, die auch als Racemat bezeichnet wird. Folglich ist eine anschliessende Trennung erforderlich, um das gewünschte Enantiomer in hoher Reinheit zu erhalten. In der vorliegenden Arbeit werden dazu kontinuierliche chromatographische Trennprozesse nach dem Simulated Moving Bed (SMB) Verfahren verwendet.

Zentrales Ziel dieser Arbeit ist die Verbesserung solcher Prozesse durch eine intelligente Kombination chromatographischer Trennunprozesse mit einer selektiven Kristallisation und/oder einer chemischen Racemisierung. Die optimale Konfiguration und die optimalen Betriebsbedingungen dieser kombinierten Prozesse hängen entscheidend von den spezifischen Kostenstrukturen und den physikalisch-chemischen Eigenschaften der betrachteten Systeme ab. Zur Bestimmung eines optimalen Design werden in der vorliegenden Arbeit geeignete Optimierungsstrategien entwickelt. In einem ersten Schritt werden Methoden der Nichtlinearen Optimierung verwendet, um optimale Betriebsbedingungen für eine gegebene Prozesskonfiguration zu bestimmen. Anschliessend wird eine erweitere Superstruktur-Formulierung zur simultanen Bestimmung einer optimalen Prozesskonfigurationen und optimalen Betriebsbedingungen eingeführt und mit Methoden der Gemischt-Ganzzahligen Nichtlinearen Optimierung gelöst. Als Anwendungsbeispiel dienen zwei verschiedene pharmazeutische Komponenten unterschiedlicher Komplexität.

Neben dem optimalen Design liegt ein weiterer Schwerpunkt der Arbeit im Gegensatz zu früheren Untersuchungen auch bei der dynamischen Betreibbarkeit und der

Regelung solcher kombinierten Prozesse mit Rückführungen. Für eine systematische Analyse werden zwei charakteristische Konfigurationen betrachtet: (1) ein SMB Prozess kombiniert mit einer enantioselektiven Kristallisation und (2) ein SMB Prozess kombiniert mit einem Racemisierungsreaktor.

Um im ersten Fall bei unvorhergesehenen Störungen die gewünschte hohe Qualität des kristallinen Produktes zu erzielen, ist es notwendig, die Kristallisation innerhalb der zugehörigen Grenzen im Phasendiagramm zu halten. In einem ersten Schritt wird der Einfluss von Störungen auf die Dynamik des ungeregelten Systems untersucht. Es wird gezeigt, dass das dynamische Verhalten der kombinierten Prozesse entscheidend von der Pumpenkonfiguration der SMB Anlage anhängt. Je nach Störung kann dabei die Kristallisation des unerwünschten Produktes beobachtet werden. Außerdem können Instabilitäten in Form nichtlinearer Oszillationen auftreten. Daher wird in einem zweiten Schritt eine anlagenweite Regelungsstrategie vorgeschlagen, um eine robuste Betriebsweise zu gewährleisten. Es wird gezeigt, dass die direkte Regelung des SMB Prozesses nicht notwendig ist, um den Gesamtprozess zu stabilisieren und die gewünschten Produktreinheiten einhalten zu können. Alternativ wird eine neues einfach umzusetzendes Regelkonzept vorgeschlagen, bei dem nur die Menge des abzuziehenden bzw. hinzuzufügenden Lösungsmittels geregelt wird. Weiterhin wird gezeigt, dass sich diese Regelungsstrategie auch auf den zweiten Fall anwenden läst, wenn die Racemisierungsreaktion im kinetischen Regime liegt und die Reinheitsanforderungen an die Produkte moderat sind. Anschliessend wird gezeigt, dass eine direkte Regelung des SMB Prozesses zwingend notwendig ist, wenn sich die Reaktion im Gleichgewichts-Regime befindet.

Zum Schluss wird eine mögliche Erweiterung dieser einfachen Regelkonzepte für komplexere SMB-Prozesskonfigurationen diskutiert.

Abstract

Enantiomers are stereoisomers, which are structured like mirror images of each other. They play an important role in pharmaceutical industries. Typically, they have identical physico-chemical properties in an achiral environment but may have different physiological effects. This requires the production of enantiopure drugs. Such production processes are often based on a nonselective chemical synthesis delivering a 50:50 mixture of both enantiomers called the racemate. Hence, a subsequent separation is required to obtain the desired enantiomer with high purity. In the present work continuous chromatographic separation by means of simulated moving bed (SMB) processes is considered.

The thesis aims at improving the production of single enantiomers by clever combination of the chromatographic separation with selective crystallization and/or racemization. The optimal configuration and the optimal operating conditions of such a combined process crucially depend on specific cost structures and physico-chemical properties of the system to be considered. For model-based computer-aided optimal design, various optimization strategies are developed in this thesis. In a first step, nonlinear programming is applied to determine optimal operating conditions for a given process configuration. Afterwards, an extended superstructure formulation is introduced to determine optimal process configurations and optimal process conditions simultaneously by means of mixed integer nonlinear programming. Application is demonstrated for two different compounds from pharmaceutical industries with increasing complexity.

Besides the optimal design, focus is on the dynamic operability and control of such combined processes with recycles, which has not been considered so far. For a systematic analysis two characteristic benchmark problems are considered: (1) an SMB process combined with an enantio-selective crystallization, and (2) an SMB process combined with a racemization reactor.

To achieve the desired high purity of the crystalline product, in the first case, it is required to keep the crystallizer operation within the corresponding region in the phase diagram in the presence of unforeseen disturbances. In the first step, the effect of such disturbances on the open loop dynamics is investigated. It is shown that the dynamic behavior of the combined process crucially depends on the pump configuration of the SMB plant involved. Depending on the disturbance, the formation of the crystals of the undesired product is observed. Further open loop instability in the form of self sustained oscillations may arise. Therefore, in a second step a simple plantwide control strategy is proposed in order to ensure a robust process operation. It is shown that the direct control of the SMB unit is not required to stabilize the process combination while maintaining the desired product specifications. Instead, we show that this can be achieved easily by controlling the amount of the solvent that is removed or added to the system. Further, it is shown, that a similar strategy can be applied to the second process combination. However, for good controllability in the second case, it is required that the racemization reaction is in the kinetic regime and that the product purities are not too high. Afterwards, it is illustrated that a direct control of one of the SMB flow rates is mandatory when the reaction is in the equilibrium regime.

Finally, the possibility of extending these simple control concepts to more complicated process schemes involving SMB is also briefly addressed.

Chapter 1

Introduction

1.1 Introduction

The production of pure enantiomers is essential and challenging due to their wide application in pharmaceutical industries. Enantiomers are a class of stereoisomers. They exist in two different forms, which are non-superimposable mirror images of each other. The asymmetry in the three dimensional arrangement in space arises from the presence of a chiral carbon atom, chiral axes etc. [1] [Figure 1.1]. Different conventions have been used for classifying these two forms of enantiomers such as +/-, D/L, R/S etc. The two enantiomers have identical physico-chemical properties in achiral environments but may have different physiological impacts. The effects of the two different forms of enantiomers can be widely dissimilar as in the case of ethambutol where the human consumption of R-form could lead to blindness while the S-form has antimycobacterial properties [2]. In these cases, the production of pure single enantiomers is of fundamental importance.

Preparative large scale production methods for pure enantiomers can be broadly classified into two major types. One of the approaches is to perform a stereo-selective synthesis of the desired enantiomer. Methods based on selective synthesis rely on the use of biological or chemical catalysis in order to produce the desired enantiomer. Although this approach seems to be much more simple, asymmetric catalysis is industrially often not economical and requires elaborate process development. The other method which is primarily used in industrial production is based on a non-selective chemical synthesis of the racemic (50/50) mixture and a subsequent enantio-separation. In this method the synthesis is comparatively easy while the separation is the major challenge due to the identical physico-chemical properties of the two enantiomers.

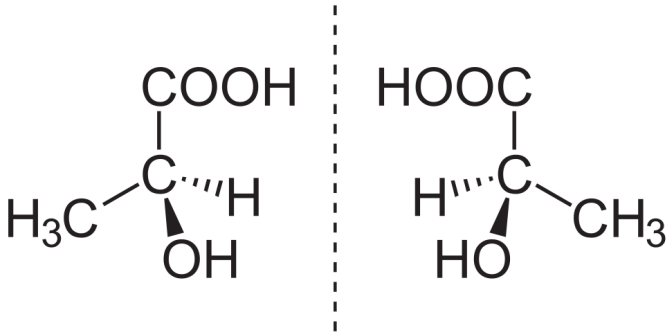

Figure 1.1: Enantiomer forms of Lactic acid. Non-super imposable mirror images of each other. Dashed lines represent a hypothetical mirror

Most of the enantiopure production methods are performed in an isolated manner using stand-alone chromatography, crystallization, etc. These methods are feasible and established, but there exists a significant potential for cost reduction by using improved process concepts combining one or more of the separation methods and/or (bio)chemical reactions which will be discussed within the course of this thesis.

Due to the tremendous advancements made in simulated moving bed (SMB) chromatography during the last decade, it has become a powerful option for separating enantiomeric mixtures [3]. Main advantages compared to classical batch chromatography are increased productivity and reduced solvent consumption.

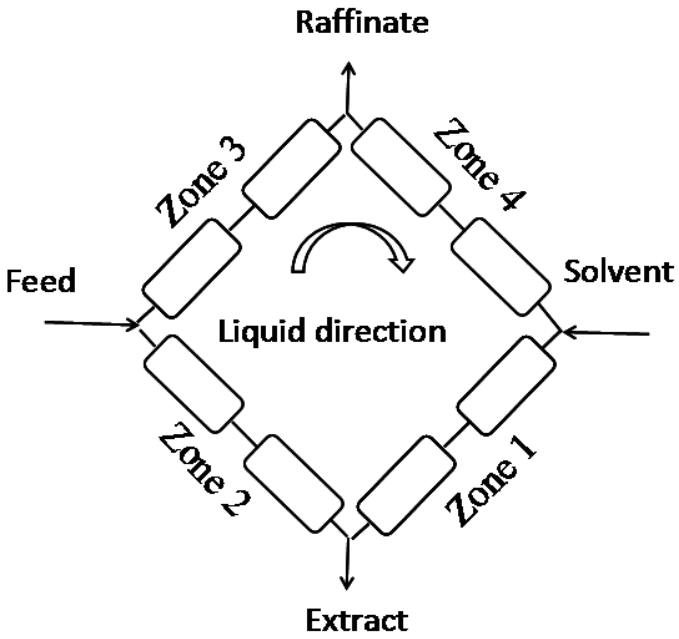

Figure 1.2: Schematic of an SMB process

An SMB chromatography unit consists of a series of interconnected columns with a continuous flow of liquid along these as shown in Figure 1.2. A periodic switching of the inlet and outlet ports in the direction of liquid flow is carried out to simulate a counter-current flow of solid and liquid phases. A feed, consisting of a binary mixture is introduced into the SMB. The less adsorbed component (component 2 in this thesis) is carried along with the liquid flow and can be collected at the raffinate. The more adsorbed component (component 1 in this thesis) can be drawn off at the extract.

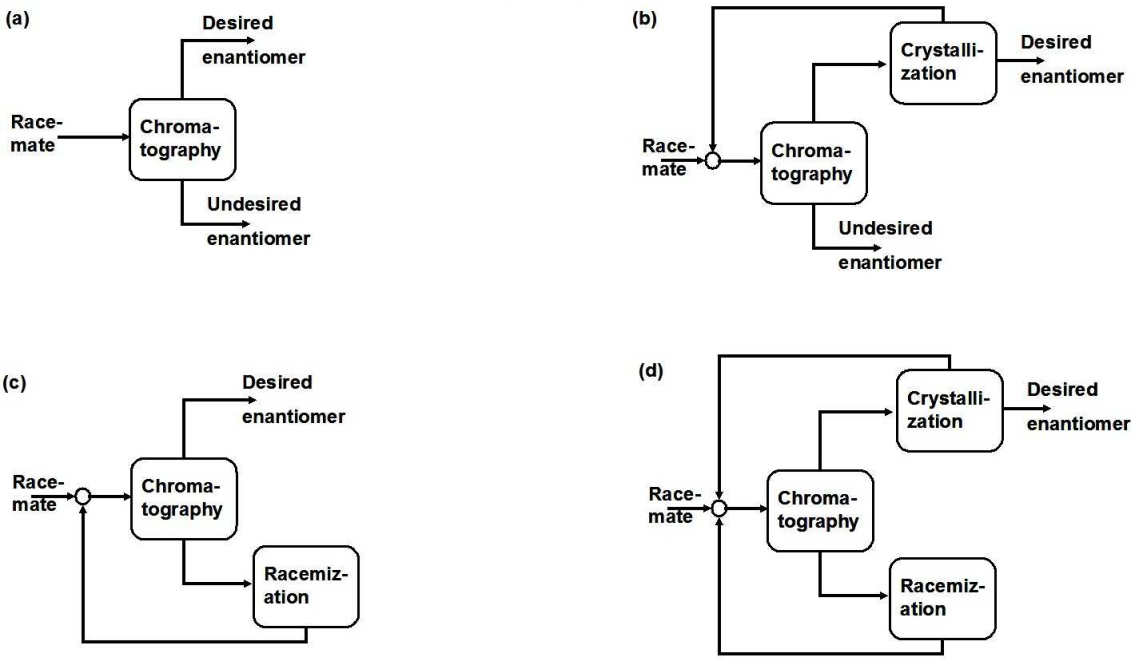

Figure 1.3: Different possible SMB based process combinations to produce pure enantiomers (a) stand-alone SMB process, (b) SMB-crystallization, (c) SMB-racemization, (d) SMB-crystallization-racemization

It has been shown earlier that the productivity of an SMB process increases exponentially with decrease in purity requirements [4, 5]. As enantiomers are often required in pure crystalline form, the combination of an SMB with crystallization can be a very favorable process option. The scheme for such a process combination is illustrated in Figure 1.3(b). This process combination helps to reduce the separation load on the SMB and simultaneously distributes the load between the SMB and the crystallization. Crystallization can be enantio-selective [6, 7] or preferential [8, 9].

Another benefit of such a process combination arises from the use of less efficient and shorter and therefore cheaper columns within the SMB. It can be seen from Figure 1.3(a), that half of the produced material becomes waste as it is of the undesired enantiomer. This translates mathematically to a maximum yield of 50%. This limitation of any pure separation process can be overcome by performing a racemization (isomerization) of the undesired enantiomer and recycling the reactor outlet to the feed of the separation unit [Figure 1.3(c)] and thereby increasing the yield of the desired enantiomer upto 100%. The concept shown in the Figure 1.3(c) was considered, for example, applying thermal racemization of Troeger's base [10], Chlorthalidone [11] and enzymatic racemization of amino acids [12, 13]. Further, it is also possible to have a process combination involving SMB-racemization-crystallization such as the one shown in Figure 1.3(d). Under such conditions, racemization occurs at the undesired enantiomer outlet and crystallization at the desired enantiomer outlet. Besides these, there are other non-intuitive process structures possible such as an SMB with a crystallizer at the undesired enantiomer outlet which can improve the process performance. These processes will be discussed in the subsequent chapter which focuses on the optimal design. It is evident that there are a lot of new process variants available which can enhance the efficiency of the state-of-the-art enantio-separations. Design and operation of such novel processes forms the essence of this thesis.

1.2 State-of-the-art and Objectives

1.2.1 SMB-crystallization

The importance of SMB-crystallization in the enantiomer domain is clear from the amount of literature which has appeared during the last decade. Lim *et al.* [14] experimentally showed that a partial resolution using SMB, followed by crystallization, is a promising process route to produce pure praziquantel enantiomers. However, they have not explored the benefits of operating such a process with reduced SMB purity. Blehaut and Nicoud [15] were the first to promote the economic potential of an integrated SMB-crystallization. They discussed it from an industrial perspective and showed that the robustness of the process can also be improved. Lorenz *et al.* [6] demonstrated the advantages of SMB-crystallization using numerical simulations for mandelic acid enantiomers. Since numerical optimization of the complete process is computationally challenging, an alternate shortcut method was developed. This method was used to evaluate the potential of the process combination [7]. The authors conclude that there is an optimal coupling purity (SMB outlet purity) at which

the productivity of the process is maximized. These methods were later extended to study an enantiomeric and an epimeric system. The importance of recycling the mother liquor back to the chromatography unit was underlined in Gedicke *et al.* [16]. Since there is an optimal coupling purity which is not known a priori, the equilibrium design methods for SMB processes are insufficient for the design of SMB-crystallization [5, 17]. A detailed dynamic optimization using multi-objective optimization was employed to study the performance of the SMB-crystallization process for different but fixed coupling purities which necessitates numerous computationally expensive parametric optimizations [18] . In this work, a detailed model was used for the SMB, while the Solid-Liquid-Equilibrium (SLE) was not accounted for in detail and the recycle stream from the crystallizer was always at the eutectic composition which implies that the crystallization process is highly unrobust. In Amanullah and Mazzotti [18] as well as in Kaspereit [4] the focus was on the steady state design of combined SMB-crystallization processes and the optimal coupling purities were determined by performing extensive parametric studies. Most of the limitations of these earlier works have been avoided within this thesis by performing a "total process" design in a single step. This implies the SMB flow rates, the optimal coupling purities and the solvent enrichment/dilution have been determined simultaneously, avoiding extensive parametric optimization studies.

1.2.2 SMB-racemization

Another major drawback of the SMB is its yield limitation which becomes evident from Figure 1.3(a). Combining the separation with the isomerization (racemization) of the undesired enantiomeric form has the obvious benefit of increasing the yield of the desired enantiomer from a maximum of 50% to a maximum of 100%.

There are three possible options to achieve this. The three different options are 1. fully integrated processes [19–21], 2. partially integrated processes with side reactors which is known as the Hashimoto process [22] and 3. classical reactor-separator schemes.

In the third option discussed previously, an external racemization reaction is performed to increase the yield to a theoretical maximum of 100% as shown in Figure 1.3(c). This option is studied within this thesis. Some of the recent applications of such process schemes are available [12, 23]. The optimal design or dynamics of such reactor-separator schemes involving SMB with an isomerization reactor has not been discussed using mathematical optimization approaches. Further, the optimal design of such processes is not straight forward due to the reduced purity at SMB

outlet coupled to the reactor. Hence, in this work, we bridge this gap by using a Non-Linear-Programming (NLP) optimization based approach to design such hybrid process schemes and discuss the dynamics and control of such a combined process.

1.2.3 Advanced optimization approaches

Until now, the discussion was focused on the benefits which can arise by using hybrid process combinations of an SMB. However, to design such processes, powerful numerical optimization tools are necessary. Therefore, in this section we look at the approaches which have been used to design such processes. As the number of process alternatives available to produce enantiomers is quite large, it would be ideal if the optimal process structure and the operating conditions are determined simultaneously. This can be achieved using either a qualitative heuristic decision tree [24] or by means of a rigorous Mixed-Integer-Non-Linear-Programming (MINLP) optimization. In this thesis, the latter approach has been employed.

Early work in using MINLP optimization in chemical process design was concerned, for example, with the determination of the optimal feed plate location and the optimal number of stages in a single distillation column [25]. These studies on single distillation systems were later extended to synthesize distillation sequences using Generalized Disjunctive Programming (GDP) or MINLP reformulation [26]. MINLP optimization has been applied extensively for the optimal design of reactive distillation columns [27, 28]. MINLP approaches have also been applied successfully to optimize heat exchanger networks [29], water distribution networks [30], reactor networks [31], etc. Lima and Grossmann [32] addressed the crystallizer design problem for p-xylene by formulating a superstructure entailing multiple possible process streams. There the focus is on the superstructure for crystallization. The details regarding the primary step which is often adsorption have been neglected.

Superstructure optimization approaches were employed by Kawajiri and Biegler [33, 34] for SMB chromatography processes. However, focus in this work was on optimizing SMB process operation using e.g. cyclic modulation of flow rates and asynchronous column switching corresponding to the POWERFEED [35, 36] and VARICOL [37, 38] concepts introduced earlier.

Palacios *et al.* [20] used a superstructure based optimization approach to design an integrated reactive SMB process.

Besides the two approaches mentioned above, no further work on super structure optimization for the design of SMB processes and its process combinations has been done so far to the best of the authors knowledge. Due to the success achieved in

other areas of process design, it is clear that the use of MINLP based superstructure optimization for SMB based process combinations can have a huge potential. For this purpose, a superstructure which subsumes all possible sub-structures and determines the optimal process configuration and operating conditions simultaneously for a specific objective, physico-chemical parameters etc. is developed in this thesis for the first time and applied to some challenging application examples from pharmaceutical industries with increasing complexity. Results have been published partly in Kaspereit *et al.*[24]. Further, the applicability of these methods to large scale problems has also been presented.

1.2.4 Process dynamics and control

It is clear from the earlier discussion that an efficient process design can create a huge step forward in the enantiomer production. However, since most of the design is performed at steady state, the practical implementation of these optimal process schemes may not be straight forward as the most economical processes often contain recycle streams. The dynamics of such processes are non-trivial and needs to be addressed for the process operability. The effect of recycle on non-linear processes could result in various phenomena such as snow balling (steady state sensitivity), inverse response, loss of stability, multiple steady states, self sustained oscillations, etc. Studies on the non-linear effects of reactor-separator recycle systems concentrated mostly on distillation/flash separators. Pushpavanam and Kienle [39] investigated the behavior of ideal reactor-separator systems. The importance of fixing the appropriate flow rates was highlighted. One of the later investigations from the same group revealed the importance of control structure selection on the overall process operation [40]. A steady state phenomenon called the "snowball" effect was reported for systems involving reactor-separator recycles [41]. It was reported that these effects crucially depend on the control structure which has been chosen.

The earlier described literature advocates the necessity of controlling the appropriate flow rates (control structure) for a smooth plant operation. This problem translates to the determination of a suitable pump configuration in SMB process operation. Understanding the dynamics of stand-alone SMB systems itself is quite challenging. The effect of SMB pump configuration plays a critical role on the performance. The effect of different SMB pump configurations have already been presented in [42, 43]. A sensitivity analysis with respect to a disturbance on flow rates for an amino acid separation system was also published in Lee *et al.*[44]. However, to the best of our knowledge, there has not been any work so far which focused on

the pump configurations and the resulting process dynamics of SMB-crystallization or SMB-racemization systems. Dynamic operability of such process combinations is addressed in the present thesis for the first time.

It turns out that suitable control strategies are required to compensate the negative effects of unforeseen disturbances. The control of a stand-alone SMB represents a challenging issue since it represents a switched non-linear system with distributed parameters. SMB control has been addressed at various levels of complexities. Most approaches have focused on model predictive control (e.g. [45–49]). Schramm *et al.* [50] applied simple PI controllers based on non-linear wave propagation to control the chromatographic unit. Another approach based on input-output linearization was reported in [35]. Most recently, non-linear wave propagation was also used to find a simple and efficient problem and controller formulation in discrete time [51, 52]. Though there has been numerous studies on stand-alone SMB control, there has been no work to date which addressed plantwide control concepts for process combinations involving SMB-crystallization or SMB-racemization processes.

From the literature analysis mentioned above, it is clear that there are many gaps which need to be addressed. One of those involve applying advanced optimization concepts to design SMB based enantiomer production processes, thus avoiding extensive parametric optimization or highly approximated shortcut methods. It is also noticeable that the dynamics and control of SMB based processes has rarely been addressed, which can be crucial in view of the practical operation. This gives rise to the following objectives of the present thesis:

- To determine the steady state optimal design for chromatography based enantioseparation processes
  - Design for fixed process configurations involving SMB-crystallization, SMB-racemization and multiple combinations of the above (NLP optimization)
  - Determine the optimal process configuration and operating conditions simultaneously, thus developing new process routes for the production of pure enantiomers (MINLP optimization)
- To understand the dynamics of process combination involving **SMB-crystallization** and to develop simple control strategies to ensure a robust process operation
- To understand the dynamics of process combination involving **SMB-racemization** and to extend the previously developed control strategies

1.3 Outline of the thesis

In order to fulfill the objectives mentioned above and to convey the ideas smoothly, the thesis has been structured as follows

Chapter 2: In the initial part of this chapter the modeling methodology which has been used within the thesis is described. In the next section, optimization methods are introduced for optimal design of combined processes for the production of pure enantiomers. In a first step, methods from Non-Linear-Programming (NLP) are applied to optimize the operating conditions for a given process configuration. Application is demonstrated for two different compounds from the pharmaceutical industry. The first is an intermediate named PDE [4]. The second is 2',6'-Pipecoloxylidide which is called PPX for brevity in the remainder. In a second step, Mixed-Integer-Non-Linear-Programming (MINLP) is applied to determine optimal process configurations and optimal operating conditions simultaneously.

Chapter 3: The chapter starts with the analysis of process dynamics corresponding to the optimal design obtained in the previous chapter for SMB-crystallization processes. Focus is on the PDE system. The effect of different disturbances are studied which reveal the need for a controller to maintain the necessary product specifications. It is shown that this can be achieved with a relatively simple control concept using PI controllers. A direct control of the SMB plant is not required.

Chapter 4: The ideas developed previously for SMB-crystallization are extended to SMB-racemization systems. Here two different case studies have been considered. The first of these corresponds to slow reaction kinetics implying that the process operation is in the kinetic regime. The second case study which was used had a high reaction rate constant implying that the process operation is in the equilibrium regime. A static controllability analysis was performed in a first step to evaluate process controllability. For the first case study, a straight forward extension of the elegant control concept developed previously for SMB-crystallization was found to be sufficient. The static controllability analysis revealed the inadequacy of this control concept for the fast kinetics scenario. Hence, a direct control based on manipulating one of the SMB flow rates was developed.

Chapter 5: This chapter summarises the major findings of the thesis and gives an outlook for possible future work in this field.

Chapter 2

Optimal design methodology

In the initial part of this chapter, the mathematical modeling approach which is used subsequently within the thesis is described. The SMB model equations have been formulated in a generalized form. Reformulation of those equations if and where necessary are highlighted in the corresponding sections. As it has been described in the previous chapter, the process performance can be enhanced significantly by using process combinations. The model equations necessary to describe these additional units are also presented. In the second part of this chapter, we focus on the steady state optimal design. Two different model compounds have been considered within this work. The first of those corresponds to a well studied enantiomer called PDE. Here, process configuration is fixed and a simple and commonly used objective function has been considered to optimize the operating conditions for the given process structures. The second model compound which has been studied is an industrial compound 2',6'-Pipecoloxylidide (PPX). The efficiency of the previously developed optimization approaches is illustrated for PPX which exhibits complex and highly non-linear adsorption characteristics. A more detailed economic cost function has been employed for this study in order to compare the potential of different process combinations. The chapter concludes with the results of an MINLP optimization, which optimizes process configuration and operating conditions simultaneously and which is a promising option at an early design stage and has not been studied in the frame work of SMB chromatography.

2.1 Mathematical formulation

Optimization of a real SMB model is extremely complex and time consuming due to the presence of periodic switching within a distributed parameter system. Hence, it

is quite a common practice to use a true moving bed (TMB) model as an approximation to the real SMB [53]. A TMB model assumes a continuous counter-current flow between the solid and the liquid phase. Fluid flow rates are fixed correspondingly, using pumps. The equivalent solid flow rate which is the same in all the four zones is linked to the switching time of the SMB plant by

$$t_{switch} = \frac{V_c(1-\epsilon)}{\dot{Q}_{solid}} \tag{2.1}$$

Continuous Chromatography model

In this work we have used an equilibrium stage TMB model. This model assumes a series of equilibrium stages with the dispersion being captured by the number of stages/cells. The mass balance for a component i on a stage k can be written as

$$\epsilon V \frac{dc_{i,k}}{dt} + (1-\epsilon)V\frac{dq_{i,k}}{dt} = \dot{Q}_{solid}\left[q_{i,k+1} - q_{i,k}\right] + \dot{Q}_{k-1}c_{i,k-1} - \dot{Q}_k c_{i,k} + \dot{Q}_{external}c_{i,external} \tag{2.2}$$

$$0 = \dot{Q}_{k-1} - \dot{Q}_k + \dot{Q}_{external} \tag{2.3}$$

In Eqs.(2.2) and (2.3), $i = 1, 2$ and $k = 1, ..N$. V is the volume of the stage, ϵ is the porosity, $\dot{Q}_{k-1}$ and $\dot{Q}_k$ are the volumetric flow rates of the liquid that enter and leave the stage k respectively. $\dot{Q}_{solid}$ is the solid flow rate which is constant in all the four zones. $\dot{Q}_{external}$ refers to possible external streams due to feed, desorbent, extract or raffinate and $c_{i,external}$ refers to the concentration of the corresponding external stream. In Eq.(2.2), $\dot{Q}_{external}$ is positive for the streams entering the plant (feed, desorbent) and negative for the streams leaving the plant (extract, raffinate). $c_{i,k}$ represents the concentration of the $i^{\,th}$ component in the liquid phase on stage k where as $q_{i,k}$ is the solid phase concentration of the corresponding component. The relation between the solid and the liquid phase is given by the thermodynamic adsorption equilibrium. This can be written mathematically for a two component system as

$$q_{i,k} = f_i(c_{1,k}, c_{2,k}) \tag{2.4}$$

In this thesis, enantiomer '1' i.e. $i = 1$ is assumed to be the stronger adsorbing enantiomer and enantiomer '2' is considered to be the weaker adsorbing enantiomer. Since enantiomer '1' is the stronger adsorbing enantiomer it would be enriched at the extract outlet and can be collected at high purity at this outlet. Similarly, enantiomer '2' being the weaker adsorbing enantiomer would be enriched at the raffinate outlet and can be obtained in high purity at the raffinate.

For the other units, simple mass balances have been applied and are assumed to be quasi-static.

Crystallizer model

The governing equations for the enrichment step before the crystallizer can be written as (see also Figure 2.1)

$$\dot{Q}^{cryst}_{evap,Feed} = \dot{Q}^{cryst}_{evap} + \dot{Q}^{cryst}_{SR} \tag{2.5}$$

$$\dot{Q}^{cryst}_{evap,Feed} c^{cryst}_{i,evap,Feed} = \dot{Q}^{cryst}_{evap} c^{cryst}_{i,evap} \tag{2.6}$$

$$c^{cryst}_{i,evap} = \rho x_{i,evap} \tag{2.7}$$

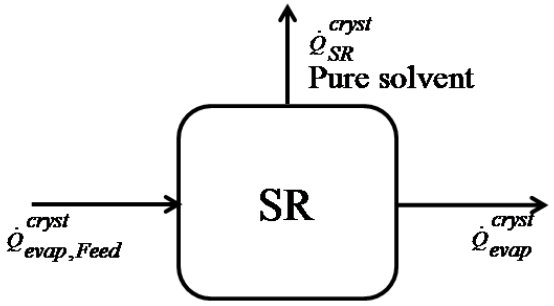

Figure 2.1: Figure illustrating the nomenclature for the solvent removal unit before the crystallizer

where the index $\dot{Q}^{cryst}_{evap}$ denotes the stream from the solvent removal to the crystallizer. $\dot{Q}^{cryst}_{SR}$ is the solvent removal rate. $x_{i,evap}$ is the mass fraction of component i in the crystallizer inlet. Crystallization characteristics being defined in terms of mass fraction in a Solid-Liquid-Equilibrium (SLE) diagram [Eqns.(2.8) - (2.10)]. This necessitates the conversion of concentration to mass fraction.

Depending on the composition of the feed to the crystallizer $c^{cryst}_{i,evap}$ or $x_{i,evap}$, different regimes of operation of the crystallizer can be distinguished according to the phase diagram in Figure 2.2. For simplicity, a SLE of conglomerate type is considered in this thesis. For the ease of presentation, rectangular coordinates are used as shown in Figure 2.2. The composition is specified in terms of mass fractions x_i. The phase diagram has four different regions which are labeled from I to IV in Figure 2.2 and which give rise to different patterns of behavior. Region I corresponds to a single liquid phase, whereas regions II and IV correspond to the two phase regions, where a liquid phase coexists with pure crystals of enantiomer '1' in region II, or pure crystals of the enantiomer '2' in region IV, respectively. Hence, pure crystals of the enantiomer '1' can be produced by crystallization in region II and pure crystals of the enantiomer

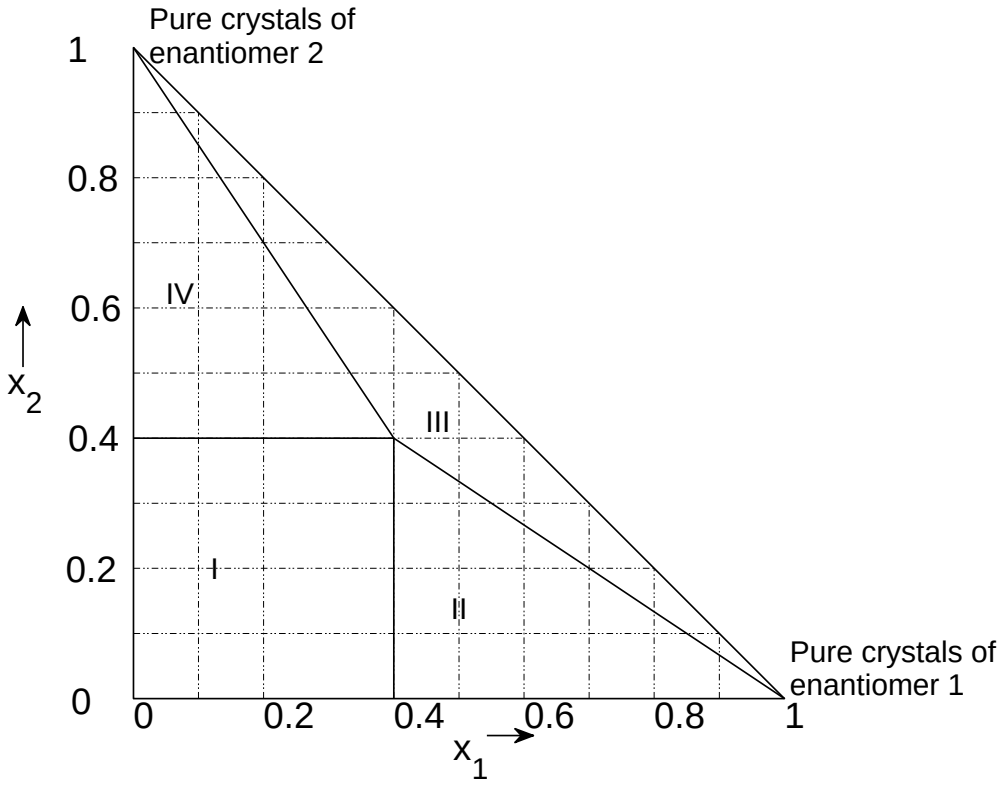

Figure 2.2: SLE for a conglomerate on a rectangular diagram

II by a crystallization in region IV. So the nominal operation for producing pure crystals of enantiomer '1' is located in region II. Accordingly, the nominal operation for the production of pure crystals of enantiomer '2' is in region IV of Figure 2.2. In the region III, all the three phases coexist, i.e. a liquid phase and a mixture of pure crystals of the enantiomer '1' and pure crystals of the enantiomer '2'.

The simple crystallizer model to be used subsequently is based on the following assumptions

- quasi-static behavior
- isothermal operation
- ideal solubility as in Figure 2.2
- equal density of the liquid and the solid

Under these assumptions the model of the crystallizer accounting for the different

operational regions in Figure 2.2 is given by

$$\dot{Q}_{evap}^{cryst} = \dot{Q}_{ml} + \sum_{1}^{2} \dot{Q}_{i,crystal} \quad (2.8)$$

$$\dot{Q}_{evap}^{cryst}\, x_{i,evap} = \dot{Q}_{ml}\, x_{i,ml} + \dot{Q}_{i,crystal} \quad (2.9)$$

$$\dot{Q}_{i,crystal} = k_i \left[x_{i,ml} - x_i^*\right] \quad (2.10)$$

$$\text{for all}\, coupled process i = 1, 2$$

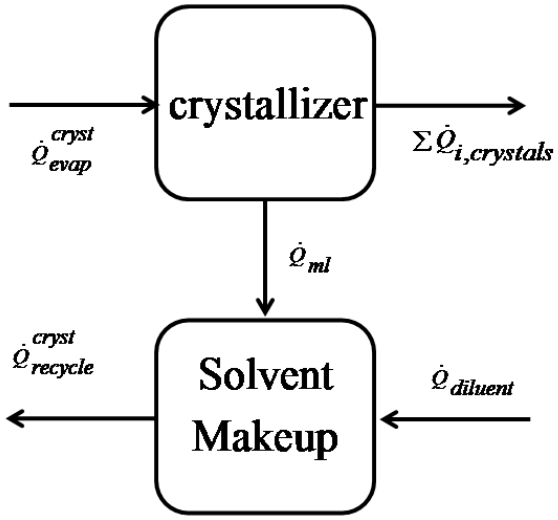

Figure 2.3: Figure illustrating the nomenclature around the the crystallizer and the solvent makeup

where Eq.(2.8) represents the total mass balance of the crystallizer, Eqs.(2.9) are the corresponding component mass balances, and Eqs.(2.10) represent the component material balances of the solid phase. Therein, x_i^* is the equilibrium composition of the fluid phase. The k_i values are assigned in such a way that in the two phase region the corresponding k_i is non-zero (e.g. in region II, $k_1 = 1000.0$ and $k_2 = 0.0$), for the crystallization that occurs within the three phase region both k_i's are non-zero (e.g. in region III, $k_1 = 1000.0$ and $k_2 = 1000.0$) and for the single phase region both k_i's are zero (e.g. in region I, $k_1 = 0.0$ and $k_2 = 0.0$). k_i can be understood as the crystallization rate constant. A nonzero k_i value of 1000 has been used for all the studies within this thesis corresponding to the limit of thermodynamic equilibrium.

The liquid outlet from the crystallizer needs to be diluted before feeding back into the SMB chromatographic unit. The unit is assumed to be an ideal mixer. A constant diluent flow rate is maintained with a corresponding pump. This stream is

in turn mixed with the fresh feed.

$$\dot{Q}^{cryst}_{recycle} = \dot{Q}_{ml} + \dot{Q}_{Diluent} \tag{2.11}$$

$$\dot{Q}^{cryst}_{recycle}\, x_{i,recycle} = \dot{Q}_{ml}\, x_{i,ml} \tag{2.12}$$

Reactor model

As in the case of crystallization, we have used an enrichment step before the reactor which can be written mathematically as,

$$\dot{Q}^{reac}_{evap,Feed} = \dot{Q}^{reac}_{evap} + \dot{Q}^{reac}_{SR} \tag{2.13}$$

$$\dot{Q}^{reac}_{evap,Feed} c^{reac}_{i,evap,Feed} = \dot{Q}^{reac}_{evap} c^{reac}_{i,evap} \tag{2.14}$$

where the index $\dot{Q}^{reac}_{evap}$ denotes the stream from the solvent removal to the reactor. $\dot{Q}^{reac}_{SR}$ is the solvent removal rate, which could be done by evaporation, nano filtration etc. For the racemizer it is adjusted in such a way, that the concentration of the undesired component in the recycle is equal to the concentration in the external feed of the corresponding component.

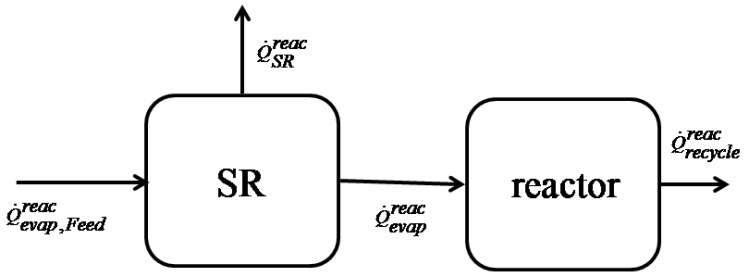

Figure 2.4: Figure illustrating the nomenclature around the the reactor and the solvent removal before the reactor

The racemization reactor is modeled as a continuous stirred tank reactor with an isomerization reaction according to

$$\dot{Q}^{reac}_{evap} = \dot{Q}^{reac}_{recycle} \tag{2.15}$$

$$\dot{Q}^{reac}_{evap} c_{i,evap} = \dot{Q}^{reac}_{recycle} c^{reac}_{i,recycle} - \nu_i V_{reac} k_{forward} \left[c^{reac}_{1,recycle} - c^{reac}_{2,recycle} \right] \tag{2.16}$$

The reaction reads

$$\text{enantiomer '1'} \rightleftharpoons \text{enantiomer '2'}$$

with $k_{forward}$ being the reaction rate constant. Note that the equilibrium constant is equal to 1 for a racemization. ν_i is the stoichiometric coefficient, which is equal to +1 for the desired enantiomer '2' and -1 for the undesired enantiomer '1'.

The recycle stream from the reactor and crystallizer or from the two crystallizers are mixed with the fresh feed before feeding it to the SMB. It is assumed to be an ideal mixer. It can be written as

$$\dot{Q}_{feed} = \dot{Q}_{F_0} + \dot{Q}^{reac}_{recycle} + \dot{Q}^{cryst}_{recycle} \tag{2.17}$$

$$\dot{Q}_{feed}\, c_{i,feed} = \dot{Q}_{F_0}\, c_{i,F0} + \dot{Q}^{reac}_{recycle}\, c^{reac}_{i,recycle} + \dot{Q}^{cryst}_{recycle}\, c^{cryst}_{i,recycle} \tag{2.18}$$

2.2 Model system 1: PDE (Simple system)

In this section, we show the results of the optimal design for a pharmaceutical intermediate called PDE. The adsorption equilibrium is of Langmuir type and the solid-liquid-equilibrium for the crystallizer assumes ideal solubilities. The physicochemical parameters for PDE are provided in Appendix A. SMB-crystallization has already been proposed as an interesting option for this compound [4, 16]. Chromatographic separation parameters are also available [54]. SLE for this system is of conglomerate type [55]. Crystallization is assumed to occur at a fixed temperature of 40°C. This corresponds to a mass fraction of 0.4 at the eutectic. The SMB unit considered within this section is assumed to consist of 400 stages distributed equally among the four zones.

In order to perform an optimal design, it is necessary to define an objective function. As an initial case, a simple well studied objective function is used, which is the specific solvent consumption. It can be written mathematically as

$$\frac{\dot{Q}_{Solvent}}{\dot{Q}_{F_0} * (c_{1,F0} + c_{2,F0})} \tag{2.19}$$

Solvent is defined as $\dot{Q}_1 - \dot{Q}_4$. The objective function given by Eq.(2.19) simultaneously minimizes solvent consumption and maximizes throughput. Optimization has been performed within the modeling environment GAMS [56]. As fixed process structures such as SMB, SMB-crystallization, SMB-racemization etc. are optimized, it is sufficient to solve a NLP problem. The CONOPT 3 solver based on a generalized reduced gradient has been used for solution purposes [57].

A general NLP problem can be written as

$$\begin{aligned} &\min\ f(\overline{x}) \\ &\text{s.t. } h(\overline{x}) = 0, \\ &\quad g(\overline{x}) \leq 0\,. \end{aligned} \tag{2.20}$$

Eq.(2.20) formulates the task of minimizing an objective or cost function f that depends on continuous variables $\overline{x}$. Equality constraints h are the mass balances, thermodynamic relations and other process model equations. The inequality constraints g arise from the user restrictions such as minimum purity, yield etc. In the present case, inequality constraints are imposed on SMB purities as well as on the positive flow rates into and out of the SMB unit at the corresponding stages.

Optimal design is based on the steady state version of the model introduced in the previous section.

2.2.1 SMB-crystallization

Depending on the location of the crystallizer two different scenarios can arise. First of these would be called the extract configuration within this work. In this configuration, the crystallizer occurs at the extract outlet and the stronger adsorbing enantiomer, i.e. enantiomer '1', is the desired product. The second scheme consists of a crystallizer at the raffinate outlet of the SMB which is called the raffinate configuration. This is the desired scenario when the weaker adsorbing enantiomer, i.e. enantiomer '2', is the desired product.

Slightly modified crystallization equations have been used for optimization purposes. Instead of accounting for the different crystallization characteristics depending on the region of the SLE, additional inequality constraints are imposed to restrict the optimal design to region II for the extract configuration, or to region IV for the raffinate configuration, respectively. The non crystallizing SMB outlet purity is maintained at a value of 99% in order to limit the loss of the desired enantiomer. The amount of diluent ($\dot{Q}_{Diluent}$) added to the recycle is adjusted in such a way that the concentration of the crystallizing component in the internal feed is equal to the concentration in the external feed.

SMB-crystallization for the extract configuration was found to be 23.7% more efficient than a stand-alone SMB using cost function given by Eq.(2.19). While for the raffinate configuration, the process combination outperformed the stand alone unit by 26.3%. Improvement will be even more pronounced for the lower stage numbers.

The effect of stage number will be discussed in detail for the PPX system.

Kaspereit [4] has shown earlier that such an SMB-crystallization can be highly beneficial using a computationally intensive approach. He combined the SMB characterisitcs obtained from extensive parametric optimization of TMB with algebraic relations defining the mass balances across the solvent removal and crystallization units. While in this thesis, a more elegant model formulation optimizing all the units simultaneously has been performed whereby the computational efficiency is increased drastically. Optimal operational variables to be determined by the optimizer are the flow rates of the SMB unit, the coupling purity and the solvent removal/addition ($\dot{Q}_{SR}^{cryst}/\dot{Q}_{Diluent}$) rate. The operational parameters corresponding to the optimal design for both the extract and the raffinate configurations are listed in Table 2.1.

Table 2.1: Optimal design for an SMB-crystallization process

Variables	Extract	Raffinate
$\dot{Q}_1[ml/min]$	2.1796	1.4644
$\dot{Q}_2[ml/min]$	0.2861	0.75
$\dot{Q}_3[ml/min]$	1.0876	1.511
$\dot{Q}_4[ml/min]$	0.6811	0.7209
$\dot{Q}_{solid}[ml/min]$	1.8696	1.8696
$\dot{Q}_{SR}^{cryst}[ml/min]$	1.8647	0.4168
$\dot{Q}_{Diluent}[ml/min]$	0.2009	0.075
$Purity_{coupling}$	78.75	83.23
$\dot{Q}_{F_0}[ml/min]$	0.5868	0.321

2.2.2 SMB-racemization

As has been done before, a steady state version of the model equations is used here too. Two different case studies have been considered within this chapter. One of them corresponds to what we call the "slow kinetics" for which $V_{reac}k_{forward} = 0.1$ and the purity requirements at the non-racemizing outlet have been fixed to 90 %. The second case study corresponds to a $V_{reac}k_{forward} = 10000.0$ which would be referred to within this thesis as "fast kinetics". The purity requirements for the latter scenario has been maintained at a high value of 99 %.

The amount of solvent which needs to be removed ($\dot{Q}_{SR}^{reac}$) is adjusted in such a way that the concentration of the undesired enantiomer in the reactor outlet is equal to the concentration in the external feed. Optimal operational variables to be determined by the optimizer are the flow rates of the SMB unit, the coupling purity and the solvent removal ($\dot{Q}_{SR}^{reac}$). The optimal design parameters corresponding to

the two case studies for racemization at the extract are given in Table 2.2. The calculations have been repeated for the scenario when the racemization occurs at the raffinate outlet and are provided in Table 2.3.

The primary benefit of SMB-racemization with respect to a stand-alone SMB arises from the increase in yield from a maximum of 50% to a maximum of 100%. In addition, a reduction of specific solvent consumption by around 20% was observed when the reaction is in the equilibrium regime (fast reaction) for both the extract and raffinate configurations. But, in the later part of this chapter it is shown that by using a more detailed cost function, the improvement can be much more significant.

Table 2.2: Optimal design for an SMB-racemization process with racemization at the extract

Variables	slow reaction	fast reaction
$\dot{Q}_1[ml/min]$	1.7432	2.1796
$\dot{Q}_2[ml/min]$	0.25	0.2857
$\dot{Q}_3[ml/min]$	1.2074	1.0876
$\dot{Q}_4[ml/min]$	0.9852	0.6811
$\dot{Q}_{solid}[ml/min]$	1.8696	1.8696
$\dot{Q}_{SR}^{reac}[ml/min]$	0.6127	1.3884
$Purity_{coupling}$	82.22	78.72
$\dot{Q}_{F_0}[ml/min]$	0.0769	0.2963

Table 2.3: Optimal design for an SMB-racemization process with racemization at the raffinate

Variables	slow reaction	fast reaction
$\dot{Q}_1[ml/min]$	1.1291	1.4644
$\dot{Q}_2[ml/min]$	0.7313	0.7499
$\dot{Q}_3[ml/min]$	2.5	1.1511
$\dot{Q}_4[ml/min]$	0.6479	0.7209
$\dot{Q}_{solid}[ml/min]$	1.8696	1.8696
$\dot{Q}_{SR}^{reac}[ml/min]$	0.1579	0.1912
$Purity_{coupling}$	62.82	83.23
$\dot{Q}_{F_0}[ml/min]$	0.0746	0.1621

2.2.3 SMB-racemization-crystallization

After having discussed the optimal design of the two simple and straightforward process combinations, we shift our attention to coupled processes which involve multiple combinations of the former two. The first multi-unit process combination which

Table 2.4: Optimal design for an SMB-extract.racemization and raffinate.crystallization

Variables	values
$\dot{Q}_1[ml/min]$	1.434374
$\dot{Q}_2[ml/min]$	0.315376
$\dot{Q}_3[ml/min]$	1.024929
$\dot{Q}_4[ml/min]$	0.635821
$\dot{Q}_{solid}[ml/min]$	1.8696
$\dot{Q}_{SR}^{reac}[ml/min]$	0.726818
$\dot{Q}_{SR}^{cryst}[ml/min]$	0.371214
$\dot{Q}_{Diluent}[ml/min]$	0.111113
$Purity_{extract}$	75.321035
$Purity_{raffinate}$	85.437920
$\dot{Q}_{F_0}[ml/min]$	0.198606

Table 2.5: Optimal design for an SMB-raffinate.racemization and extract.crystallization

Variables	values
$\dot{Q}_1[ml/min]$	1.32327440
$\dot{Q}_2[ml/min]$	0.39210279
$\dot{Q}_3[ml/min]$	1.00477873
$\dot{Q}_4[ml/min]$	0.63442873
$\dot{Q}_{solid}[ml/min]$	1.8696
$\dot{Q}_{SR}^{cryst}[ml/min]$	0.91194584
$\dot{Q}_{SR}^{reac}[ml/min]$	0.09062685
$\dot{Q}_{Diluent}[ml/min]$	0.14944738
$Purity_{extract}$	81.05755237
$Purity_{raffinate}$	80.96352825
$\dot{Q}_{F_0}[ml/min]$	0.17321029

is studied is called the "total process combination". The scheme consists of an SMB unit coupled with a crystallization at the desired enantiomer outlet and a racemization at the undesired enantiomer outlet. Fast kinetics for racemization has only been considered here. Two different possible options are available. Since it is a generic investigation, both the situations, extract being the desired product outlet or raffinate being the desired product outlet have been considered. The result of the optimization for this "total process combination" when crystallization is at the raffinate (desired product) is shown in Table 2.4. In Table 2.5, the optimal design parameters for the counter scenario, i.e. the extract outlet being the desired product has been provided. It is also worth mentioning that including a crystallization can not only have an economic impact, it can also increase the process robustness.

In such a process combination, the productivity can be improved because of the presence of a crystallizer coupled to the SMB unit. This stems from the fact that SMB can be operated at lower purities and simultaneously delivering pure crystals. Further, due to the presence of racemization and recycle at the other outlet, the separation scheme has a single product stream. Thus the yield of such a process becomes 100%. In addition, the specific solvent consumption is reduced by about 44% irrespective of the location of the crystallizer and racemizer.

2.2.4 SMB-crystallization-crystallization

Here, we calculate the optimal design of a process which involves crystallization at both outlets. Unlike for racemization which can occur only at the undesired enantiomer outlet, crystallization may occur at both the outlets irrespective of whether both the enantiomers are desired or not. Table 2.6 shows the optimal operating conditions for a hybrid process which involves SMB with enantio-selective crystallization at both the outlets. In fact, it was observed that for certain cases, crystallizing the undesired enantiomer alone may be economically beneficial depending on the stage number, crystallizing outlet etc. (Results of section 2.3).

In contrast to a single crystallizer, here both the outlets can be operated at reduced purities. This leads to a significant reduction in the solvent consumption. Also, since the crystallizer delivers pure products, the loss of desired enantiomer at the undesired outlet can be eliminated. These effects lead to a reduced specific solvent consumption. An improvement of 57% is observed with respect to a stand-alone process in the objective function. It needs to be mentioned that there are additional investments and operating costs associated with the presence of additional crystallization and racemization units. In this study, they have been neglected. These additional costs may affect overall economics. Therefore, in the next section, a more detailed cost function which takes into account these additional cost factors have been formulated and the effect of those on process combinations have been discussed.

Table 2.6: Optimal design for an SMB-raff.crystallization and extr.crystallization process

Variables	values
$\dot{Q}_1[ml/min]$	1.460361
$\dot{Q}_2[ml/min]$	0.407649
$\dot{Q}_3[ml/min]$	1.049641
$\dot{Q}_4[ml/min]$	0.655810
$\dot{Q}_{solid}[ml/min]$	1.8696
$\dot{Q}^{cryst}_{SR,extract}[ml/min]$	1.033040
$\dot{Q}^{cryst}_{SR,raffinate}[ml/min]$	0.376999
$\dot{Q}_{Diluent,extract}[ml/min]$	0.144091
$\dot{Q}_{Diluent,raffinate}[ml/min]$	0.102864
$Purity_{extract}$	82.348184
$Purity_{raffinate}$	85.701256
$\dot{Q}_{F_0}[ml/min]$	0.378024

2.3 Model system 2: 2',6'-Pipecoloxylidide (PPX)

2',6'-Pipecoloxylidide (PPX) is an intermediate in the manufacture of several anaesthetics. It has a number of properties that make its production through an integrated process interesting. A specific process combination for the production of the pure S-enantiomer i.e enantiomer '2' according to this thesis convention by steady state recycling (SSR) chromatography, metal-catalyzed racemization and enantioselective crystallization has been studied very recently [58]. Here focus is on continuous processing and a systematic evaluation of different process options. The discussion in section 2.3 was in part already published in Kaspereit *et al.* [24].

In this publication a three step approach was proposed for the optimal design of combined processes for the production of pure enantiomers [24]. The first of these steps involves discarding/selecting the impossible/possible candidates based on a qualitative criteria. For enantiomer production, the qualitative criteria can be based on a decision tree such as the one shown in Figure 2.5. One of the characteristic examples of the use of a decision tree would be to discard hybrid SMB-crystallization processes when the eutectic purity is high. In the second step, short cut methods which are already available and based on equilibrium theory (analytical/semi-analytical) are applied to analyze the potential of the selected process candidates. In the last step, a detailed numerical optimization is employed to obtain optimal process configurations and/or optimal operating conditions.

The three step approach has been employed for the development of improved production processes for PPX. PPX is a compound-forming substance with a favorable eutectic purity of 67%. Based on this property and the ease of racemization, the decision tree suggests a process combination consisting of chromatography, crystallization and racemization as illustrated in Figure 1.3(d). Since the statement of a "reasonable" eutectic composition is not quantitative, the chromatography-racemization process in Figure 1.3(c) is also an interesting candidate.

The details of the chromatography, racemization and crystallization are available elsewhere [58].

Since the adsorption isotherms are extremely complex i.e quadratic isotherm, as can be seen from Appendix A, there are no shortcut methods available to design SMB processes. Since it is not the primary topic of this thesis, we shift our attention directly to the final step of the three step approach. For that purpose, a detailed numerical optimization of the equations, developed in section 2.1 has been carried out. .

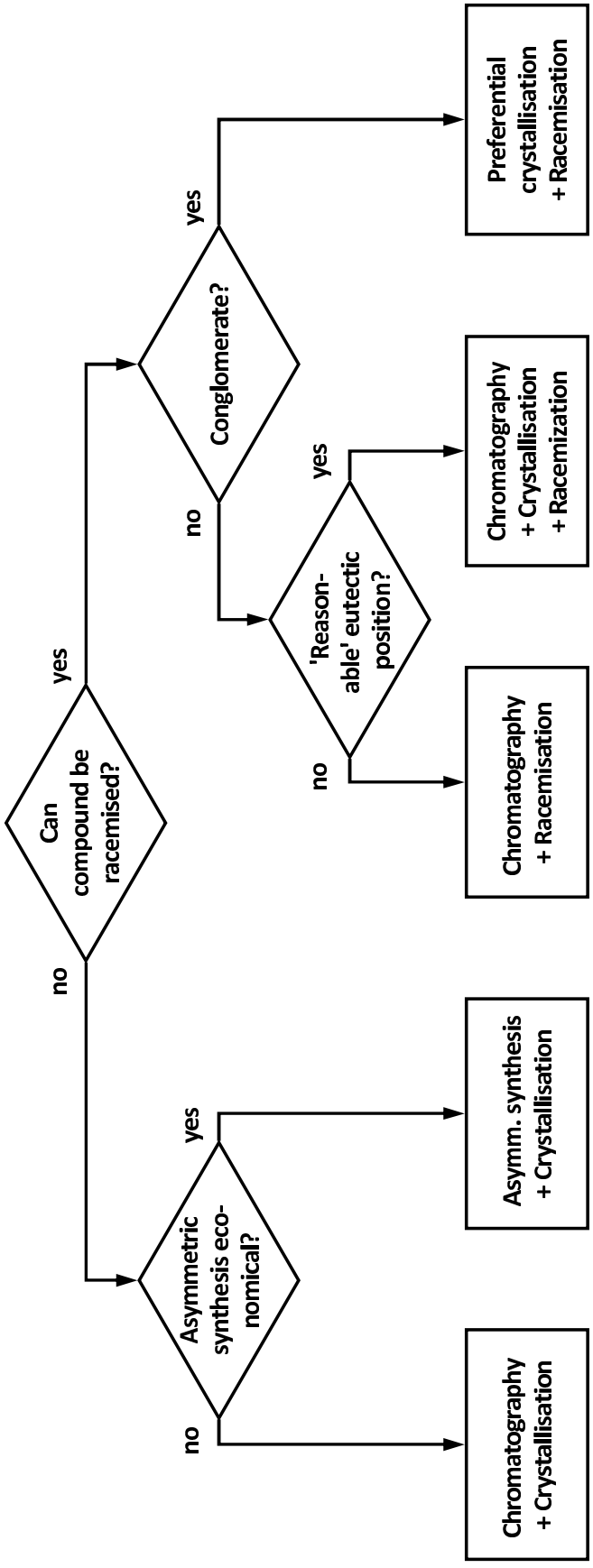

Figure 2.5: Decision tree based on simple qualitative criteria for the selection of a suitable combined or integrated process concept for the production of a pure enantiomer [24].

2.3.1 Design of fixed process structures (NLP optimization)

In order to compare the effect of the various process combinations, it is necessary to formulate a more detailed objective (cost) function based on process economics than the one used for the model system 1, i.e. Eq.(2.19). So, for that purpose, we propose and apply a cost function which is sufficiently general and does not depend on highly industry/compound specific cost structure. Here, costs are measured in money units per kg of product, i.e. [MU/kg product]. The cost function used here comprises of cost contributions due to the feed cost C_f, personnel costs C_{op} and investment costs C_{inv} according to

$$f = C_f + C_{op} + C_{inv} \tag{2.21}$$

Feed and investment costs depend on the amount of racemate to be processed M_{rac} in [kg racemate/hr], personnel costs are fixed in a given time frame leading to

$$f = \frac{(w_f + w_{inv})M_{rac} + w_{op}}{Y\,M_{rac}} = \frac{(w_f + w_{inv})M_{prod}/Y + w_{op}}{M_{prod}} \tag{2.22}$$

with cost or weighting factors w_f in [MU/kg racemate], w_{inv} in [MU/kg racemate] and w_{op} in [MU/hr]. $M_{prod} = YM_{rac}$ in [kg product/hr] is the amount of desired enantiomer produced, with Y being the yield.

Examining the expression in Eq.(2.22), it can be seen that at low production rates M_{prod}, the personnel costs are dominating and tending to infinity as the production rate goes to zero. At high production rates, the other costs are dominating and tending towards the asymptotic value $(w_f + w_{inv})/Y$.

Mathematical optimization using the cost function defined by Eq.(2.22) is applied to determine the optimal operating conditions for different process configurations. Process configurations which have been considered for this model system are:

1. Stand-alone SMB process
2. SMB with racemization
3. Three different types of SMB processes with crystallization, namely :
   (a) SMB with a crystallizer at the raffinate (product stream)
   (b) SMB with a crystallizer at the extract (waste stream)
   (c) SMB with a crystallizer at the raffinate as well as the extract

4. SMB with racemization at the extract and crystallization at the raffinate outlet.

The six different process candidates mentioned above have been compared using the cost function given by Eq.(2.22). However, it is worth mentioning, that an implementation of much more detailed cost functions such as in Jupke *et al.* [59] into the optimization framework discussed here is straightforward.

The cost function given by Eq.(2.22) also allows a preliminary discussion of the basic effects of racemization and crystallization on process economics. The initial objective is to evaluate the effect of racemization. In order to achieve that, a stand-alone SMB chromatographic unit is compared with a coupled process, where the undesired enantiomer is racemized and the reactor outlet is subsequently recycled back to the SMB unit according to Figure 1.3(c). This corresponds to the 2nd candidate in the list of possible process configurations mentioned previously. In the PPX example the undesired enantiomer is obtained at the extract outlet of the SMB. The most important effect of the racemization is an increase of the overall yield from 50% in the stand-alone SMB to a maximum of 100% in the process combination. It is worth noting, that this effect on the simple cost function can be readily predicted without knowing the optimal process conditions, i.e. without a detailed mathematical optimization. The effect is illustrated in Figure 2.6 as a function of the production rate. For demonstration purposes, equal cost factors of 1.0 for w_f, w_{inv}, w_{op} are assumed for the stand-alone process, whereas a 20% increase in investment and operational costs are assumed for the process with racemization (i.e. $w_{inv}, w_{op} = 1.2$ for the coupled process) in Figure 2.6(a). At low production rates the personnel costs are dominant and thus minimizing the benefit through an improved overall yield. At high production rates, the other costs are dominating leading to a significant cost reduction for the coupled process. In between, there is a break even point at a production rate of 0.1 in Figure 2.6(a). The difference between the stand-alone and the coupled process increases with increasing feed costs as illustrated in Figure 2.6(b) for $w_f = 10$, shifting the break even point to even lower production rates not shown anymore in Figure 2.6(b). The cost reduction for the coupled process will tend to a maximum of 50% for increasing production rates and increasing feed costs due to a 100% increase of yield compared to the stand-alone process.

An additional scope for improvement of the coupled process follows from the fact that the purity requirements for the feed to the racemizer can be relaxed leading to an increase of productivity of the SMB unit. However, to quantify this effect, rigorous optimization of the coupled process is required. Details will be discussed later in this chapter.

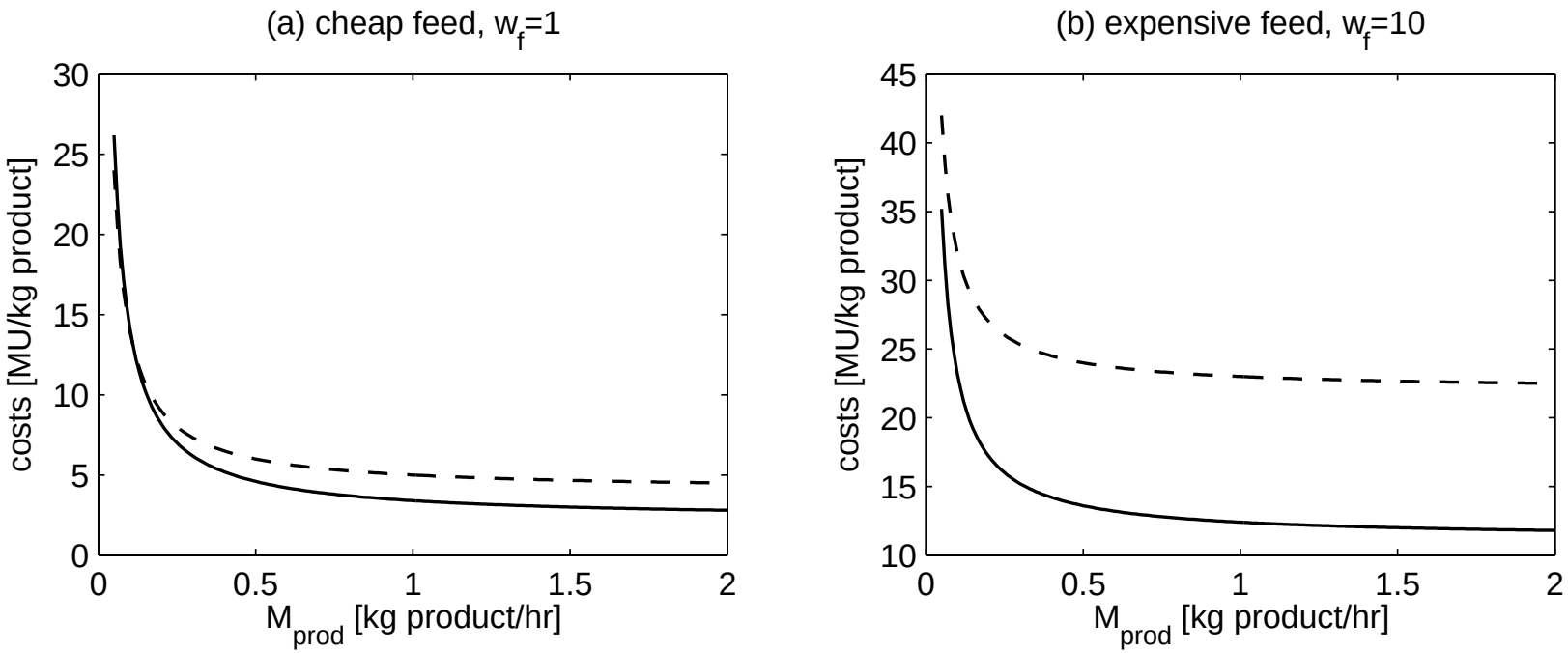

Figure 2.6: Costs as a function of production rate of a stand-alone SMB as in Figure 1.3(a) (dashed line), compared to an SMB process coupled with a racemizer as in Figure 1.3(c) (solid line) for two different feed cost scenarios.

A similar effect can be observed, when selective crystallization is coupled to an SMB chromatographic unit to "share the separation workload" between the two processes shown in Figure 1.3(b). The overall yield is not affected by this hybrid separation process but coupling purities can be relaxed, leading to an increased productivity of the SMB sub-unit in this coupled process. Further, investment costs for the chromatographic columns may be reduced due to reduced purity requirements and finally, the solvent consumption can also be reduced. To explain the main effects, solvent cost contributions have been neglected within the thesis but could be included easily in a more detailed cost evaluation.

To quantify the effects mentioned above for PPX, a parametric optimization study is presented in the Figures 2.7 - 2.9 using the models described in section 2.1 and parameters in Appendix A. As in the case of PDE, the optimization has been performed in the environment GAMS using the CONOPT3 solver [57] . In all the three cases, a fresh feed concentration of 25 g/l of racemate is used, which was found optimal for the present system due to the rather specific adsorption behavior described in Appendix A.

Figure 2.7 compares the maximum production rate of a stand-alone SMB chromatographic unit with a coupled SMB-crystallization process, when the crystallizer is located at the product, i.e. the raffinate port. The maximum production rate was obtained by rigorous optimization for different numbers of theoretical stages of the SMB unit. Furthermore, the corresponding coupling purities between the SMB unit and the crystallizer are shown. For the optimization, the outlet purities of the SMB were fixed to 99.8%. Coupling purities were restricted to a range between the eutectic composition of 67.5% and 99.8%.

In Figure 2.7, a large difference in productivity between the stand-alone SMB and the coupled process is observed for moderate numbers of theoretical stages below 300. For a fixed number of 160 theoretical stages, the maximum production rate of the coupled process is almost two times higher than that of the stand-alone SMB. On the other hand, if the production rate is fixed in Figure 2.7, the number of theoretical stages can be reduced significantly by using a coupled process in comparison to the the stand-alone SMB. In the remainder, the total number of theoretical stages will be fixed to 160.[1] Similar effects can be observed in Figure 2.8, where the SMB is coupled to a crystallizer at the extract outlet delivering the undesired enantiomer, and in Figure 2.9 where each of the two outlets is coupled to a crystallizer.

[1]Rigorous optimization of the number of theoretical stages using an extended MINLP formulation is discussed in Appendix B

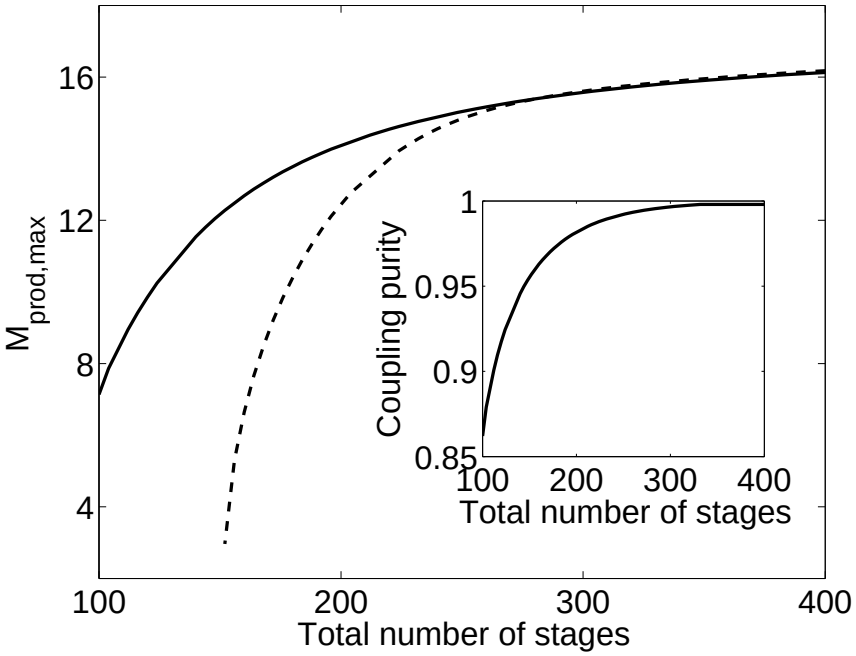

Figure 2.7: Maximum production rates and coupling purity as a function of the total number of theoretical stages of a stand-alone SMB (dashed line) compared to an SMB process with a crystallizer at the raffinate.

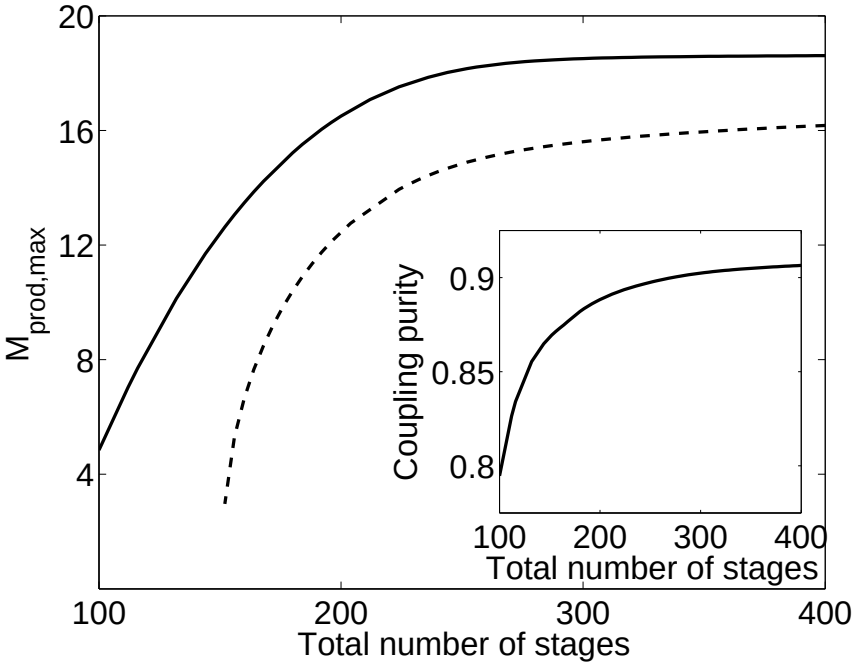

Figure 2.8: Maximum production rates and coupling purity as a function of the total number of theoretical stages of a stand-alone SMB (dashed line) compared to an SMB process with a crystallizer at the extract.

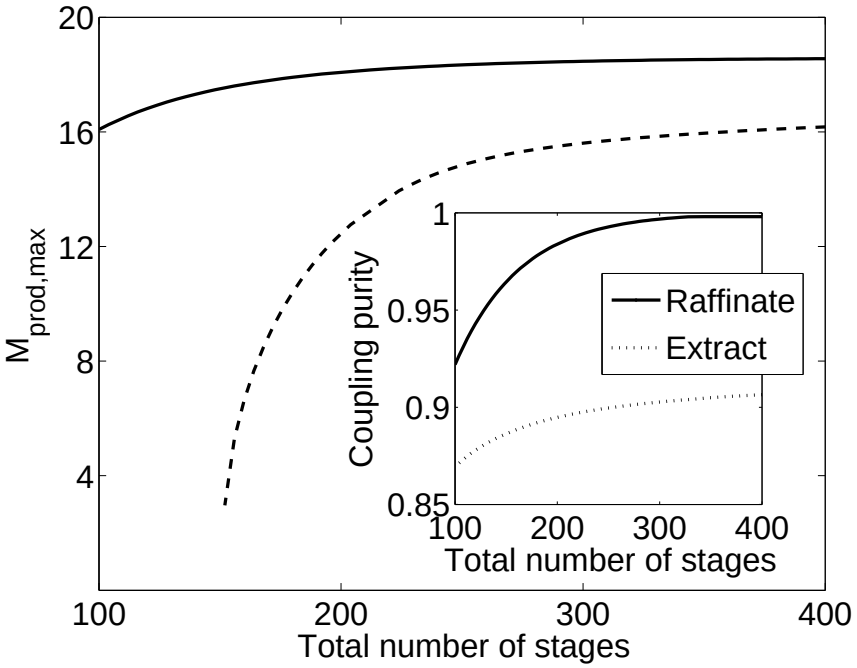

Figure 2.9: Maximum production rates and coupling purity as a function of the total number of theoretical stages of a stand-alone SMB (dashed line) compared to an SMB process with a crystallizer at the raffinate and a crystallizer at the extract.

After illustrating the basic effects, the effect of various process combinations mentioned above on the simplified cost functions will be evaluated in detail by means of rigorous NLP optimization. Results are provided in Table 2.7. Cost factors w_f, w_{inv}, w_{op} for the SMB unit are assumed to be equal to one. Again, for the racemization a twenty percent increase in investment and operational costs are assumed. Since crystallization is required anyhow in most cases to obtain crystalline products, no extra costs for the crystallization have been taken into account.

Rigorous optimization results as presented in Table 2.7 are fully consistent with our earlier discussion. Namely, the productivity of the overall process can be increased significantly if a crystallizer is coupled to the SMB process. Although the effect on costs is moderate for the present arbitrary cost model, it can be much more pronounced if operational (personnel) costs have a stronger weight. The strongest improvement is observed for the racemization, which leads to a reduction in costs of 45%. Besides the increased overall yield by factor 2 an additional increase in the optimal production rate is observed due to reduced coupling purity as discussed above.

Table 2.7: NLP calculations for PPX for a total number of 160 theoretical stages

Process	Objective function	Optimal production rate	raff., extr. purity
SMB	4.301	3.315	99.8, 99.8
SMB-raff.cryst	4.158	6.330	96.3, 99.8
SMB-extr.cryst	4.148	6.735	99.8, 87.3
SMB-two.cryst	4.113	8.831	97.0, 88.8
SMB-rac	2.364	7.289	99.8, 79.0
SMB-rac-cryst	2.318	10.211	96.2, 74.4

2.3.2 Simultaneous design of the process structure and operating conditions (MINLP optimization)

Until now, the focus has been on the design of a priorily fixed process configurations. But often, at an early design stage, the optimal configuration is not known and needs to be determined along with the operating conditions for the same. This can be achieved using either a Mixed Integer Non Linear Programming (MINLP) approach or by an extensive enumeration techinique. In the latter approach, we evaluate all the possible process options by means of NLP optimization and determine the best candidate. This approach can be computationally challenging when the number of process combinations is large.

In this thesis, we use the more elegant MINLP approach for simultaneous determination of process structure and operating conditions. A generalized MINLP problem can be written as

$$\begin{aligned} &\min\ f\left(\overline{x},\overline{y}\right) \\ &\text{s.t. } h\left(\overline{x},\overline{y}\right)=0, \\ &\quad g\left(\overline{x},\overline{y}\right)\leq 0\,. \end{aligned} \tag{2.23}$$

Depending on the objective function, process constraints etc., the optimization algorithm calculates the optimal process configuration (sub-structure) from the superstructure by means of binary decision variables $\overline{y}\in\{0,1\}$. Since the formulation involves both the integer $\overline{y}$ and continuous variables $\overline{x}$, the optimal process structure as well as the optimal perating conditions are obtained simultaneously from Eqs.(2.23).

The superstructure to be discussed subsequently is shown in Figure 2.10. In this figure, 'SR' stands for solvent removal, 'SM' for solvent makeup, 'Rac' for racemization, 'Crys' for crystallization. The binary decision variables y_i with $i = RR, RO, RC, EC, ER, EO$, also shown in Figure 2.10, specify, whether the corresponding flowrate is zero ($y_i = 0$) or finite ($y_i = 1$). In this notation, the first index refers to the raffinate ('R') or extract ('E') outlet of the SMB whereas the second index refers to the type of process connected to this outlet, i.e. 'R' for racemizer, 'C' for crystallizer and 'O' if no further processing step is connected to the stream. In the present case, additional constraints have to be taken into account according to

$$y_{RR}=0, \qquad \sum_i y_{R,i}=1, \qquad \sum_i y_{E,i}=1 \tag{2.24}$$

meaning that exactly one flow is active at the raffinate and the extract side. Also, additional conditions are enforced so that no racemizer is located at the raffinate side, where the desired enantiomer is obtained with high purity. It is worth noting, that the number of stages for the SMB unit can also be optimized in a similar way with additional binary decision variables, which specify whether a tray in a given SMB superstructure is active or not. Such strategies are illustrated in Appendix B. For simplicity, however, focus in the following is on a fixed total number of 160 stages like in the previous section.

For the MINLP optimization with fixed number of stages, the simplified cost function from the previous section is extended to account for the various process

combinations in an explicit way. The extended cost function can be written as

$$f = \frac{(w_f + w_{inv})M_{rac} + w_{op}}{((1 - y_{ER})0.5 + y_{ER}Y)M_{rac}} \tag{2.25}$$

with

$$w_{inv} = w_{inv,SMB} + y_{RC}w_{inv,RC} + y_{EC}w_{inv,EC} + y_{ER}w_{inv,ER}$$

and

$$w_{op} = w_{op,SMB} + y_{RC}w_{op,RC} + y_{EC}w_{op,EC} + y_{ER}w_{op,ER}$$

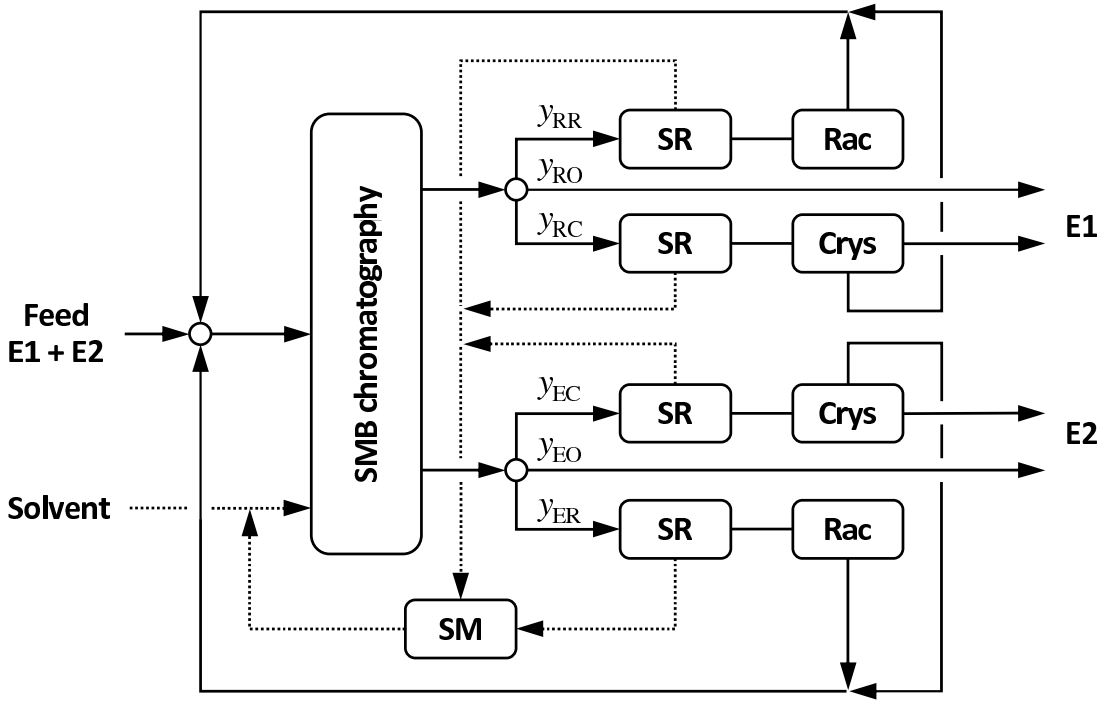

Figure 2.10: Superstructure for MINLP optimization

Besides feed costs w_f, the cost function comprises investment costs of the SMB process $w_{inv,SMB}$, a possible raffinate $y_{RC}w_{inv,RC}$ and/or extract crystallizer $y_{EC}w_{inv,EC}$, and a possible extract racemizer $y_{ER}w_{inv,ER}$. Additional operational costs are covered in a similar manner. As was considered in NLP, feed and investment costs are proportional to the amount of racemate M_{rac} to be processed. Further, it should be noted, that the formula for the production rate in the denominator also admits racemization with overall yields smaller than 100%.

At this point it is important to mention that the optimal process configuration depends crucially on the specific cost factors of the different cost contributions in the

Eq.(2.25). For a given cost function, the optimal process can be determined directly by MINLP optimization. Exemplary results are given in Table 2.8.

The process configuration given in the first line of Table 2.8 is obtained when using the same weighting factors as in the cost function of section 2.3.1. As expected, the SMB plus the racemization at the extract and the crystallization at the raffinate is the best configuration, if no additional costs for the crystallization are taken into account according to our earlier argument. In the second line, additional costs for crystallization are considered which counterbalances the benefit of potential crystallizers leading to an elimination of the crystallizers in the optimal process structure, given in the first row. In a similar way, the racemizer will be eliminated for an expensive racemization with reduced yields in line 3. High investment costs may be due to an expensive catalyst, as an example. Racemizers and crystallizers will be eliminated if the two previous cost factors are added which leads to a stand-alone SMB in line four. In a similar way, the SMB plus the crystallizer at the extract or raffinate are obtained in line 5 and 6 of Table 2.8 for an expensive racemization with low yield, if the respective other crystallizer is penalized with high costs. The two latter examples are a bit artifical, but are useful to demonstrate the full capacity of the MINLP optimization employed here.

All MINLP calculations were done in GAMS [56] using the DICOPT MINLP solver [60] with CPLEX for the MILP sub problems and CONOPT for the NLP sub problems.

2.4 Summary

In this chapter, methods for optimal design of combined processes for the production of pure enantiomers were introduced and illustrated with two case studies. For the first system, an intermediate chemical compound called PDE, NLP optimization was used to determine optimal operating conditions for some given SMB-racemization-crystallization processes. For demonstrating the potential of the process combinations, specific solvent consumption was considered as a simplified cost function. A more detailed cost function together with a simultaneous MINLP optimization pf process configuration and process structure was demonstrated here for the first time for a second compound with highly nonlinear adsorption behavior called PPX. For simplicity the number of stages was fixed in a first step. Extended formulations with variable number of stages are presented in Appendix B. This gives rise to a large number of additional binary variables which clearly underlines the usefulness

of advanced optimization methods in this context

In most of the cases, the optimal design consisted of single or multiple recycle streams. The dynamics of these non-linear recycle systems is non-trivial and requires a critical analysis. Therefore, in the next step, we study the effect of disturbances on process behavior. This is decisive in view of practical operability of the process. The results of these dynamic investigations are discussed in the next two chapters for the two different process combinations namely SMB-crystallization and SMB-racemization.

Table 2.8: MINLP calculations for PPX for a total number of 160 theoretical stages. All MINLP calculations were performed in GAMS using the DICOPT MINLP solver with CPLEX for the MILP sub-problems and CONOPT for the NLP sub-problems.

Optimal process	w_f	$w_{inv,SMB}$	$w_{inv,ER}$	$w_{inv,EC}$	$w_{inv,RC}$	$w_{op,SMB}$	$w_{op,ER}$	$w_{op,EC}$	$w_{op,RC}$	Y
SMB-rac-cryst	1.0	1.0	0.2	0.0	0.0	1.0	0.2	0.0	0.0	1.0
SMB-rac	1.0	1.0	0.2	0.2	0.2	1.0	0.2	0.2	0.2	1.0
SMB-two-cryst	1.0	1.0	0.5	0.0	0.0	1.0	0.2	0.0	0.0	0.7
SMB	1.0	1.0	0.5	0.2	0.2	1.0	0.2	0.2	0.2	0.7
SMB-extr.cryst	1.0	1.0	0.5	0.0	0.2	1.0	0.2	0.0	0.2	0.7
SMB-raff.cryst	1.0	1.0	0.5	0.2	0.0	1.0	0.2	0.2	0.0	0.7

Chapter 3

Dynamics and control of SMB-crystallization processes

It has already been shown that the process combinations such as SMB-crystallization, SMB-racemization, SMB-crystallization-racemization etc. outperform the standalone SMB in terms of process performance. In the previous chapter, optimization techniques were introduced to design those favorable process structures, one of them being SMB-crystallization, which is the investigated process within this chapter. Since the optimal process schemes are often multi-unit recycle systems with inherent nonlinearities, process dynamics is non-trivial. This implies that the steady state optimal design described in the previous chapter alone is not sufficient to ensure process operability. Process dynamics is also very important in terms of practical implementation. Thus, in the first step, we study the dynamics of an SMB-crystallization process subjected to step disturbances of the external feed flow rate and concentration. Since the dynamic investigations reveal undesired characteristics, simple feed back control strategies are proposed. They form the basis for the current chapter. As a benchmark problem the PDE enantiomers are considered [4, 55]. Numerical investigation for the dynamic process models has been performed using the simulation environment DIVA [61]

3.1 Open loop dynamics

3.1.1 Robust design

In chapter 2, optimal design of SMB-crystallization process has been addressed. Figure 3.1 shows the optimal design for the extract and the raffinate configuration

Table 3.1: Robust design for an SMB-crystallization process

Variables	Extract	Raffinate
$\dot{Q}_1[ml/min]$	2.1856	1.5721
$\dot{Q}_2[ml/min]$	0.3949	0.7571
$\dot{Q}_3[ml/min]$	1.1067	1.1861
$\dot{Q}_4[ml/min]$	0.6981	0.7344
$\dot{Q}_{solid}[ml/min]$	1.8696	1.8696
$\dot{Q}_{SR}^{cryst}[ml/min]$	1.7663	0.4374
$\dot{Q}_{Diluent}[ml/min]$	0.148	0.0806
$Purity_{coupling}$	85.77	86.96
$\dot{Q}_{F_0}[ml/min]$	0.5538	0.3429

in the rectangular phase diagram. The optimal process is always located at the boundary between the two and the three phase regions in Figure 3.1. This is due to the fact, that the maximum amount of crystalline product is obtained at the boundary. However in view of practical operation, this may not be the ideal solution since process operation around this point would be extremely sensitive. The smallest disturbance in the wrong direction would move the process into the three phase region whereby the product specifications would be lost. Hence, to be operable at all, an extra safety margin was introduced in the optimization and a new set of design parameters referred to as "Robust design" have been obtained. Robust design parameters have been calculated with a safety margin of 15% with respect to the eutectic purity. This corresponds to about 25% decrease in the mass fraction of the undesired enantiomer from the eutectic composition of 0.4. They are also shown in Figure 3.1 and serve as the optimal/nominal operating point for the dynamic analysis studied in the next section. The robust design parameters are given in Table 3.1. The procedure has been repeated for both the extract as well as raffinate.

3.1.2 Extract configuration

In order to study the process dynamics, a standard SMB pump configuration is applied (see e.g. [62]). Figure 3.2 shows a combined SMB-crystallization process with a crystallizer at the extract outlet of the SMB unit which is studied in the initial part of this chapter. This is termed as the extract configuration within this thesis. It is worth noting that the direction of the liquid flow in combination with the pump configuration introduces a certain asymmetry. Operational consequences of this asymmetry for the extract configuration will be discussed subsequently. Afterwards, the consequences of this asymmetry on the process dynamics when the crystallizer is

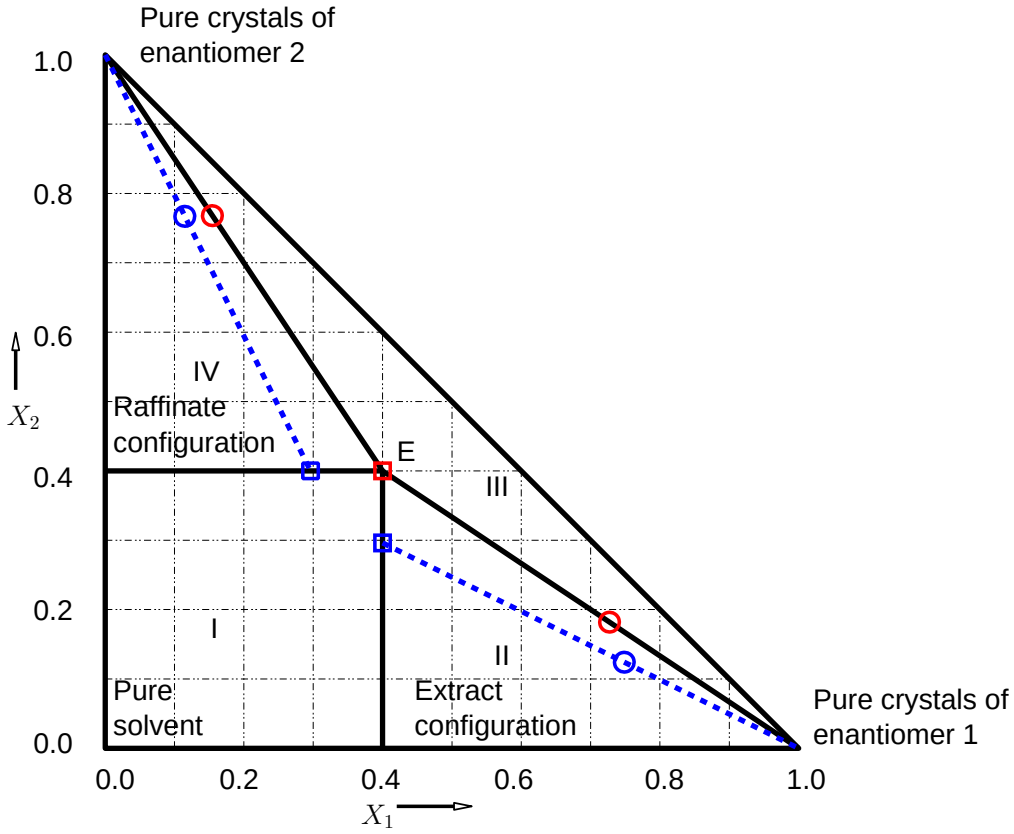

Figure 3.1: Optimal and robust operating points obtained from steady state optimization. Red indicates the optimal operating points and blue shows the robust operating points. ∘ – composition of feed to the crystallizer, □ – composition of the mother liquor. x_i represents the mass fraction of the corresponding enantiomer.

at the raffinate outlet of the SMB will also be treated.

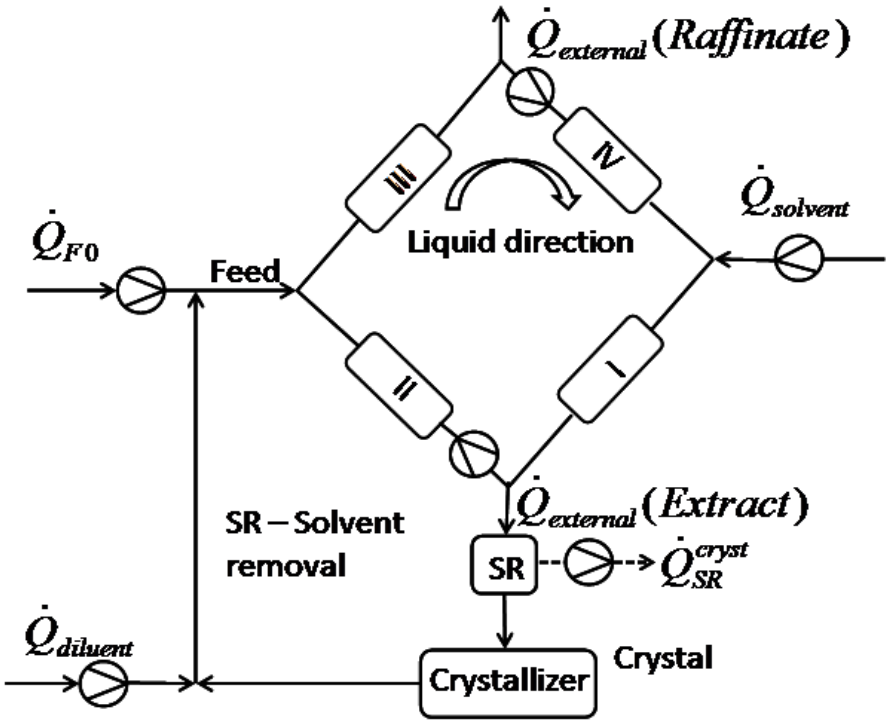

Figure 3.2: Schematic diagram for an SMB-crystallization with a crystallizer at the extract

Two different types of disturbances are investigated, namely step disturbances of the external feed flow rate and of the external feed concentration. Disturbances of the external feed composition show similar effects like external feed concentration and are therefore not explicitly considered. Nominal operating points for the studies within this chapter correspond to the robust design parameters presented in Table 3.1.

Let us first focus on the extract configuration shown in Figure 3.2. In Figure 3.2 $\dot{Q}_{external}(Raffinate)$ denotes the raffinate flow rate which is given by $\dot{Q}_3$ - $\dot{Q}_4$. Figure 3.3 shows the effect of positive disturbances of the external feed concentration with +5, +10 and +17.5% of magnitude. Figure 3.3(a) shows the mass flow rate of crystals out of the crystallizer of the desired (thick lines) and the undesired enantiomer (thin lines). Initially, only the desired enantiomer is crystallized. Due to the robust design, i.e. the design of Table 3.1, the process can tolerate a small disturbance of +5% of the external feed concentration without moving to the three phase region and crystallizing the undesired enantiomer. In contrast to this, the larger disturbances of +10 and +17.5% lead to the crystallization of the undesired enantiomer and loss of the product specifications. In addition, for the largest disturbance of 17.5%, stability

is lost, leading to self sustained oscillations located entirely in the three phase region. A more detailed analysis revealed, that in this case, stability is lost through a Hopf bifurcation [63].

The effect on the flow rates illustrated in Figure 3.3(b) and (c) is less pronounced. This is a direct consequence of the type of disturbance and a consequence of the pump configuration of the SMB unit illustrated in Figure 3.2. It must be noted that this pump configuration implies that the extract flow rate is implicitly fixed. As a consequence the recycle rate is almost constant. Changes in the flow rates of the SMB unit are transmitted directly to the raffinate flow rate. This is even more obvious regarding disturbances of the external feed flow rate to be discussed below.

Step disturbances of the external feed concentration in the negative direction were also examined. For a decrease of the feed concentration from the nominal value, the process moved further into the two phase region, which was therefore not critical and is not discussed any further.

Figure 3.4 shows the effect of disturbances of the external feed flow rate by -5, -10 and -33%. As explained above, the recycle flow rate is almost constant as a consequence of the pump configuration. Changes of the external feed flow rate are directly transmitted to the raffinate outlet and therefore have only a moderate effect on the product purities of the SMB unit as illustrated in Figure 3.4(d) and in turn also a moderate effect on the operation of the crystallizer. Only for a very large disturbance of the external feed flow rate of -33%, small amounts of undesired enantiomer are crystallized as illustrated in the zoom of Figure 3.4(a).

Disturbances of the external feed flow rate in the positive direction were found to be even less critical.

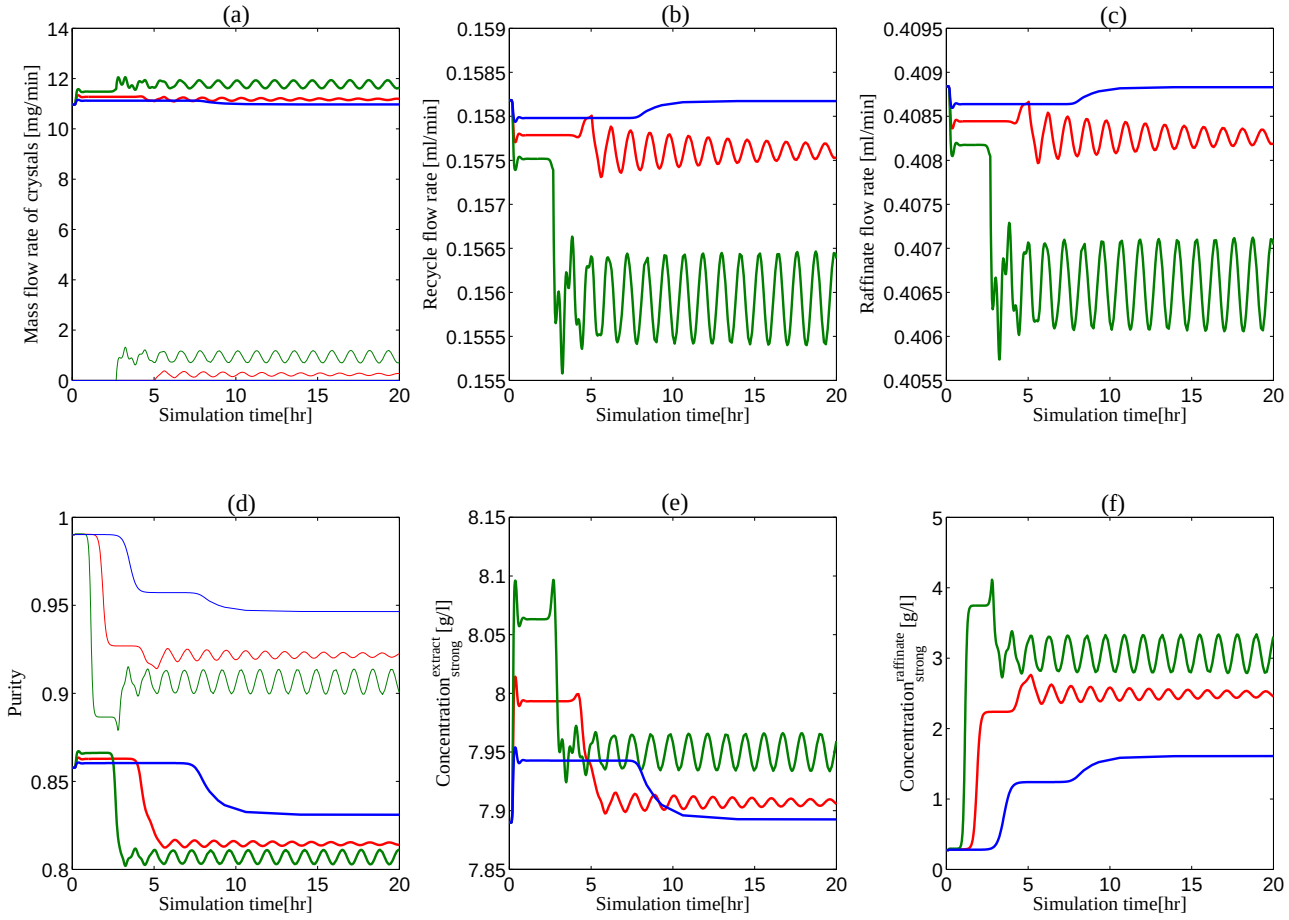

Figure 3.3: Effect of step disturbances of the external feed concentration for a crystallizer at the extract. Blue is for +5% disturbance, red is for +10% and green is for +17.5%. Thick lines in the figure (a) denote the crystals of the enantiomer 1 and thin lines in figure (a) denote crystals of the enantiomer 2. Thick lines in the figure (d) represent the extract purities and thin lines in the figure (d) represent the raffinate purities.

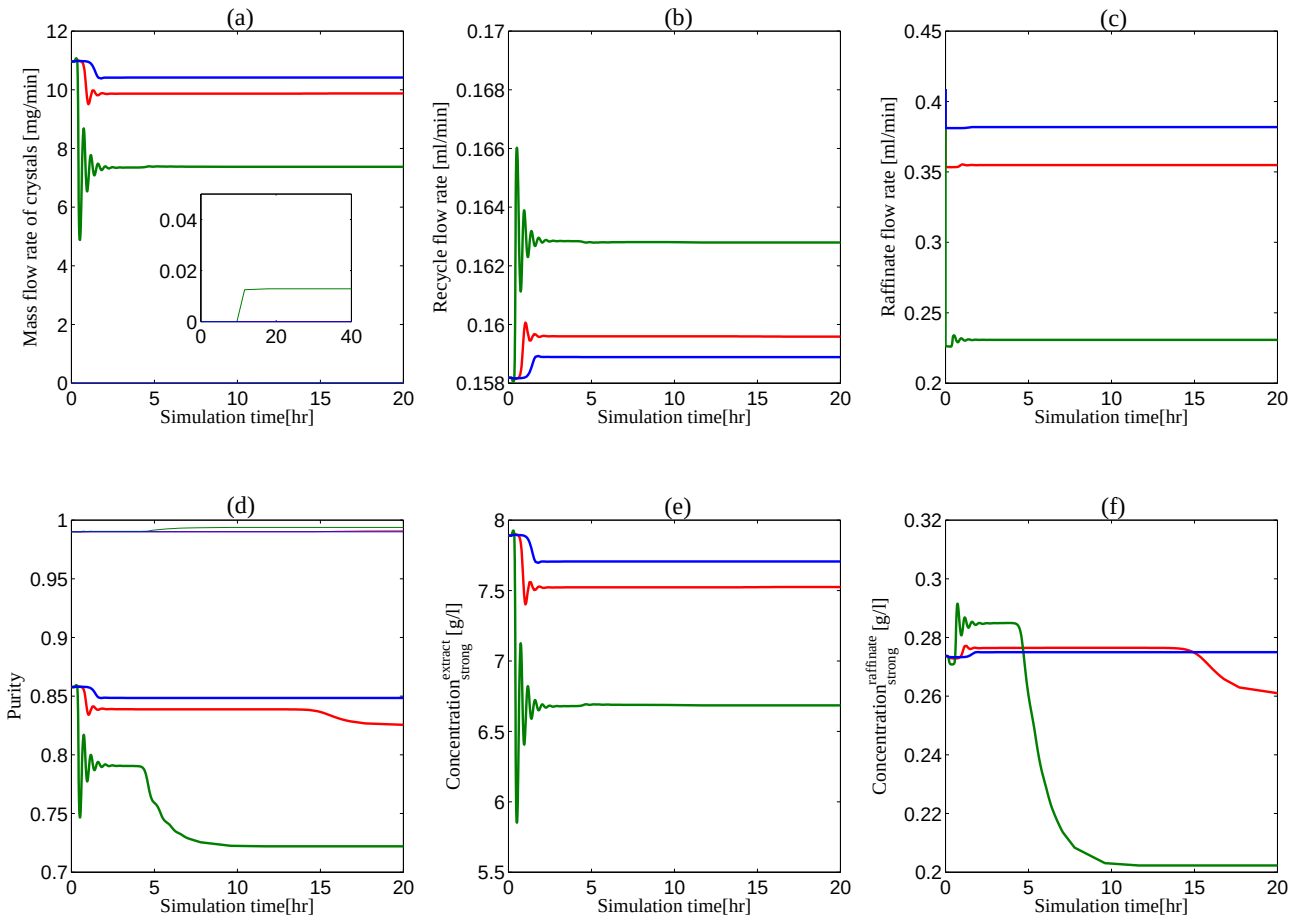

Figure 3.4: Effect of step disturbances of the external feed flow rate for a crystallizer at the extract. Blue is for -5% disturbance, red is for -10% and green is for -33%. Meaning of the thick and the thin lines in figures (a) and (d) is as in Figure 3.3.

3.1.3 Raffinate configurations

Next, discussion is extended to an SMB-crystallization process with a crystallizer at the raffinate outlet of the SMB unit. In a first step a pump configuration according to Figure 3.2 is also applied to the raffinate configuration (configuration 1). Due to this pump configuration flow rate as well as the composition of the raffinate stream may change. This makes this configuration much more sensitive to disturbances of the external feed concentration as well as to the disturbances of the external feed flow rate compared to the process configuration with a crystallizer at the extract of the previous section. The amount of solvent removed from the system ($\dot{Q}_{SR}^{cryst}$) remains constant irrespective of the changes on the raffinate stream flow rate.

Figure 3.5 illustrates the open loop dynamics for a positive (+20% red)and a negative (-12.5%, blue) step disturbance of the external feed concentration. In general, a larger sensitivity to negative disturbances was observed. However, in contrast to the extract configuration, for both, the positive and negative disturbance, formation of crystals of undesired enantiomer is observed in Figure 3.5. This is due to changes of the composition and the flow rates in the recycle loop and their mutual interaction. In contrast to the extract configuration, no oscillations were observed for the raffinate configuration.

Due to the specific pump configuration, sensitivity with respect to the disturbances of the external feed flow rate is even more pronounced. This is illustrated in Figure 3.6 for small disturbances of about $\pm 0.5\%$, which have already large effects, especially on the raffinate flow rate. For the positive disturbance (red lines in Figure 3.6), the raffinate flow rate is decreased. Since the solvent removal rate is fixed, this causes a shift to the three phase region leading to the formation of crystals of an undesired enantiomer. For the negative disturbance (blue lines in Figure 3.6), the raffinate flow rate is increased significantly and the process is shifted towards the single phase region (region I in the Figure 3.1) leading to a drastic reduction in crystals of the desired enantiomer.

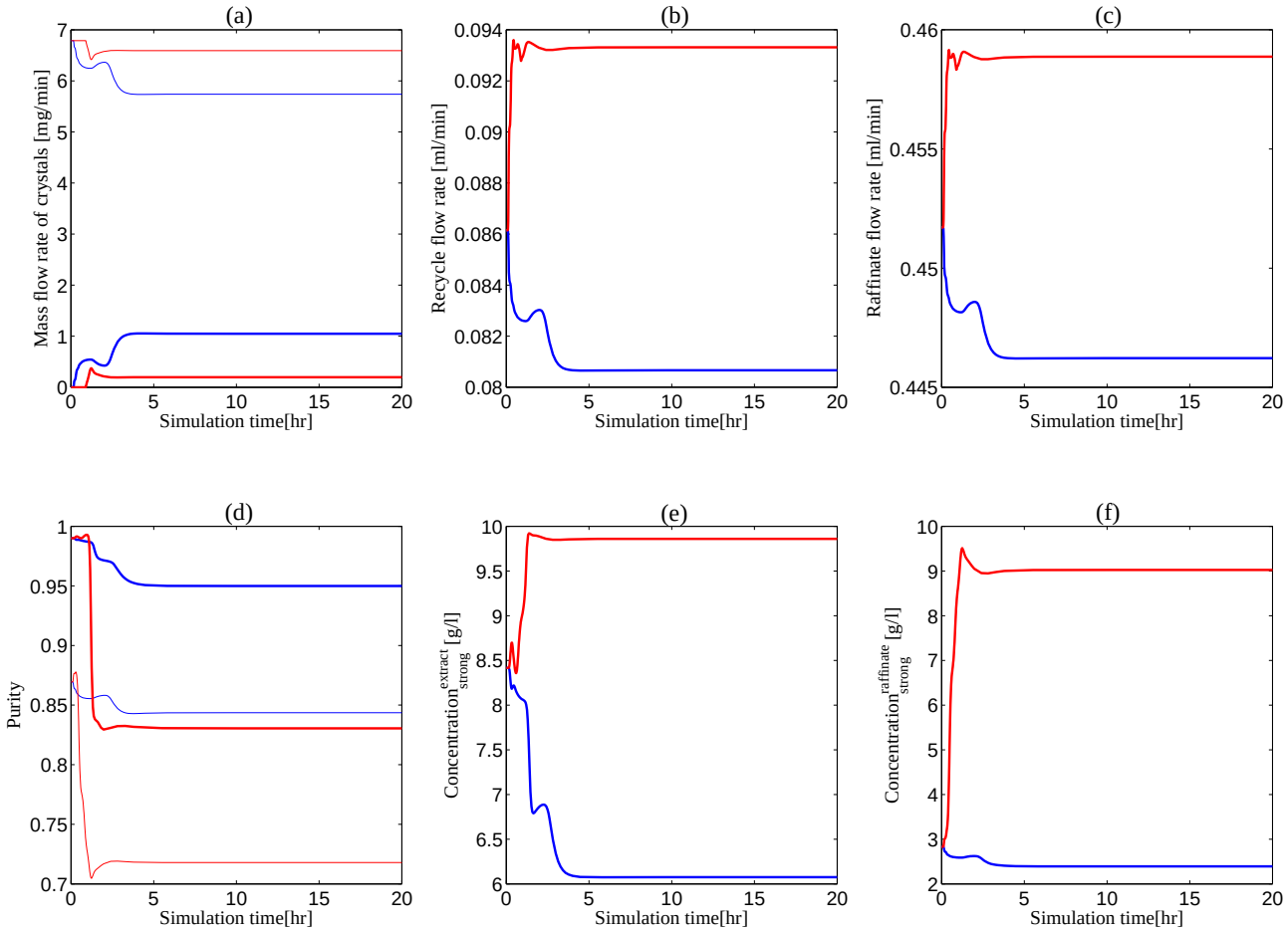

Figure 3.5: Effect of step disturbances of the external feed concentration for a crystallizer at the raffinate (configuration 1). Red is for +20% disturbance and blue is for -12.5%. Meaning of the thick and the thin lines in figures (a) and (d) is as in Figure 3.3.

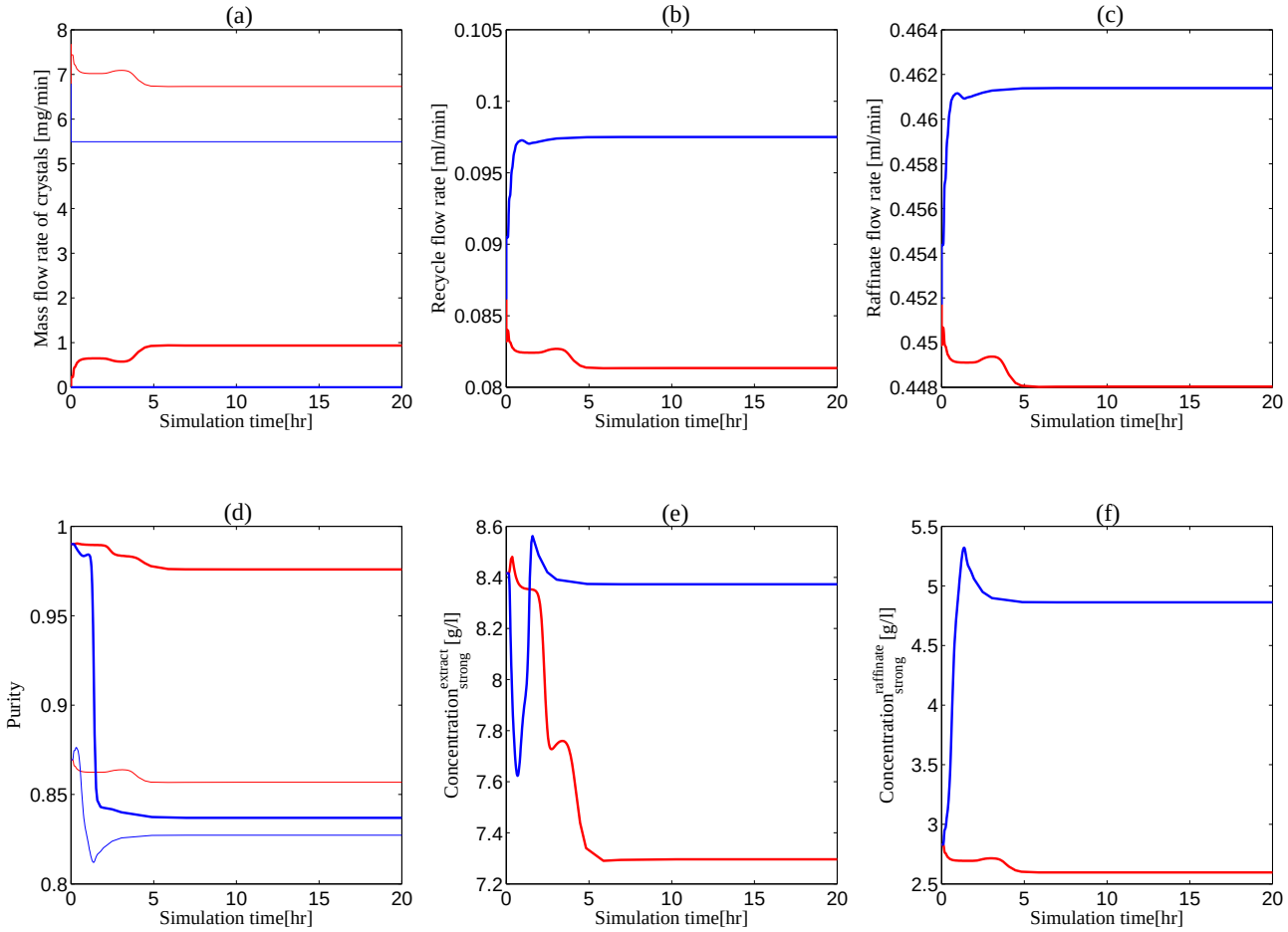

Figure 3.6: Effect of step disturbances of the external feed flow rate for a crystallizer at the raffinate (configuration 1). Blue is for -0.5% disturbance and red is for + 0.5%. Meaning of the thick and the thin lines in figures (a) and (d) is as in Figure 3.3.

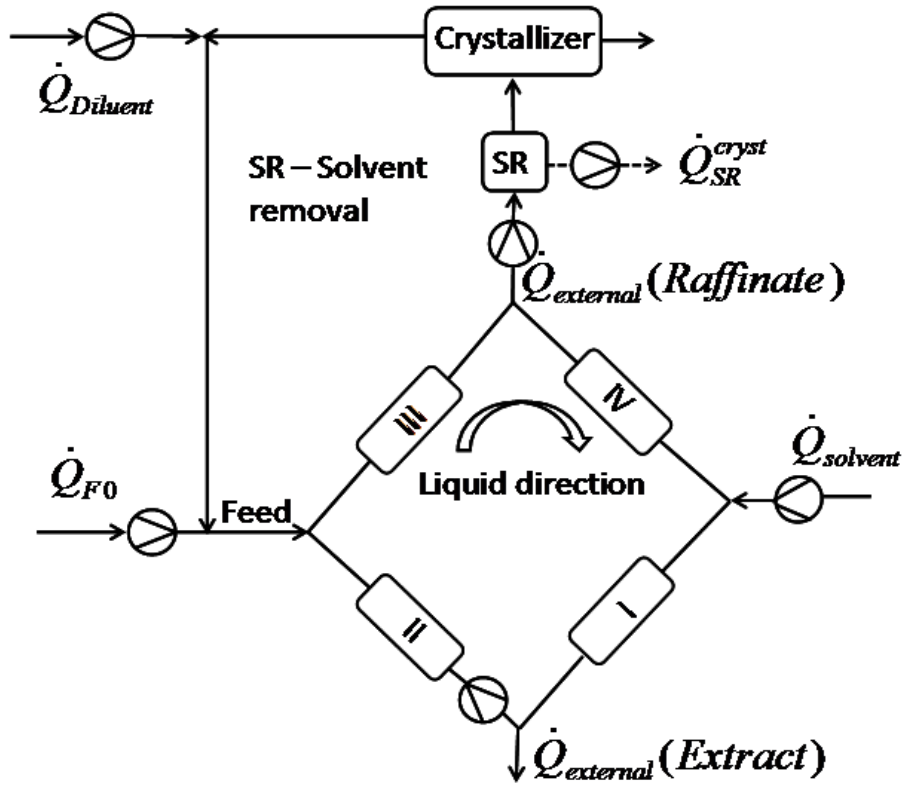

Figure 3.7: Schematic diagram for the alternative raffinate configuration (configuration 2)

This high sensitivity to disturbances of the raffinate configuration can easily be rectified by adapting the pump configuration to fix the raffinate instead of the extract flow rate. One corresponding alternative pump configuration (configuration 2) is shown in Figure 3.7. For validation, the open loop dynamics for disturbances of the external feed flow rate with the alternative pump configuration are illustrated in Figure 3.8. From Figure 3.8 we conclude that the alternative configuration can tolerate much larger disturbances ($\pm$ 7.5% in Figure 3.8 compared to $\pm$ 0.5 % in Figure 3.6) without the formation of crystals of the undesired enantiomer and achieves a similar performance like the extract configuration in Figure 3.2. Nevertheless, tolerable disturbances are of course limited, underlining the necessity of control which is discussed in the next section.

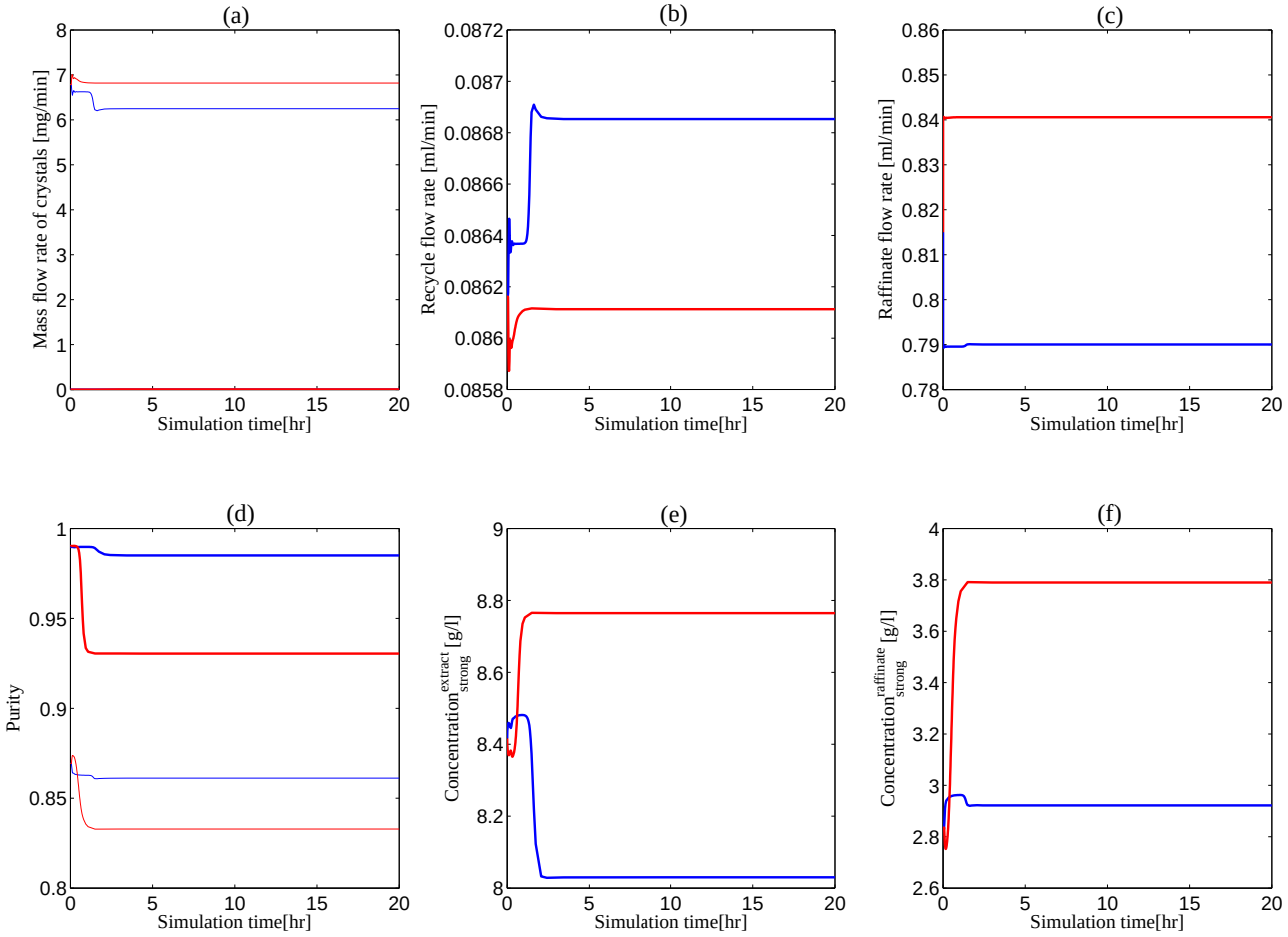

Figure 3.8: Effect of step disturbances of the external feed flow rate for a crystallizer at the raffinate (configuration 2). Blue represents -7.5% disturbance and red represents +7.5% disturbance. Meaning of the thick and the thin lines in figures (a) and (d) is as in Figure 3.3.

3.2 Feedback control

In this section, suitable plantwide control concepts for SMB crystallization processes are introduced. The focus is on the extract configuration illustrated in Figure 3.2. It should be noted, however, that analogous concepts can be applied to the raffinate configuration. For the latter, the modified pump arrangement i.e. configuration 2 according to Figure 3.7 should be used.

The main objective of the control is to guarantee high purity of the crystalline product from the crystallizer also in the presence of unforeseen disturbances. This in turn requires that the feed to the crystallizer has to stay all the time in the corresponding two phase region of the phase diagram. In case of the extract configuration in Figure 3.2, which will be discussed below, this is region II in Figure 3.1.

The aim of the control can be achieved via different approaches. A straight forward approach would be to directly control the purity in the extract outlet of the SMB plant by manipulating the corresponding flow rates. For this, different control concepts have been developed during the last years as briefly summarized in Chapter 1. However, easier options are available for the coupled SMB-crystallization process considered within this chapter. Instead of controlling the SMB plant, crystallizer operation can be manipulated directly by controlling the amount of solvent removed or added to the system (Figure 3.2). In a first step, the solvent removal between the SMB unit and the crystallizer (unit SR in Figure 3.2) is considered as a manipulated variable. As a second option, solvent addition after the crystallizer is briefly discussed as a manipulated variable. In both cases, the measured variable is the mass fraction of the weaker adsorbing component in the crystallizer outlet, which is directly related to the location of the feed to the crystallizer according to Figure 3.1. This quantity could be measured relatively easily online using a combination of a UV detector and a polarimeter.

For both control concepts discussed before, simple PI controllers are used. The controller tuning was performed using the step response method by Ziegler and Nichols [64]. However, any other tuning method for single input single output linear systems could be applied including auto tuning methods [65]. The controller parameters are provided in Table 3.2

The performance of this simple control concept is displayed in the Figures 3.9 through 3.11 for some characteristic disturbances used already in the previous section. All of these figures give a direct comparison between the open loop dynamics (red lines) and the closed loop dynamics (blue lines). Figures 3.9 and 3.10 are for step

Table 3.2: Controller parameters for an SMB-extr.crys process

Parameters	Value
$K_c[min/ml]$	0.82
$\tau_I[min]$	15.0

disturbances of the external feed concentration of +10 % and +17.5 %, respectively. Figure 3.11 is for a step disturbance of the external feed flow rate of -33 %. In all of these cases without control, formation of crystals of the undesired enantiomer is observed and the product specifications are lost. In all cases with control, the formation of crystals of the undesired enantiomer can be avoided leading to pure product at all times. In addition, for a +17.5 % disturbance of the external feed concentration in Figure 3.10 the process is stabilized and any undesired oscillatory behavior is eliminated by proper feed back control. In summary, it is concluded that the proposed control concept is simple but powerful and fully serves the purpose.

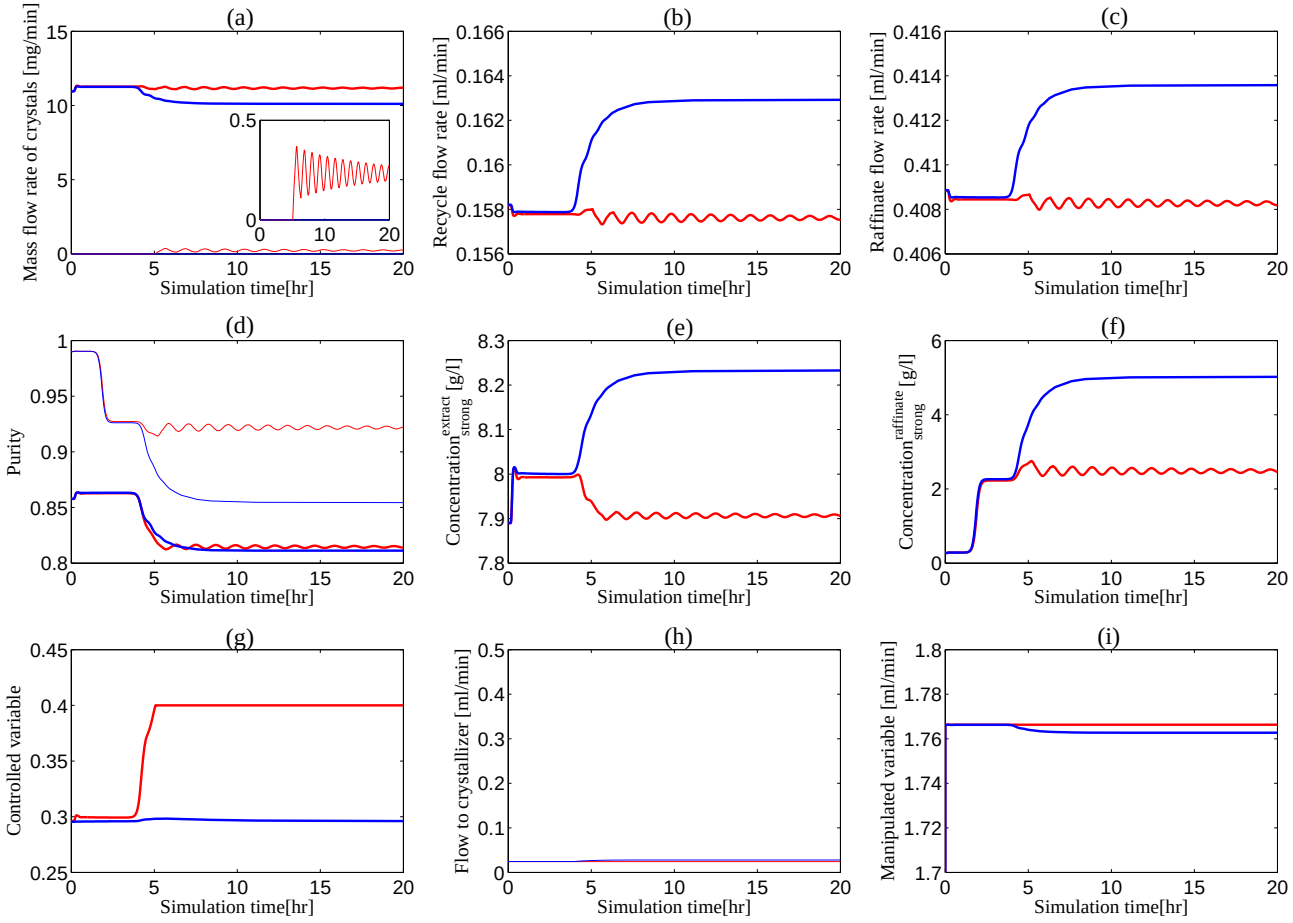

Figure 3.9: Comparison of open loop and closed loop process behavior for a step disturbance of +10.0% of the external feed concentration for a crystallizer at the extract. Blue represents the process with SR control and red represents the uncontrolled process. Meaning of the thick and the thin lines in figures (a) and (d) is as in Figure 3.3.

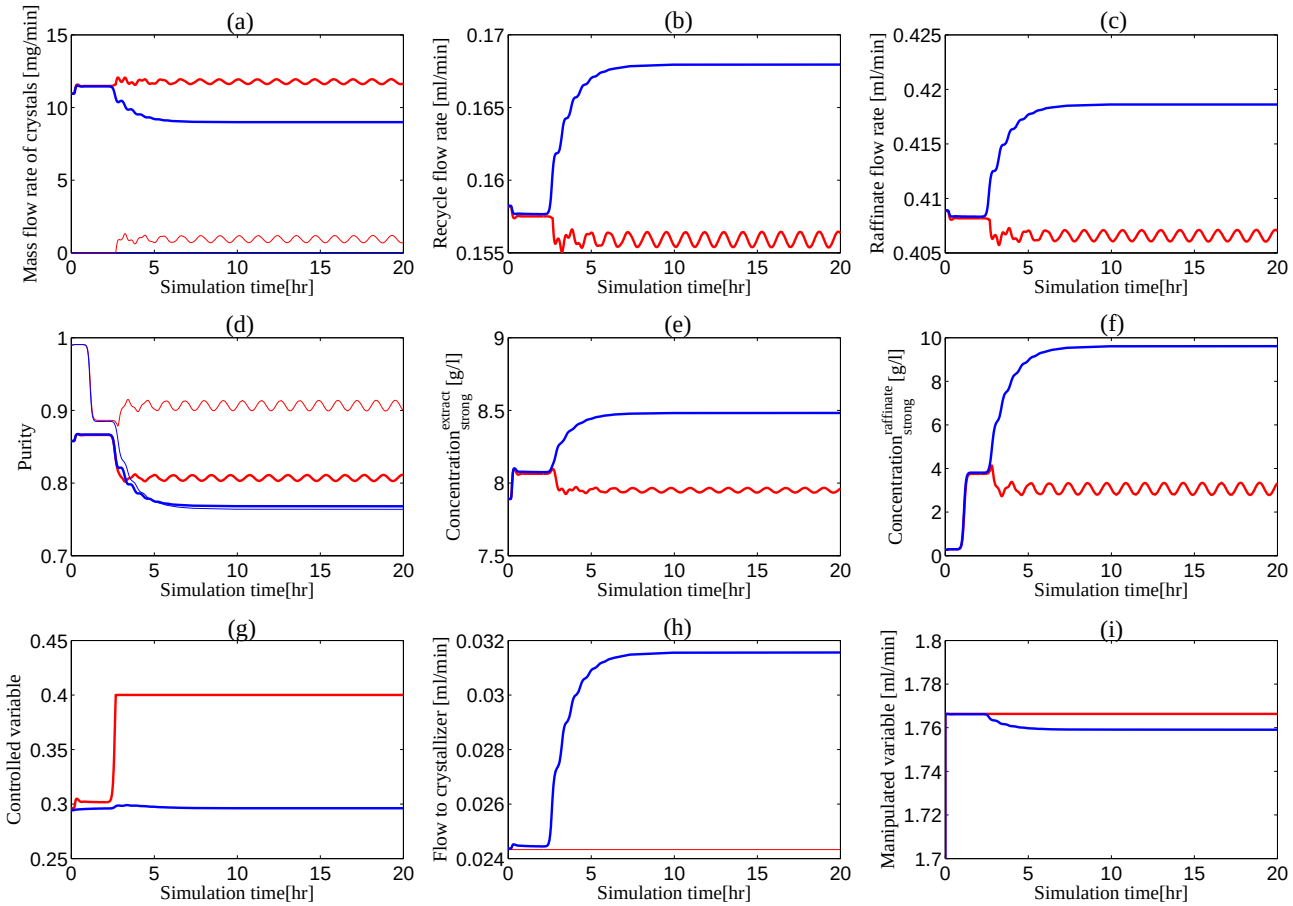

Figure 3.10: Comparison of open loop and closed loop process behavior for a step disturbance of +17.5% of the external feed concentration for a crystallizer at the extract. Blue represents the process with SR control and red represents the uncontrolled process. Meaning of the thick and the thin lines in figures (a) and (d) is as in Figure 3.3.

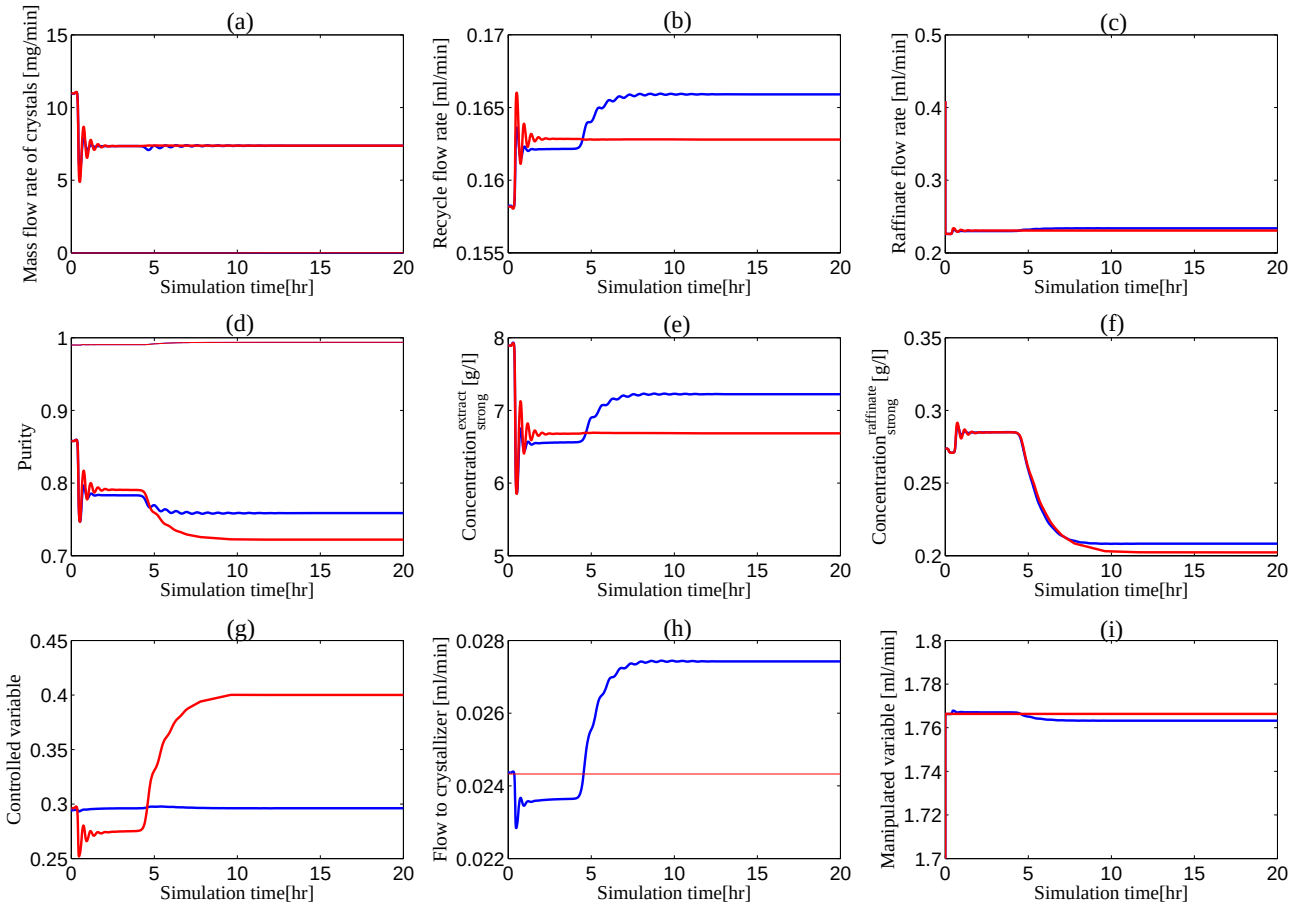

Figure 3.11: Comparison of open loop and closed loop process behavior for a step disturbance of -33% of the external feed flow rate for a crystallizer at the extract. Blue represents the process with SR control and red represents the uncontrolled process. Meaning of the thick and the thin lines in figures (a) and (d) is as in Figure 3.3.

The results in the Figures 3.9 to 3.11 have been obtained with a quasi-static model of the crystallizer. To check the influence of finite crystallizer dynamics, an extended version of this simple model with finite dynamics has also been implemented. The corresponding model equations are given in the Appendix C. The results of the open and closed loop dynamic investigations with finite crystallizer dynamics are also provided in the Appendix C. There it is shown that the simple control concept introduced with a quasistatic crystallizer model can be directly applied to finite crystallizer dynamics if the controller parameters are adjusted accordingly (see table C.1).

As mentioned earlier, instead of manipulating the amount of solvent which is removed from the extract before being fed to the crystallizer, also the amount of solvent added to the system after the crystallizer ($\dot{Q}_{Diluent}$) could be used as a manipulated variable. In principle, this also works. However, since the crucial influence on the crystallizer operation has an additional lag introduced by the SMB unit, performance of this second control structure is not as good as with the first control structure. During the transients some temporary formation of undesired crystals was observed.

3.3 Summary

This chapter discussed the dynamics and control of SMB crystallization processes. The main control objective is to restrain the process operation within the corresponding two phase region of the SLE thus ensuring a pure crystalline product. For this purpose, the optimal design of the previous chapter had to be relaxed giving rise to a so called robust design. The effect of disturbances on the "robust design" was analyzed. It was observed that due to the asymmetry introduced by the direction of the fluid flow in the SMB unit, an appropriate pump configuration turned out to be crucial to avoid high sensitivity to disturbances, especially of the external feed flow. From the investigations, it was recognized that the outlet flow rate of the SMB unit coupled to the crystallizer should be fixed to limit the variation of the flow rates in the recycle loop. This is in agreement with standard rules for plantwide control of multi-unit chemical process with recycle [66]. Nevertheless, for larger disturbances, the product purities could not be kept within the required specification. Therefore, a feedback control based on manipulating the solvent removed or added to the system was developed as a simple alternate option to standard complicated SMB control.

In the following chapter, we evaluate the dynamics of a second hybrid process combination, namely SMB-racemization.

Chapter 4

Dynamics and control of SMB-racemization processes

In the previous chapter, the effect of disturbances of the external feed on the operability and process dynamics of SMB-crystallization process were studied. Although some extra safety margins were introduced leading to a so called robust design, the magnitude of tolerable disturbances was limited and some simple plant wide control strategies were developed to compensate such disturbances. In the present chapter, the investigation of dynamics and operability is extended to SMB-racemization processes. Since dynamics and controllability crucially depends on the kinetics of the chemical reaction, two different case studies are considered

- slow reaction with $k_{forward}V_{reac} = 0.1$ and moderate product purity of 90%
- fast reaction with $k_{forward}V_{reac} = 100000$ and high product purity of 99%

Adsorption isotherms are taken from the PDE system according to Appendix A.

4.1 Slow reaction kinetics and moderate purities

In this section, focus is on the first case study with slow racemization kinetics and moderate product purity requirements. Figure 4.1 shows the schematic configuration of the process. Nominal operating points are the optimal design parameters which have been obtained in section 2.2.2 (Table 2.2). The consequence of step disturbances of the external feed concentration and of the external feed flow rate imposed to the nominal operating points have been investigated. In general, any permanent disturbance of the external feed concentration/flowrate will lead to a permanent offset

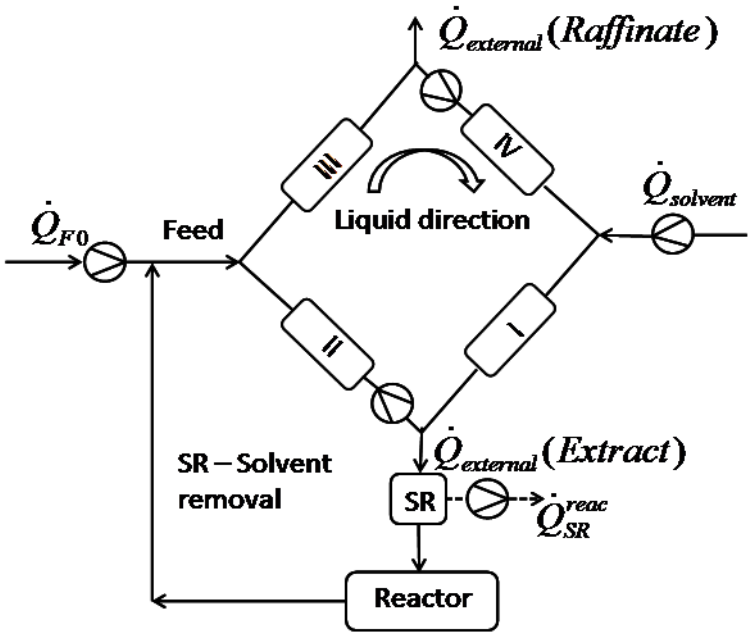

Figure 4.1: Schematic diagram for an SMB-racemization process

of the product purity from its specification. To overcome this problem suitable control strategies are introduced within this chapter step-by-step.

As an initial step, an extension of the control concepts developed previously in chapter 3 for SMB-crystallization processes to SMB-racemization processes is considered. In these concepts, the solvent removal in the recycle loop is used as a manipulated variable and product purity of the raffinate is considered as the controlled variable. Online measurement with reasonable effort is possible for the present class of mixtures by a combination of a UV detector and a polarimeter, for example [67].

4.1.1 Static controllability analysis

To check the feasibility of this control concept, static controllability of the raffinate product purity by means of the solvent removal is investigated using steady state continuation in DIVA [61]. Results are shown in Figure 4.2 for nominal operation and a 5% increase/decrease of the external feed concentration. In all cases the desired steady state purity of 90% can be achieved with some suitable values of the manipulated variable. Due to the maximum of the curves even two different values of the manipulated variable are available in each case, corresponding to an input multiplicity. The solvent removal value which would be adjusted by the control system depends on the controller tuning and/or the initial conditions and does not bother us at this point of the discussion.

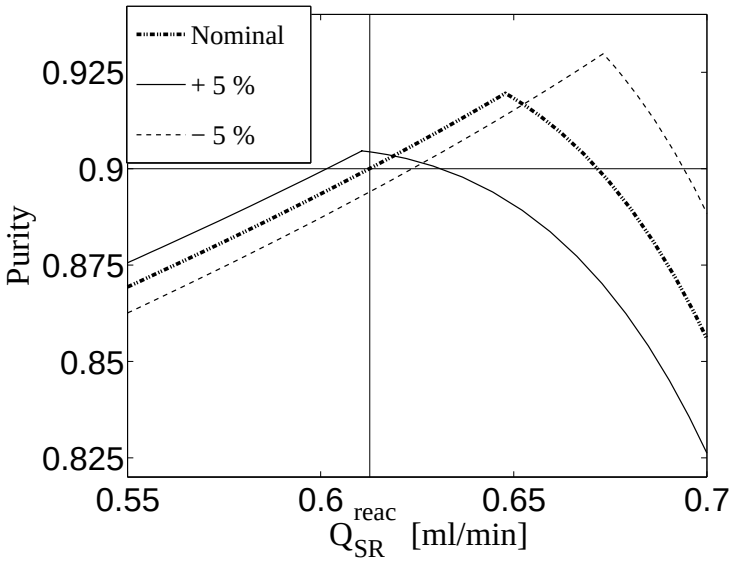

Figure 4.2: Comparison of steady state parameter continuation profiles when subjected to step disturbances of ± 5% of the external feed concentration. The solid lines are for 5%, the dotted lines for nominal and the dashed lines are for -5%. Case study corresponds to slow kinetics

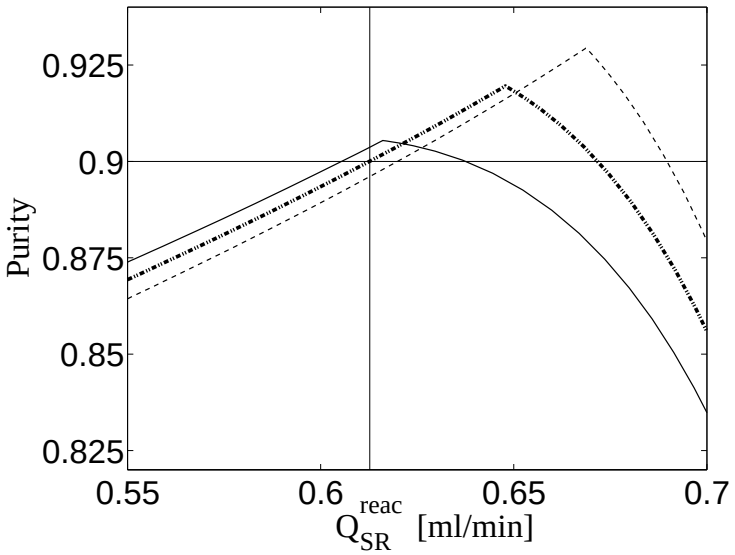

Figure 4.3: Comparison of steady state parameter continuation profiles when subjected to step disturbances of ± 5% of the external feed flow rate. The solid lines are for 5%, the dotted lines for nominal and the dashed lines are for -5%. Case study corresponds to slow kinetics. Nomenclature is same as in Figure 4.2

Table 4.1: Controller parameters for an SMB-extract.racemization process for slow kinetics

Parameters	Value
$K_c[min/ml]$	7.86
$\tau_I[min]$	18.1

Analogous patterns of behavior are illustrated in Figure 4.3 for a ± 5% increase/decrease of the external feed flow rate.

4.1.2 Open loop and closed loop process dynamics

Here, we discuss the results of the dynamic simulation for the process scheme shown in Figure 4.1. The dynamic behavior of the closed loop operation compared to the open loop operation corresponding to the feed concentration disturbances (step disturbance) in Figure 4.2 are shown in Figure 4.4, whereas the feed flow rate disturbances corresponding to Figure 4.3 are shown in Figure 4.5. The open loop step responses are illustrated in Figure 4.4 and Figure 4.5 by the dashed lines. In contrast to the previous chapter, any permanent disturbances lead to a permanent offset of the product purity. Further, from the symmetry of the open loop responses it is concluded that the system is in the linear range. The reason for this is the moderate product purity of the reference point. Further, it is concluded from Figures 4.4 and 4.5 that in closed loop operation the disturbances are well compensated by the control system through readjusting the solvent removal ($\dot{Q}_{SR}^{reac}$). For this purpose, simple PI controllers were used. Controller parameters were calculated by numerical optimization minimizing the integral of the squared controller error. The controller parameters are provided in Table 4.1. The resulting closed loop dynamics is smooth and relatively fast as shown by the solid line in the Figures 4.4 and 4.5 and it is concluded that the proposed control strategy works nicely if the disturbances are not too large.

For a larger disturbance of +7.5%, however, controllability fails for the above design specifications without safety margins as illustrated in Figure 4.6. In this figure, the maximum product purity of the corresponding dashed line is clearly below 90%. This implies that the desired product purity cannot be adjusted anymore by means of the solvent removal rate. To overcome this problem and extend the range of disturbances the control system is able to tolerate, the design is modified. In particular, the process is overdesigned for a product purity of 92% instead of 90%. Modified design parameters are determined with the optimization procedure described in the

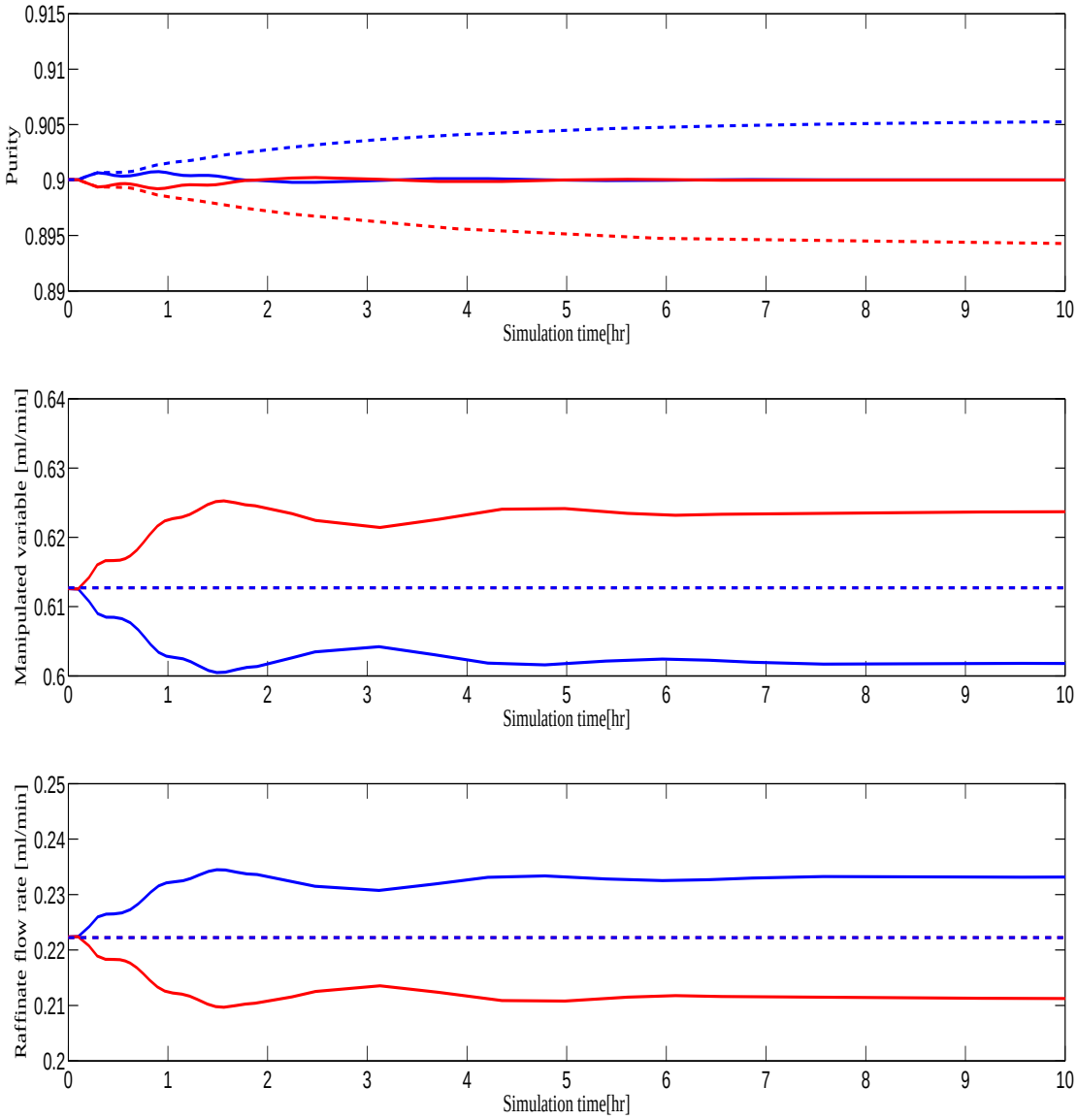

Figure 4.4: Comparison of an open loop and closed loop process for $\pm$ 5 % disturbance of the external feed concentration. The solid lines are for the process with control while the dashed lines are for the process without control. Red is for -5 % while the blue curves are for + 5 %

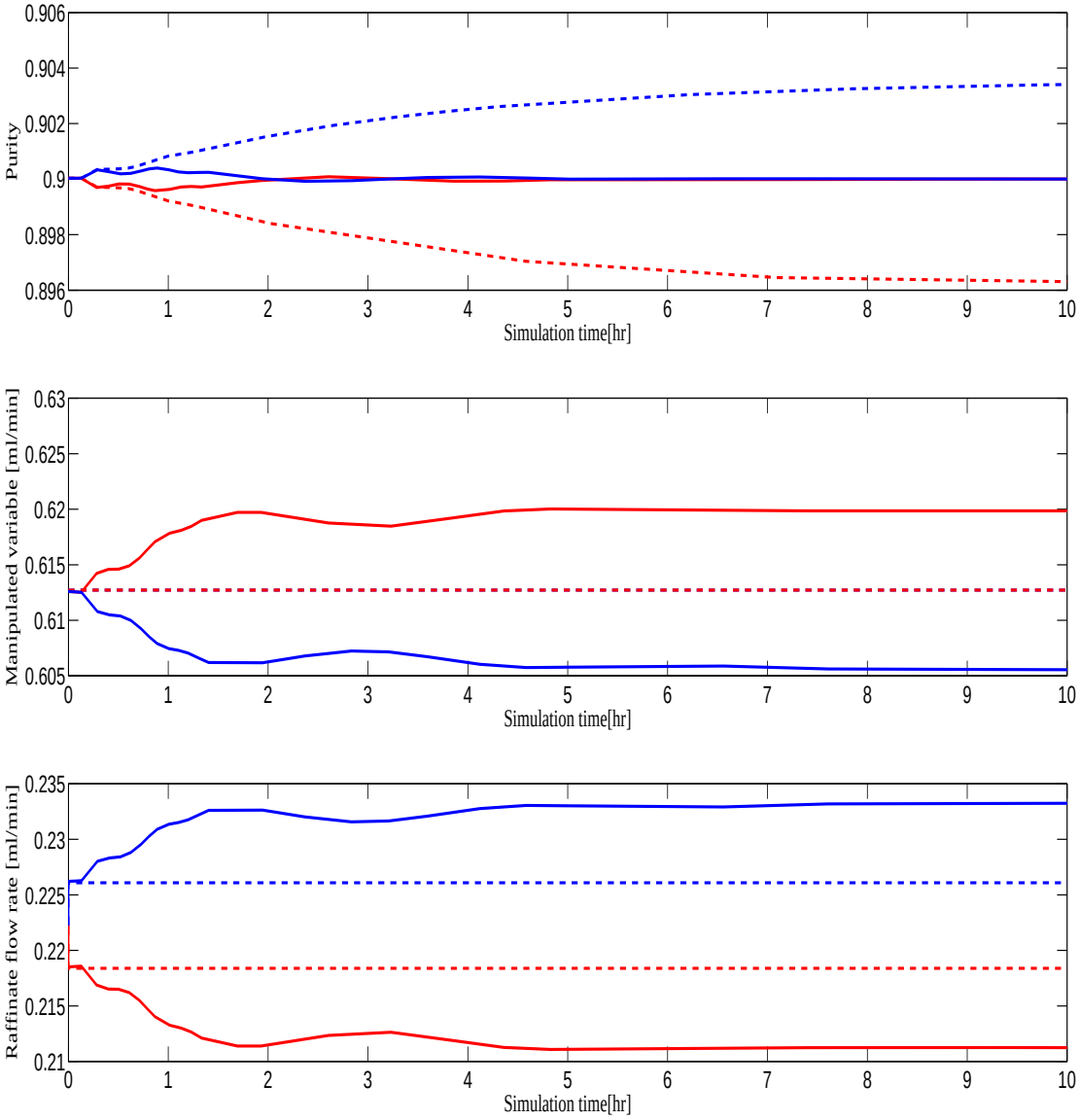

Figure 4.5: Comparison of an open loop and closed loop process for $\pm$ 5 % disturbance of the external feed flow rate. The solid lines are for the process with control while the dashed lines are for the process without control. Red is for -5 % while the blue curves are for + 5 %

Table 4.2: Robust design for an SMB-racemization process with racemization at the extract for slow kinetics

Variables	slow reaction
$\dot{Q}_1[ml/min]$	1.7846
$\dot{Q}_2[ml/min]$	0.25
$\dot{Q}_3[ml/min]$	1.2157
$\dot{Q}_4[ml/min]$	0.9858
$\dot{Q}_{solid}[ml/min]$	1.8696
$\dot{Q}_{SR}^{reac}[ml/min]$	0.6459
$Purity_{coupling}$	83.08
$\dot{Q}_{F_0}[ml/min]$	0.0770

previous chapter. Values are given in Table 4.2. Static controllability of a reference point with 90% purity for a critical increase of the external feed concentration of 7.5% is illustrated in Figure 4.6 with the solid line. The dynamic performance of the closed loop system compared to the open loop dynamics is shown in Figure 4.7 for 7.5% increase/decrease of the external feed concentration. The modified strategy again shows very good characteristics.

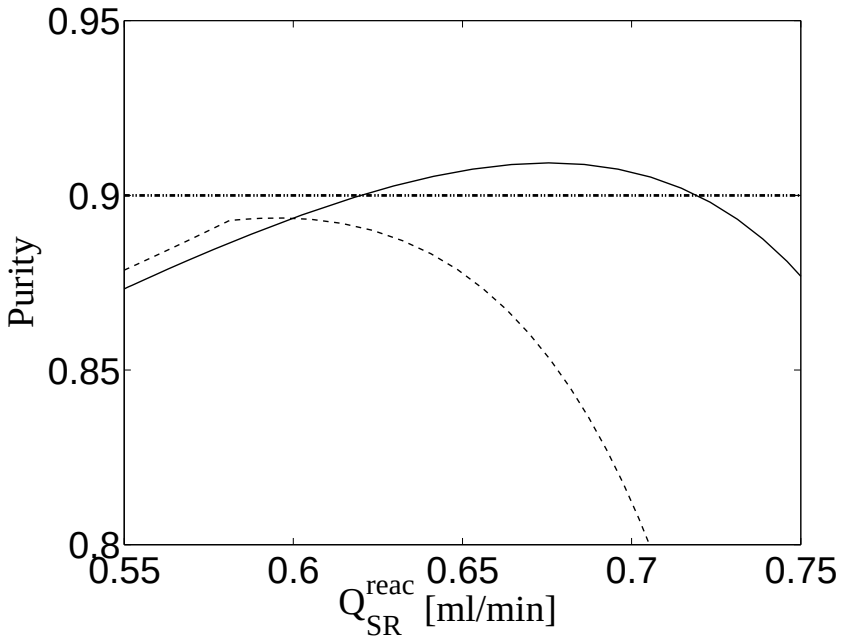

Figure 4.6: Comparison of steady state parameter continuation profiles when subjected to step disturbances of 7.5 % disturbance of the external feed concentration. The solid lines are with a safety margin while the the dashed lines are without safety margin

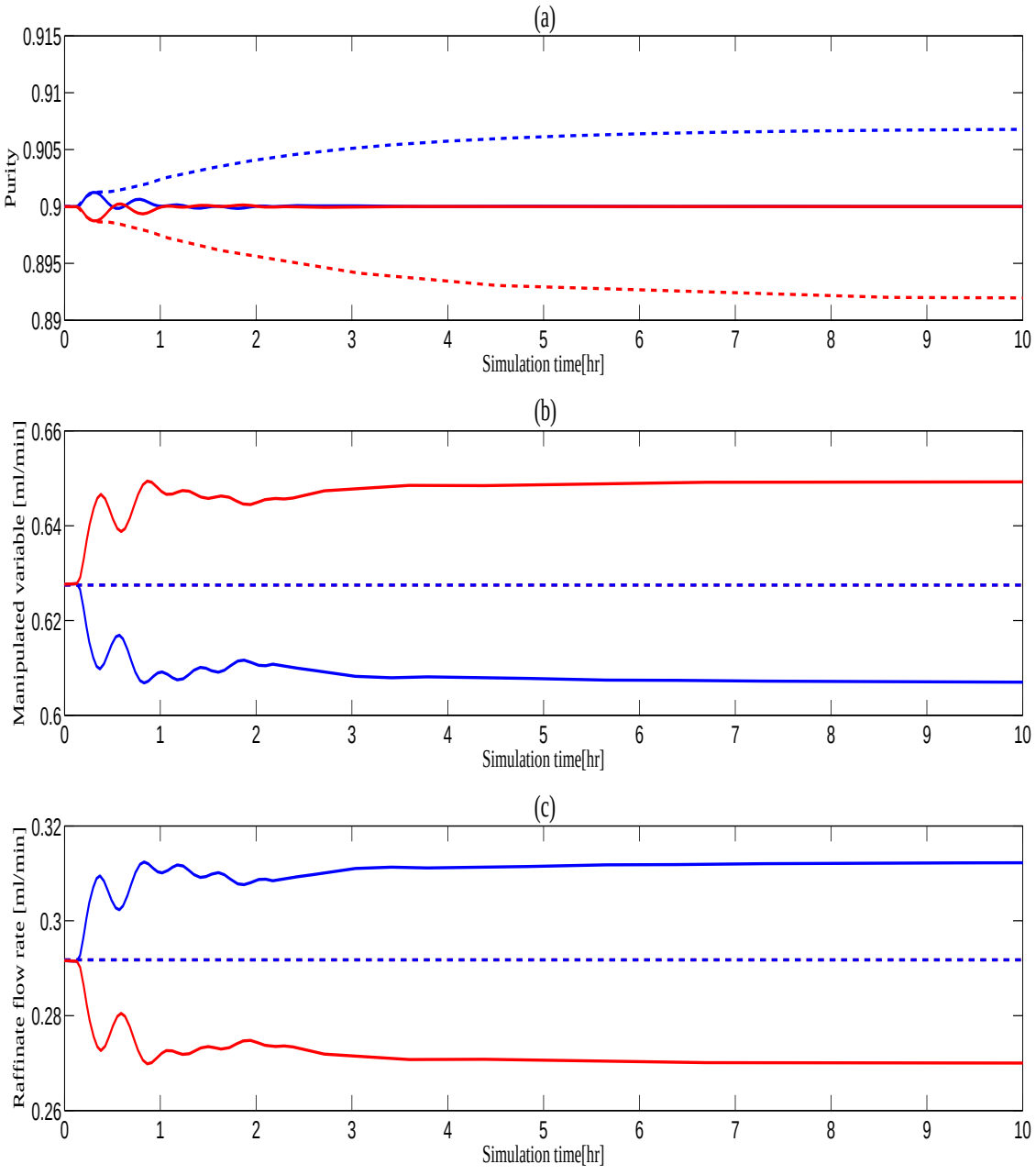

Figure 4.7: Comparison of an open loop and closed loop process for ± 7.5% disturbance of the external feed concentration. The solid lines are for the process with control while the dashed lines are for the process without control. Red is for -5% while the blue curves are for + 7.5%

In summary, we find that the proposed control strategy of manipulating product purity by means of solvent removal is very effective. It can be combined with an over design to also handle large disturbances, if necessary. Results are however for slow racemization kinetics with moderate purity requirement. Influence of fast racemization kinetics with high product purity requirement is analyzed in the next section as the second case study.

4.2 Fast reaction kinetics and high purities

Here, in this section, an increased product purity of 99% and a fast racemization kinetics with $V_{reac}k_{forward} = 100000$ are considered. As in the previous section, the effects of step disturbances of the external feed concentration and of the external feed flow rate applied to the nominal operating points are investigated. Unlike in the previous section, the recycle concentration of both components is almost symmetric and is equal to the external feed concentration which confirms that the process is in the equilibrium regime. Nominal operating points have been obtained in section 2.2.2 and are listed in Table 2.2.

4.2.1 Static controllability analysis

In order to examine if the simple control concept developed in the last section can be applied for fast racemization kinetics with high product purity requirements, a steady state continuation is applied as a first step. Results for the nominal operation compared to a $\pm$ 5% increase/decrease of the external feed concentration are shown in Figure 4.8 for the nominal design corresponding to Table 2.2. It is observed that for the nominal operation (dotted line in Figure 4.8), the maximum value of the curve coincides with the required product purity and that there is no room left for handling disturbances in the positive direction, whereas disturbances in the negative direction are not critical in that respect. Consequently, the control strategy applied to the nominal design is not feasible.

Therefore, following the ideas in the previous section, in a second step, safety margins by means of an overdesign are introduced. In the present case the process was redesigned for a product purity of 99.5% instead of 99%. Parameters are given in Table 4.3. Results of the steady state continuation can be seen in Figure 4.9. Compared to Figure 4.8, the maximum lies now a bit higher than the nominal purity of 99% giving little room to tolerate some disturbances in the positive direction. However, a disturbance of the external feed concentration of 5% which is the solid

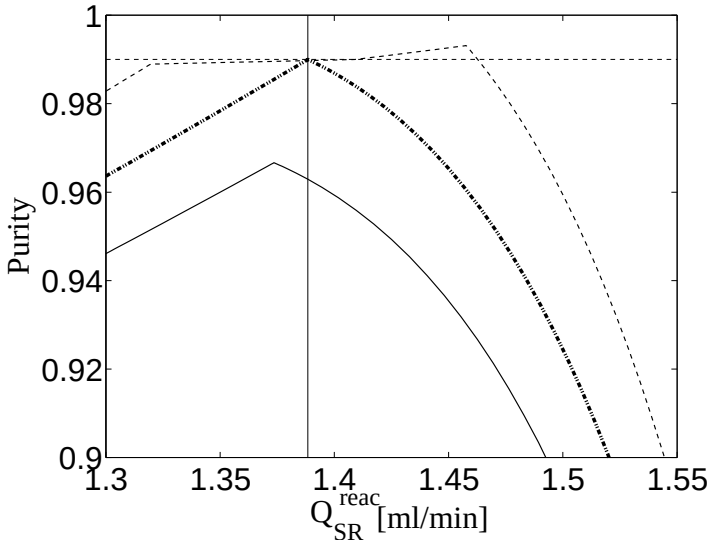

Figure 4.8: Comparison of steady state parameter continuation profiles for nominal, 5%, -5% disturbance of the external feed concentration. The solid lines are for 5%, the dotted lines for nominal and the dashed lines are for -5%. Design without safety margin. Nomenclature same as in Figure 4.2

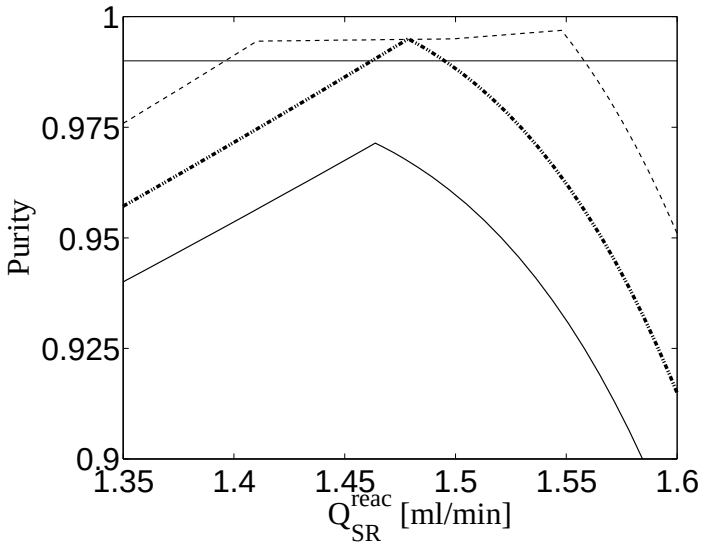

Figure 4.9: Comparison of steady state parameter continuation profiles for nominal, 5%, -5% disturbance of the external feed flow rate. The solid lines are for 5%, the dotted lines for nominal and the dashed lines are for -5%. Design with safety margin. Nomenclature same as in Figure 4.2

line in Figure 4.9 is still clearly out of reach.

Table 4.3: Robust design for an SMB-racemization process with racemization at the extract for fast kinetics

Variables	Fast reaction
$\dot{Q}_1[ml/min]$	2.2728
$\dot{Q}_2[ml/min]$	0.2865
$\dot{Q}_3[ml/min]$	1.0905
$\dot{Q}_4[ml/min]$	0.6830
$\dot{Q}_{solid}[ml/min]$	1.8696
$\dot{Q}_{SR}^{reac}[ml/min]$	1.4787
$Purity_{coupling}$	78.89
$\dot{Q}_{F_0}[ml/min]$	0.2963

Hence, in a last step, alternative handles for controlling the product purity are explored. Results are summarized in Figure 4.10 for a critical increase of the external feed concentration of 5%. Possible handles are indicated by the pumps in Figure 4.1. Besides the solvent removal, flow rates in Zone II, Zone IV and the solvent feed of the SMB plant can be manipulated. From Figure 4.10 it is concluded, that the flow rate in Zone IV is the only choice which works for a 5% increase of the external feed concentration.

4.2.2 Open and closed loop dynamics

The dynamics of the open loop system compared to the corresponding closed loop system is described in Figure 4.11 for a ± 5% change of the external feed concentration. Open loop dynamics show a strong asymmetry of the responses indicating strong nonlinearity for the high product purity requirements. The blue dashed line even shows an inverse response. Nevertheless, closed loop control works very well as indicated by the solid lines. The controller parameters were obtained by numerical optimization of the integral square error. The controller parameters are shown in Table 4.4. Similar patterns of behavior are observed in Figure 4.12 for a ± 5% change of the external feed flow rate confirming the feasibility of the alternative control concept.

Table 4.4: Controller parameters for an SMB-extract.racemization process for fast kinetics

Parameters	Value
$K_c[min/ml]$	8.93
$\tau_I[min]$	15.0

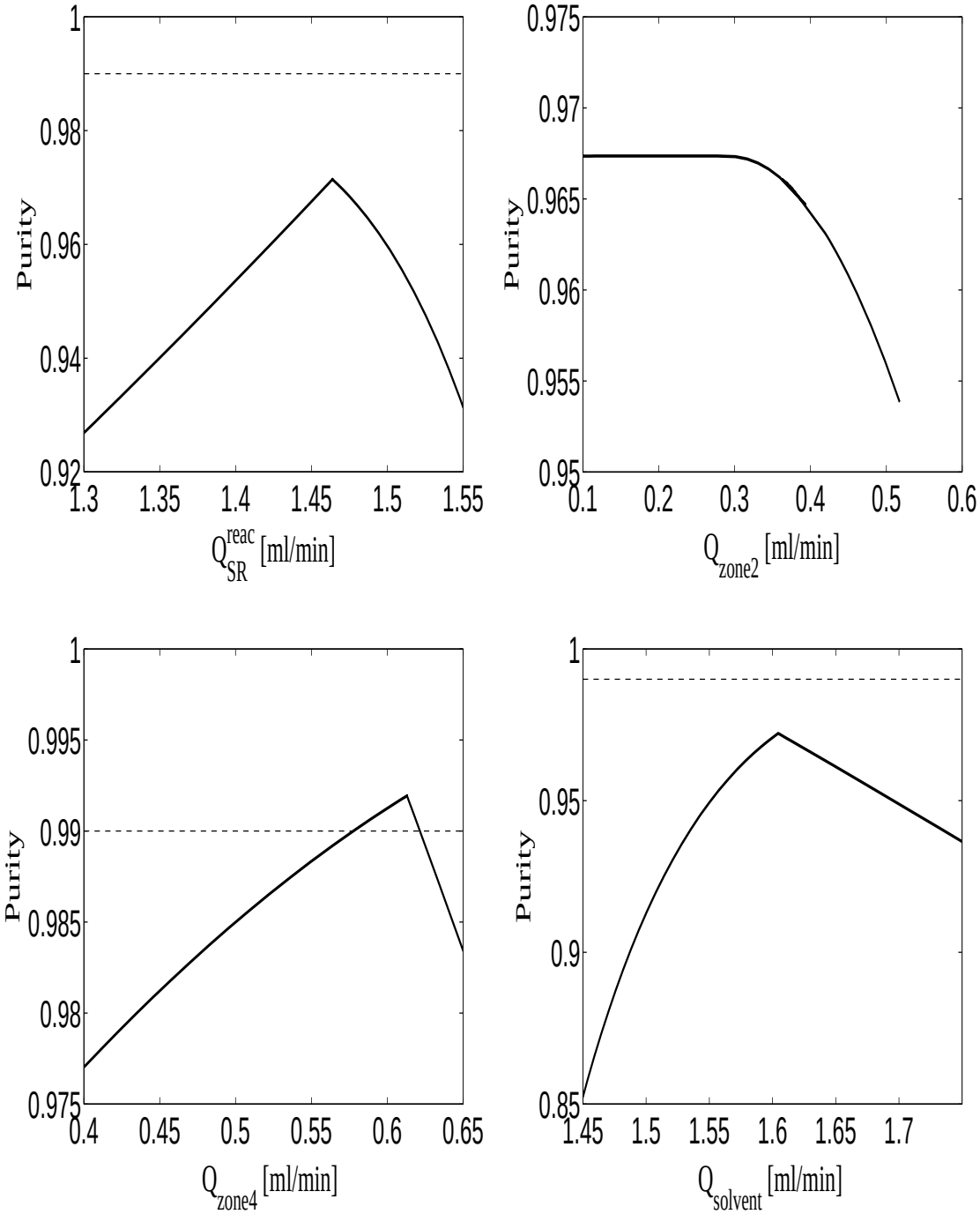

Figure 4.10: Comparison of possible control options for 5% disturbance of the external feed concentration through steady state parameter continuation for fast kinetics

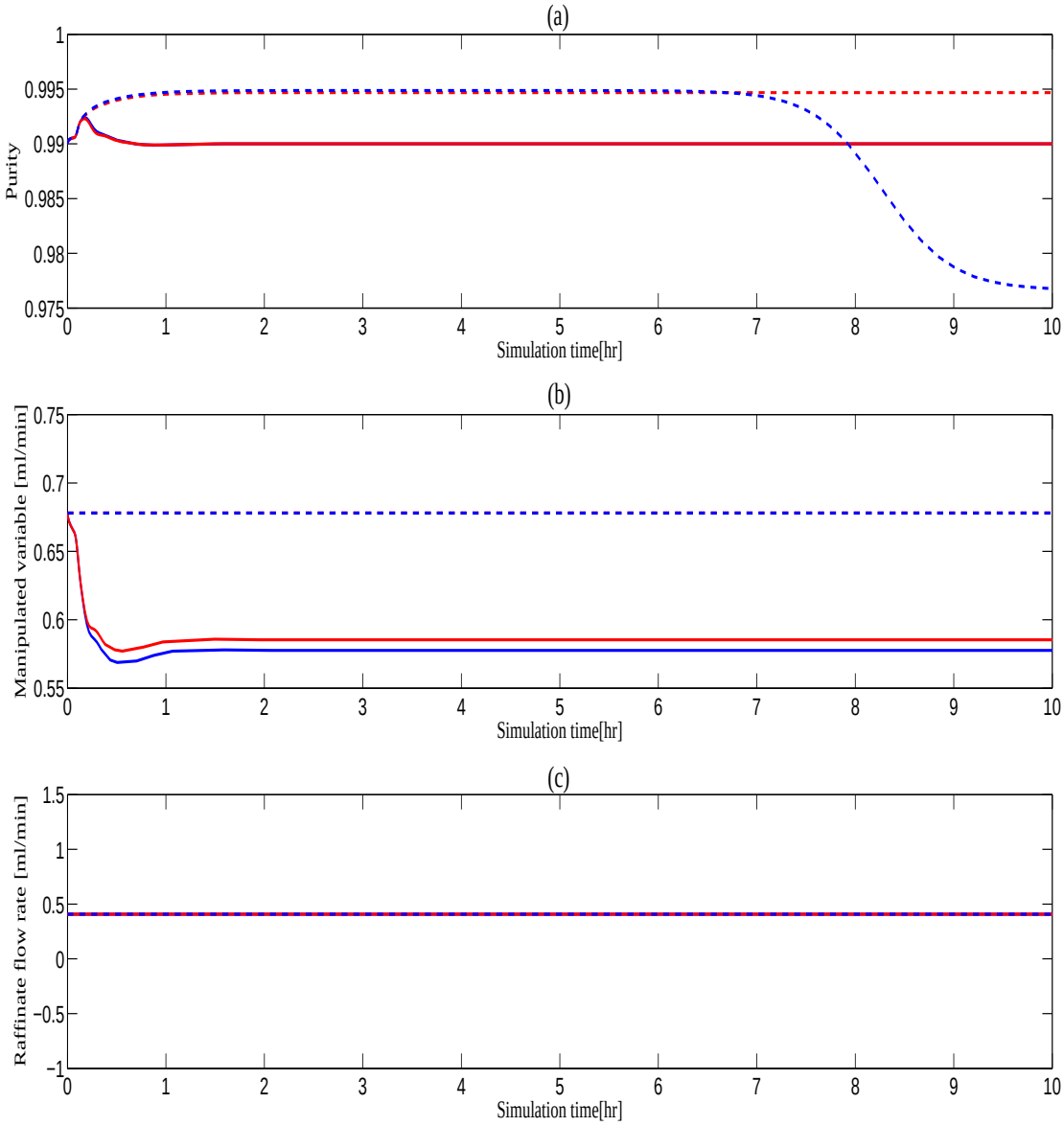

Figure 4.11: Comparison of an open loop and closed loop process for ± 5% disturbance of the external feed concentration. The solid lines are for the process with control while the dashed lines are for the process without control. Red is for -5% while the blue curves are for + 5%

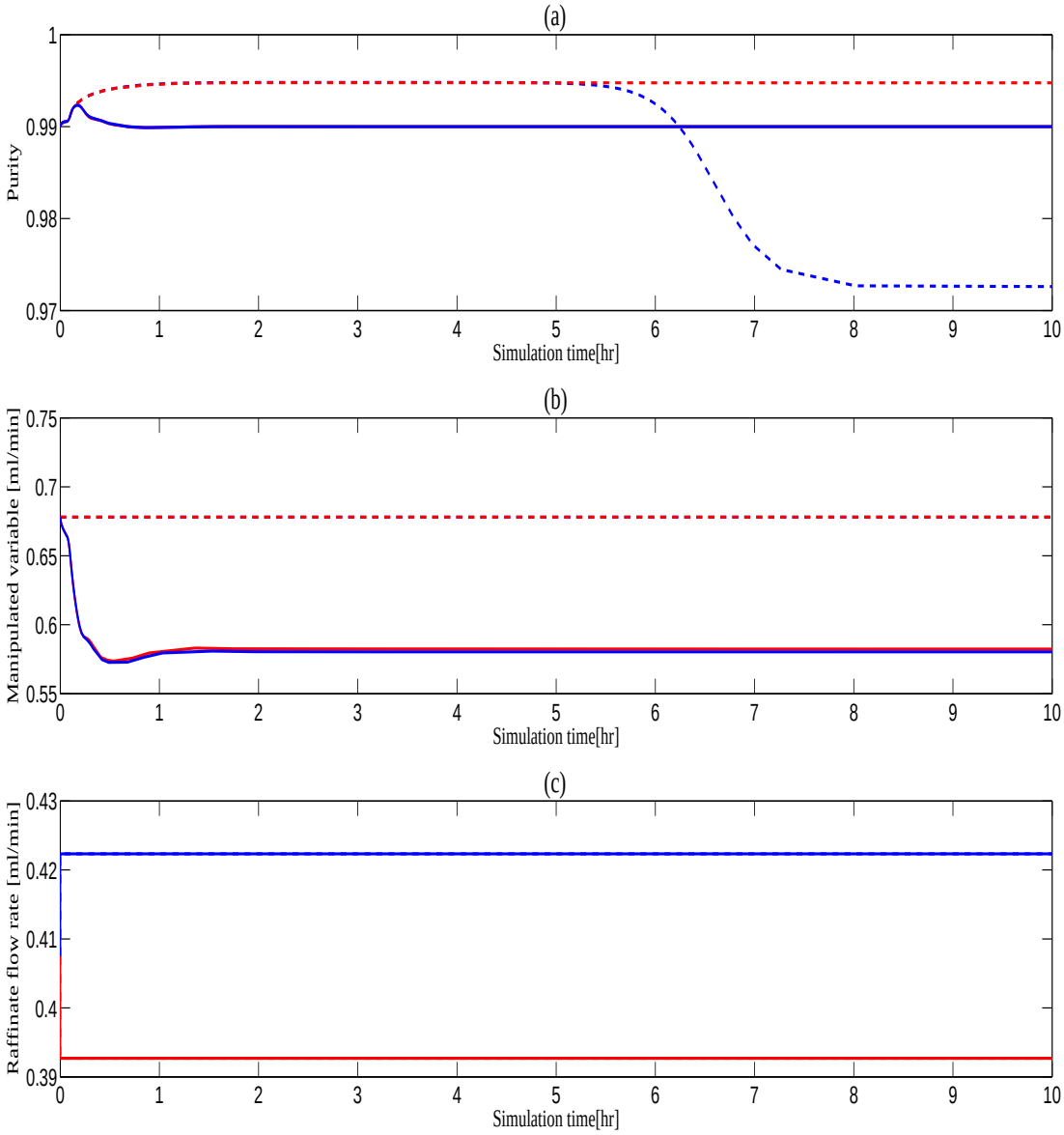

Figure 4.12: Comparison of an open loop and closed loop process for ± 5% disturbance of the external feed flow rate. The solid lines are for the process with control while the dashed lines are for the process without control. Red is for -5% while the blue curves are for + 5 %

4.3 Summary

The dynamics and control of coupled SMB-racemization processes has been explored for the first time within this thesis. Two simple control concepts have been proposed to compensate unforeseen disturbances of the external feed flow and the external feed concentration. It has been proven that for moderate product purity requirements an extension of the previous concepts for SMB-crystallization processes can be applied successfully to the present class of processes, namely SMB-racemization. For high product purity, this control concept is not applicable anymore and an alternative strategy has been developed. In both cases, an overdesign of the nominal operation point improved the controllability in respect to the magnitude of tolerable disturbances. Further, from the results of the SMB-crystallization (chapter 3) it was observed that a selective crystallizer at the product outlet introduces a certain robustness with respect to the disturbances and therefore a process comprising SMB-crystallization-racemization is an interesting option.

Chapter 5

Conclusions

Enantio-pure compounds play a decisive role in the pharmaceutical industry. Due to their significantly different physiological effects, most of the drugs are marketed in the enantio-pure form which accounts for almost 40% of the world wide drug market. This asserts that the development of innovative and economically conducive production processes is very important. Traditionally, these productions were performed using stand-alone separation or reaction units. An enormous potential for improving the performance of pure enantiomer production is provided by "smart" process schemes that combine the existing separation techniques such as chromatography and crystallization with chemical reactions. Also, due to the ever increasing need for enantio-pure drugs within the pharmaceutical industries, there is a strong demand for faster process development. A three step approach can be employed for this purpose which proves to be a useful tool to select and evaluate the interesting process options. In the first step, promising process candidates are selected based on qualitative criteria arising from industrial practice. In the second step, shortcut methods are applied for preliminary process design and preliminary evaluation of process performance.

The final step of the three step procedure involves rigorous optimization of the chosen process variants which is discussed in detail in the first part of this thesis. Initially, Non-Linear-Programming (NLP) based optimization was used to evaluate six possible process candidates derived from a qualitative decision tree. The results revealed that an ingenious and efficient approach would be to determine the optimal process structure as well as operating conditions simultaneously. This can be performed elegantly using Mixed-Integer-Non-Linear-Programming (MINLP). For the first time these advanced optimization approaches have been applied to design advanced process schemes for enantiomer production.

The results of the steady state optimal design affirmed that the hybrid process schemes involving combinations of SMB chromatography with enantio-selective crystallization and/or racemization are economically more favorable than the corresponding stand-alone processes. However, the dynamic operation of such non-linear processes with mass recycle is delicate and non-trivial. Hence, in the second step, dynamics, operability and control of such processes were considered. The first process which was investigated was the SMB-crystallization process. The operational objective of such a process is to produce a pure crystalline product irrespective of the presence of unforeseen disturbances. The open loop investigations highlighted the importance of the pump configuration on the process performance. It was also observed that the process specifications were not adhered to for moderate to large disturbances. Also for sufficiently large disturbances, the system stability was lost through a Hopf bifurcation leading to self sustained oscillations. This underlines the necessity of suitable plant wide control which was achieved by manipulating the amount of solvent added or removed from the system, thus avoiding a complicated direct SMB control.

The second process scheme which was considered for the dynamic investigations was the SMB-racemization system. Here, two qualitatively contrasting scenarios for racemization, one corresponding to the kinetic regime while the other in the equilibrium regime of the chemical reaction were considered. A steady state parameter continuation was employed as a tool to determine the necessary condition for controllability. It was observed that for the process in the kinetic regime, indirect control based on a solvent removal rate is a simple and feasible option. A direct control of the SMB plant was not required. It was further shown that this simple control concept will fail for fast racemization kinetics with high purity requirements. In this case readjustment of the SMB operational parameters is inevitable for good control performance. Further, it was also emphasized that for SMB-racemization, including an enantio-selective crystallization can improve the process robustness.

Here the design and control aspects have been dealt with sequentially. **Future work** should focus on integrating design and control. This can be achieved by formulating a dynamic optimization problem. An extension of this dynamic optimization with parametric uncertainty can be an interesting option and would ensure a robust design. Also, by formulating a Mixed Integer Dynamic Optimization (MIDO) problem, the pump configuration which can tolerate characterisitc disturbances irrespective of

the location of the crystallizer can be determined which is challenging and worth pursuing.

For a proof of concept, simple PI controllers were used in this thesis. Alternatively, one could also think of more advanced control concepts like model predictive control, for example, to explicitly account for non-linear process dynamics and hard constraints on the process dynamics introduced by the boundaries of the desired operational region in the phase diagram of enantioselective crystallization process.

Appendix A

Physico-chemical parameters

Table A.1: Parameters for the model system: PDE

a_2	a_1	$b_2[l/g]$	$b_1[l/g]$	$c_i^{feed}[g/l]$	x_i^*	$Porosity$	$L_c[cm]$	$D_c[cm]$	$N_c/zone$
0.6	1.31	0.022	0.04	20.0	0.4	0.7	25.0	0.46	2

PDE follows a Langmuir adsorption behavior which is given by

$$q_{i,k} = \frac{a_i c_{i,k}}{1 + \sum_{k=1}^{n} b_{i,k} c_{i,k}}. \tag{A.1}$$

Table A.2: Parameter values for the model system: PPX

Parameter	Unit	S-PPX	R-PPX
q_{sat}^I	[g/l]	46.78	
b_i^I	[l/g]	0.10351	0.20556
b_i^q	[l/g]	0.00555	0.02581
b_i^m	[l/g]	0.00334	0.01555
q_{sat}^{II}	[g/l]	64.66	
b_i^{II}	[l/g]	0.03162	1.63e-8
λ		0.6331	

PPX follows a quadratic thermodynamic adsorption equilibrium given by [58]

$$q_i = q_{\text{sat}}^I \frac{b_i^I c_i + 2b_i^q c_i^2 + c_S c_R \left(b_S^m + b_R^m\right)}{1 + \sum_j b_j^I c_j + \sum_k b_k^q c_k^2 + c_S c_R \left(b_S^m + b_R^m\right)} + q_{\text{sat}}^{II} \frac{b_i^{II} c_i}{1 + \sum_l c_l} + \lambda c_i \qquad \text{(A.2)}$$

The feed concentration which has been used for the PPX case studies is $c_i = 12.5$ g/l.

Appendix B

MINLP optimization of SMB processes and process combinations with variable number of stages

B.1 Model formulation

A schematic of an SMB unit allowing optimization of the number of stages i.e. a variable size SMB unit is shown in Figure B.1(a). Later, such units are included within a super structure such as the one studied in Chapter 2 [Figure B.1(b)]. The approach which has been used here is similar to the one which has been proposed for optimizing distillation columns [68].

In this work, an SMB unit is modeled using its equivalent TMB. The feed stage of the TMB is fixed. The remaining inlet and outlet stages are variable and determined by MINLP optimization. Binary variables are used to determine the location of the extract (I_E^k), raffinate (I_R^k), desorbent (I_D^k) and final stage (I_L^k) according to Eq.(B.1) and thereby define the length of the different zones. Adsorption equilibrium is described by Langmuir isotherms with parameters for the PDE system as described in Appendix A. The unit is assumed to be at steady state.

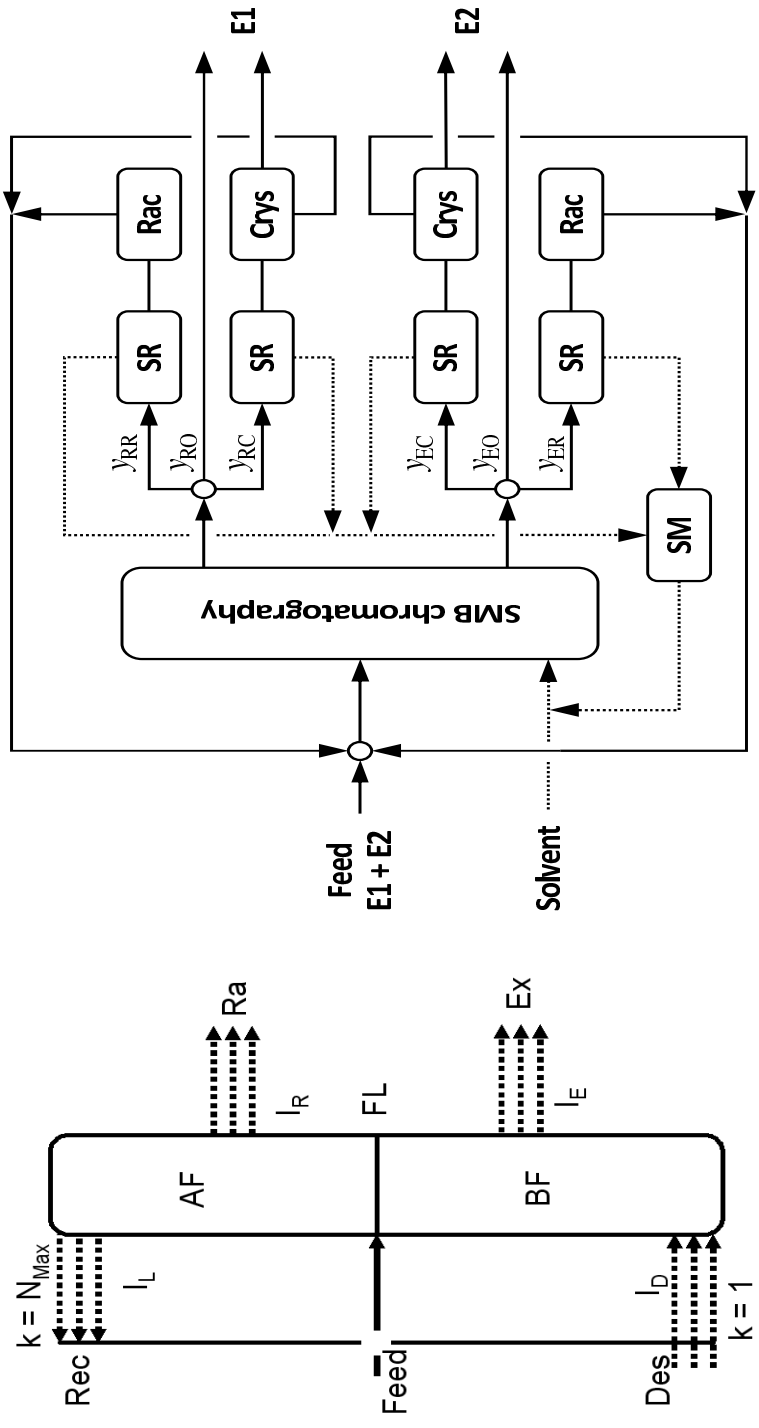

(b) Super structure

(a) TMB modeling with variable stage number

Figure B.1: Schematic models for stage number optimization for SMB processes and process combinations

The dimension of the four binary variables can be written as

$$I_E^k, I_D^k, I_R^k, I_L^k \in \{0,1\}^{FL-1} \tag{B.1}$$

Single stage conditions can be written as

$$\sum_{k=1}^{FL-1} I_E^k = 1, \qquad \sum_{k=1}^{FL-1} I_D^k = 1, \qquad \sum_{k=FL+1}^{N_{Max}} I_R^k = 1, \qquad \sum_{k=FL+1}^{N_{Max}} I_L^k = 1 \tag{B.2}$$

The steady state mass balances of the TMB unit can be written as

$$\begin{aligned}
I_D^1 \left[Des + Rec\right] - \dot{Q}^1 &= 0, && k = 1 \\
I_D^k \left[Des + Rec\right] + \dot{Q}^{k-1} - \dot{Q}^k &= I_E^k * Ex, && k = 2, ...FL-1 \\
\dot{Q}^{FL-1} - \dot{Q}^{FL} + Feed &= 0, && k = FL \\
\dot{Q}^{k-1} - \dot{Q}^k - I_L^k * Rec &= I_R^k * Ra, && k = FL+1, ...N_{Max}-1 \\
\dot{Q}^{N_{Max}-1} - \dot{Q}^{N_{Max}} - I_L^{N_{Max}} * Rec &= 0, && k = N_{Max}
\end{aligned} \tag{B.3}$$

It needs to be mentioned that $\dot{Q}^{N_{Max}}$ is always fixed at zero.

The component mass balances across each stage can be written as

$$\begin{aligned}
\dot{Q}_{solid}[q_i^2 - q_i^1] + I_D^1\left[Des * c_i^{Des} + Rec * c_i^{Rec}\right] - \dot{Q}^1 * c_i^1 = 0, \qquad & k = 1 \\
\dot{Q}_{solid}[q_i^{k+1} - q_i^k] + I_D^k\left[Des * c_i^{Des} + Rec * c_i^{Rec}\right] + \dot{Q}^{k-1} * c_i^{k-1} - \dot{Q}^k * c_i^k = I_E^k * Ex * c_i^k, \qquad & k = 2, ..FL-1 \\
\dot{Q}_{solid}[q_i^{FL+1} - q_i^{FL}] + \dot{Q}^{FL-1} * c_i^{FL-1} - \dot{Q}^{FL} * c_i^{FL} + Feed * c_i^{Feed} = 0, \qquad & k = FL \\
\dot{Q}_{solid}[q_i^{k+1} - q_i^k] + \dot{Q}^{k-1} * c_i^{k-1} - \dot{Q}^k * c_i^k - I_L^k * Rec * c_i^{Rec} = I_R^k * Ra * c_i^k, \qquad & k = FL+1, ..N_{Max}-1 \\
\dot{Q}_{solid}[q_i^1 - q_i^{N_{Max}}] + \dot{Q}^{N_{Max}-1} * c_i^{N_{Max}-1} - \dot{Q}^{N_{Max}} * c_i^{N_{Max}} - I_L^{N_{Max}} * Rec * c_i^{Rec} = 0, \qquad & k = N_{Max}
\end{aligned} \tag{B.4}$$

Purity constraints can be formulated as

$$\begin{aligned}
\sum_{k=1}^{FL-1} I_E^k * c_1^k \geq Pu_{min}\left[\sum_{k=1}^{FL-1} I_E^k * c_1^k + \sum_{k=1}^{FL-1} I_E^k * c_2^k\right] \\
\sum_{k=FL+1}^{N_{Max}} I_R^k * c_2^k \geq Pu_{min}\left[\sum_{k=FL+1}^{N_{Max}} I_R^k * c_1^k + \sum_{k=FL+1}^{N_{Max}} I_R^k * c_2^k\right]
\end{aligned} \tag{B.5}$$

The above purity constraints have been written in such a way that the stronger adsorbing component is the first one.

A positive minimal zone length ($N_{minzone}$) condition has also been implemented which can be written mathematically as

$$\begin{aligned}
\sum_{k=1}^{FL-1} I_E^k * k \geq \sum_{k=1}^{FL-1} I_D^k * k + N_{Minzone}, \quad \sum_{k=FL+1}^{N_{Max}} I_L^k * k \geq \sum_{k=FL+1}^{N_{Max}} I_R^k * k + N_{Minzone} \\
FL \geq \sum_{k=1}^{FL-1} I_E^k * k + N_{Minzone}, \quad \sum_{k=FL+1}^{N_{Max}} I_R^k * k \geq FL + N_{Minzone}
\end{aligned} \tag{B.6}$$

Additional equations can be enforced or relaxed depending on whether equal zone lengths are necessary or not.

In this formulation, a fixed order of desorbent, extract, feed, raffinate and recycle stages according to Figure B.1(a) is explicitly taken into account . This reduces the number of binary variables and leads to a computational efficient implementation. The set of relations given by Eq.(B.2) ensures that there is only a single extract stage, feed stage and so on. The first equation in the set of mass balances given by Eqs.(B.3) ensures that if the first stage is inactive the fluid flow rate becomes zero. Since the first active stage below the feed is the desorbent stage i.e. $I_D^k = 1$, sum of the solvent and recycle from zone 4 represents the stream which enters and leaves this stage. Inequality constraints given by Eq.(B.6) enforce positive zone lengths i.e. the extract stage is located above the desorbent stage. Hence between the the desorbent and the extract stages there is just a transfer of components between the two phases while the solid and liquid flow rates are unchanged. Similar ideas are used in the remaining zones of the SMB unit except in the final zone. When the stage N_{Max} is inactive, $I_L^k = 0$ as well as $\dot{Q}^{N_{Max}} = 0$. This implies that the liquid flow rate is zero everywhere till the last active stage is encountered. The entire liquid stream which enters the last active stage is completely recycled back to the desorbent stage of the SMB unit.

B.2 Results

B.2.1 Simple cost function

The efficiency of this modeling approach is illustrated in a first step by using a very simple objective function. Here, the objective function corresponds to minimizing the number of active stages of a stand-alone SMB for a fixed feed flow rate. Identical purity requirements at both outlets ranging from 95 - 99.8% have been considered. Further, in a first step, the number of stages in each zone is assumed to be equal.

In Chapter 2, an enumeration approach was used to determine the maximum feed flow rate as a function of stage number. In such a calculation, the objective function was to maximize the feed flow rate. Symmetric purity constraints were enforced and the maximal feed rate was calculated for various stage numbers. Such a calculation is repeated here for the PDE enantiomer system and is shown in Figure B.2. A high purity of 99.8% was used in Figure B.2

The results of MINLP optimization needs to be validated which has been performed by comparing them with that of the parametric enumeration procedure. For this purpose, a fixed feed flow rate of 0.225 ml/s was used. This corresponds to the horizontal dashed line in Figure B.2. With a fixed feed rate of 0.225 ml/s and out-

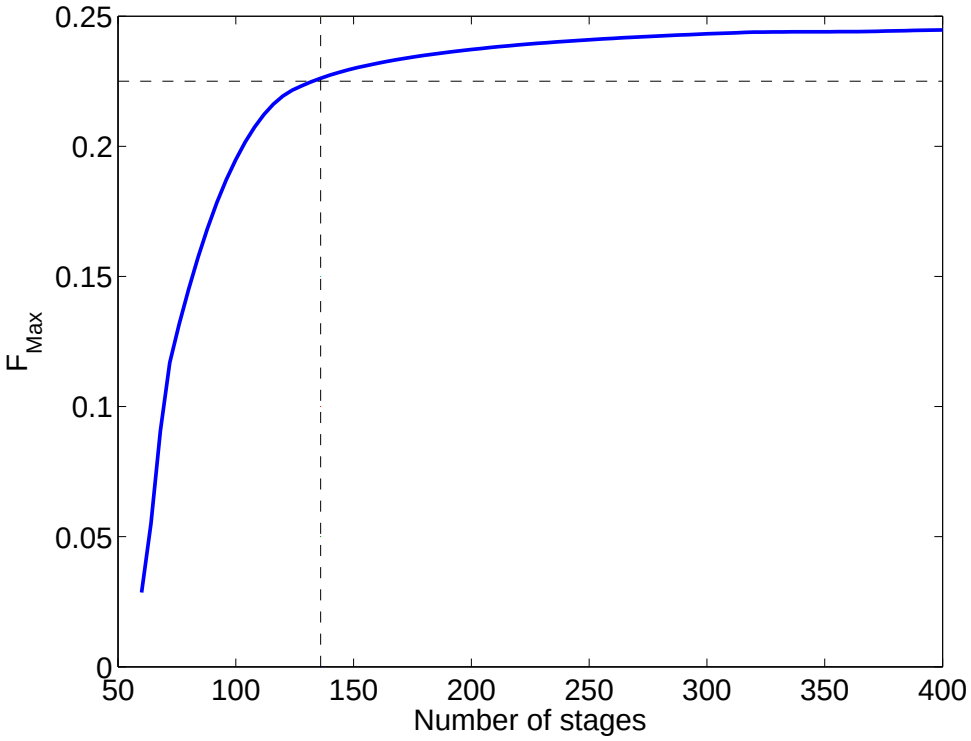

Figure B.2: Enumeration approach illustrating the effect of stage number on the maximum feed which can be processed for outlet purity of 99.8%. Results are for the PDE enantiomer

let purities of 99.8%, MINLP optimization using DICOPT in GAMS [56, 57] with CONOPT3 for the NLP subproblems and CPLEX for the MILP master problems. Parametric enumeration was done using CONOPT3. The minimum number of stages which is necessary to achieve this separation corresponds to 136 which is identical with the result of the above enumeration as indicated in Figure B.2. This proves that the number of stages determined by the NLP based enumeration approach and the more elegant MINLP approach is identical. The solid flow rate was assumed to be 1.0 ml/s.

Once the validation between the two methods was established, the computational efficiency of the two methods were compared. For this purpose, the feed flow rate was fixed to 0.225 unit/time in MINLP optimization and the extract and raffinate purities were varied. In the parametric enumeration based approach, the maximum feed flow rate as a function of stage number was calculated similar to Figure B.2 for different purity requirements as shown in Table B.1. In the case of parametric enumeration, the entire curve was generated ranging from a maximum of 400 stages to a minimum of 40 stages irrespective of the location of the desired operating point. Table B.1 clearly demonstrates the efficiency of the MINLP optimization compared to the parametric approach.

In Figure B.3(a), we show the effect of product purity on the number of stages. The results have been generated using MINLP optimization. The number of stages required to achieve the necessary purity decreases exponentially with a decrease in purity requirements which is perfectly along the lines of expectation. These are for a feed flow rate of 0.225 units/time which is identical to that in the Table B.1.

Figure B.3(b) shows the effect of feed flow rate on the minimum number of stages which is necessary to achieve a certain separation. These are similar to the calculations shown earlier. Here the blue curve is for a product purity of 99.8% while the red curve is for 97.5%. The circles in the figure are the outcome of MINLP calculations. As expected, the amount of feed which can be processed increases by relaxing the purity requirements. Further, for a fixed purity, the minimum number of stages which is necessary to achieve the desired purity decreases significantly with a decrease in the feed flow rate.

Upto now focus has been on stand-alone SMB processes. In a next step, such variable stage number SMB models were coupled to other process units such as crystallization and racemization. Here, the discussion is limited to fixed process candidates. For the stand-alone SMB process, a feed flow rate of 0.225 ml/s is considered. For a feed concentration of 20 mg/ml, this corresponds to 4.5 mg/s of product. Since

Table B.1: Comparison of CPU time for the two methods to perform stage number optimization. Computations were performed on a linux 2GHz, AMD Athlon single core processer

Purity	N_{tot}	TIME (sec)	Method
95.0 %	40	70	MINLP
97.5 %	60	66	MINLP
99.0 %	84	47	MINLP
99.5 %	104	101	MINLP
99.8 %	136	92	MINLP
95.0 %	40	289	Parametric
97.5 %	60	259	Parametric
99.0 %	84	251	Parametric
99.5 %	104	243	Parametric
99.8 %	136	257	Parametric

Table B.2: Minimum number of stages for the different process schemes

Process	N_{tot}
SMB	136
SMB-cryst	60
SMB-rac	132
SMB-rac-cryst	28

SMB units have to be compared with the SMB-racemization systems, the calculations here are based on a product rate of 4.5 mg/s at the extract. This in turn makes sure that the stand-alone SMB which has already been optimized previously can be compared with the more advanced process options. Table B.2 shows the results of the optimization for four different processes. It can be seen that there is a significant reduction in the number of stages necessary to produce the fixed amount of products by using a crystallization. This is clear from the results for SMB-crystallization as well as for SMB-racemization-crystallization. In the case of SMB-racemization, there is no significant improvement for this hypothetical cost function. This is due to the fact that the reduction in feed material cost by half does not have a direct effect on the number of stages.

Another important parameter which has a significant effect on the number of stages is the separation factor. In order to evaluate the effect of separation factor, the adsorption isotherm parameter of the stronger adsorbing enantiomer is varied while simultaneously maintaining the weaker adsorbing isotherm parameter constant. The separation factor is defined as the ratio of the adsorption isotherm parameters i.e. $\frac{a_1}{a_2}$ according to the convention used in this thesis. The results of such an investigation

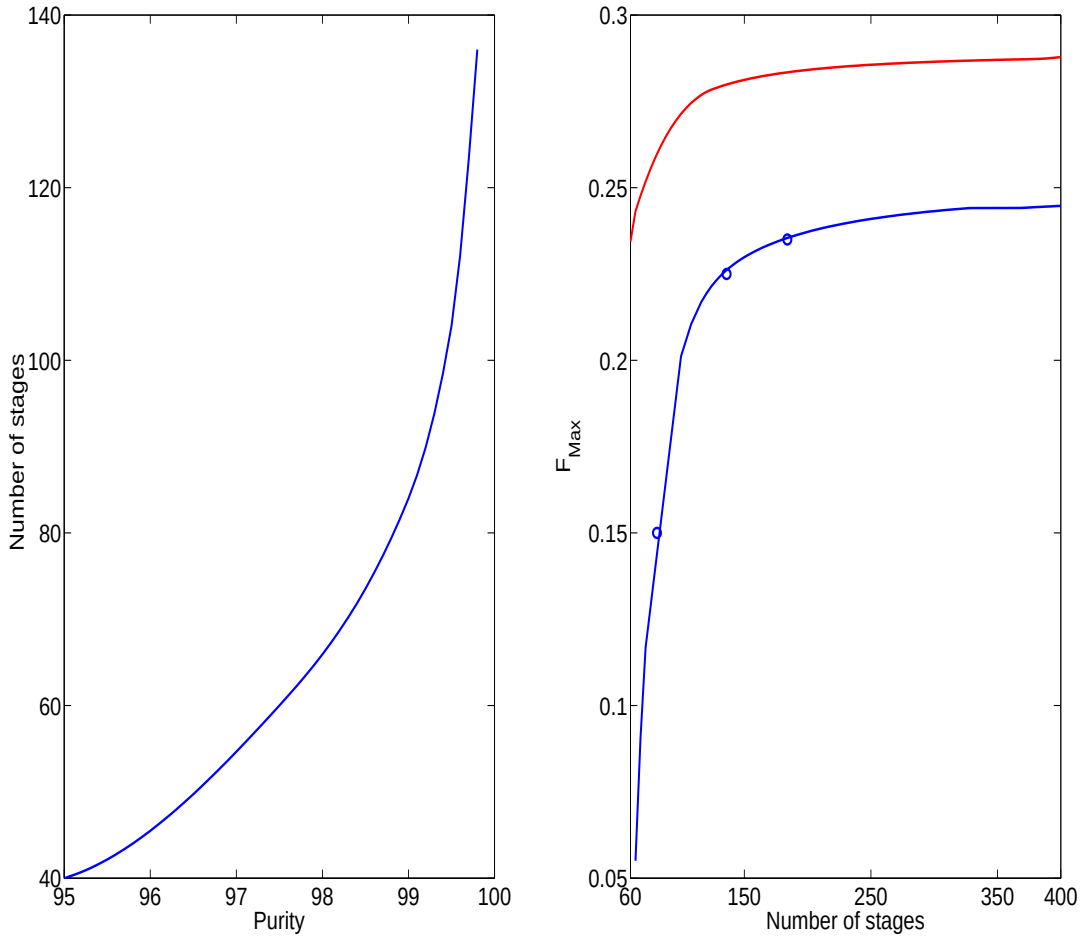

Figure B.3: (a) Minimum number of stages as a function of the product purity (b) Minimum number of stages as a function of the feed flow rate

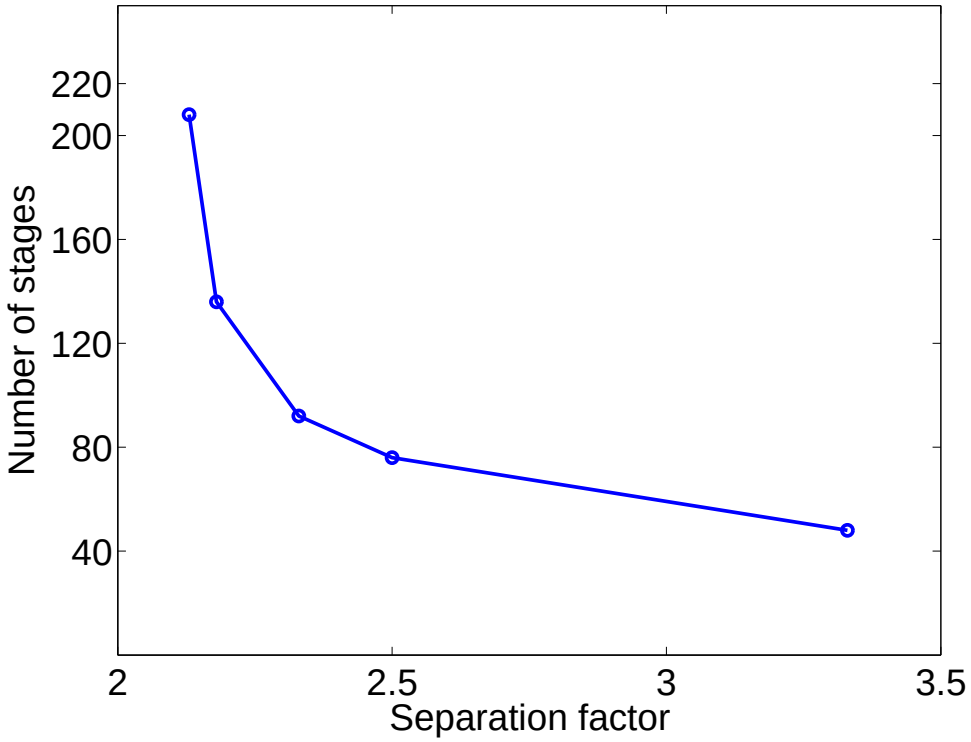

Figure B.4: Effect of separation factor on the number of stages

is shown in Figure B.4. The results have been generated for a feed flow rate of 0.225 ml/s and extract and raffinate outlet purities of 99.8%. It can be seen from the figure that the qualitative profiles are in accordance with intuition.

Upto this point, the number of stages were assumed to be equally distributed among the four zones of the unit. But it is interesting to realize that an optimization formulation such as the one given by Eqs.(B.1 - B.6) allows to optimize unequal number of stages in the four zones of the SMB. Table B.3 shows the results for this second set of optimization. By using unequal stage numbers in each zone, the minimum number of stages required to achieve the separation is much smaller. The results correspond to a fixed feed flow rate of 0.225 ml/s which has already been investigated for the equally distributed scenario. It must also be mentioned that here the number of stages in the zones 1 and 4 are very small. This could be due to the fact that in the present formulation there is no restriction on the amount of solvent added to the SMB. Nevertheless, these results emphasize the computational potential of such a formulation.

Table B.3: Minimum number of stages for unequal stage number for stand alone SMB with symmetric purities

Purity	No. of stages in zone				N_{tot}
	1	2	3	4	
95.0 %	3	12	9	3	27
99.0 %	6	15	27	3	51
99.8 %	5	30	26	4	65

B.2.2 Super structure based optimization for process combinations

From the results of the MINLP optimization with fixed stage numbers in Chapter 2, it is clear that the weighting factors, production rates etc. play a critical role in determining the optimal process scheme. Figure B.1(b) shows a super structure which includes a variable stage SMB unit coupled with a racemization reactor and enantio-selective crystallizer. Here, additional binary variables are used to denote the existence/non-existence of the different auxiliary units. Optimizing such a super structure for the user defined process and product specifications as well as user defined cost factors would provide the optimal process structure including the SMB size and the optimal operating conditions. A more detailed cost function along the lines of chapter 2 can be written for a variable stage SMB unit as

$$f = \frac{(w_f + w_{inv})M_{rac} + w_{op}}{((1 - y_{ER})0.5 + y_{ER}Y)M_{rac}} \tag{B.7}$$

with

$$w_{inv} = \tilde{w}_{inv,SMB} * N_{tot} + y_{RC}w_{inv,RC} + y_{EC}w_{inv,EC} + y_{ER}w_{inv,ER}$$

and

$$w_{op} = w_{op,SMB} + y_{RC}w_{op,RC} + y_{EC}w_{op,EC} + y_{ER}w_{op,ER}$$

Here, N_{tot} is the total number of active stages of the SMB unit. Depending on the different weighing factors, various process schemes were obtained as optima.

Until now, the results were calculated using a hypothetical TMB model. But in reality, the parameters obtained need to be converted to SMB design parameters. For designing an SMB unit, the $\dot{Q}^k$ and $\dot{Q}_{solid}$ values need to be converted to real flow rates and switching times along with an additional pressure drop constraint. Converting the optimized TMB results to actual SMB operational parameters can be performed using relations already available in the literature [53]. In the next section, we use these translation strategies to design an SMB unit incorporating the additional restriction on pressure drop.

B.2.3 SMB design using TMB parameters

In order to design an SMB, the model equations used in the previous section are appended to the Eqs.(B.8) - (B.22). This in turn ensures that the optimal $\dot{Q}^k$ values which are determined are in accordance with the minimum switch time or maximum pressure drop limitations. The additional optimal design parameters besides the ones which were determined for the TMB calculations are the column length (L_c), column diameter (D_c), switch time (t_{switch}). The equations which are used for the TMB to SMB translation can be written as.

$$A_c = 3.1416 * D_c * D_c/4 \tag{B.8}$$

$$V_c = A_c * L_c \tag{B.9}$$

$$t_{switch} = \frac{V_c * (1-\epsilon_t) * \left[\sum_{k=1}^{FL-1} I_D * \dot{Q}^k - \sum_{k=1}^{FL-1} I_E * \dot{Q}^k\right]}{QE} \tag{B.10}$$

$$HETP = (aVD + bVD * ULIN) \tag{B.11}$$

$$NTPCOL * HETP = Lc \tag{B.12}$$

$$NTP = 4 * NTPCOL \tag{B.13}$$

$$NTP = (FNP - DPR + 1) \tag{B.14}$$

$$dP_j = \frac{1 * KdP * L_c * Q1}{\epsilon_b * A_c} \tag{B.15}$$

$$Q_1 * t_{switch} = \sum_{k=1}^{FL-1} I_D * \dot{Q}^k * (1-\epsilon_t) * V_c + \epsilon_t * Vc \tag{B.16}$$

$$Q_2 * t_{switch} = \sum_{k=1}^{FL-1} I_E * \dot{Q}^k * (1-\epsilon_t) * V_c + \epsilon_t * Vc \tag{B.17}$$

$$Q_3 * t_{switch} = \dot{Q}^{FL} * (1-\epsilon_t) * V_c + \epsilon_t * Vc \tag{B.18}$$

$$Q_4 * t_{switch} = \sum_{k=Fl+1}^{N_{Max}} I_R * \dot{Q}^k * (1-\epsilon_t) * V_c + \epsilon_t * Vc \tag{B.19}$$

$$ULIN = \frac{Q1 + Q2 + Q3 + Q4}{4 * PORB * Ac} \tag{B.20}$$

$$dP1 + dP2 + dP3 + dP4 \leq \Delta P_{Max} \tag{B.21}$$

$$QE * \sum_{k=1}^{FL-1} I_E * \dot{Q}^k * c_2^k = MPEX \tag{B.22}$$

Here we discuss the results obtained using a more detailed cost function. The cost

function can be written as $C = C_{Inv} + C_{Feed} + C_{Solv} + C_{Oper} + C_{ads}$ [59]. Here C_{Inv} represents the investment cost arising from the different units. C_{Feed} and C_{Solv} corresponds to the feed material and solvent cost respectively. C_{Oper} is the operation/labor cost while C_{ads} arises from the cost of chiral stationary phase.

The studies in this section have been performed for a fixed production rate of 2 mg/s. The extract is assumed to be the desired product. The cost function incorporating all the former contributions can be written as

$$C = W_f * M_{rac} + W_{inv,SMB} + W_{inv,Cry} + W_{inv,Rac} + W_{solv} * SC + W_{op} + W_{ads} * Vc * 4 \quad \text{(B.23)}$$

Since the investment and operation costs are not known explicitly, it is assumed in a first step that the effect of these contributions is same for all three processes. This implies that additional equipments and operation costs associated with a crystallizer and racemizer are insignificant. Under such scenarios, the three processes namely SMB, SMB-cryst, and SMB-rac-cryst can be compared. The results for this case is given in Table B.5. Irrespective of the weighing factors as well the process scheme, the length of the column (L_c) was always observed to be at the lower bound. Hence, there was no significant effect of the number of stages on the process optimum though there is a significant reduction in the objective function value for the process combinations. A maximum pressure drop restriction of 200 bar across the four zones was considered as the limit and was always at the bound. It can be seen that there is a significant reduction in the cost by using process combinations. This arises mainly from the use of columns with smaller diameters which reduces C_{ads}. Since the effect of feed material cost is not significant in comparison with the adsorbent cost, the effect of racemization is not so pronounced. By using a larger W_f, and lower W_{ads}, the effect of racemization would be much more evident as there is a reduction in the amount of feed material by half.

Table B.4: Comparison of different processes with translation to SMB

$Process$	W_f	W_{solv}	W_{ads}	$W_{inv,SMB}$	$W_{inv,Cry}$	$W_{inv,Rac}$	W_{op}
Case 1	1.0	0.1	0.01	0.0	0.0	0.0	0.0

The entries which are in bold implies they are at their lower/upper bounds.

Table B.5: Comparison of different processes with translation to SMB for case 1 in Table B.4

$Process$	$Q1$	$Q2$	$Q3$	$Q4$	$F0$	L_c	D_c	t_s	NTP	$Objective$
SMB	2.983	1.722	1.822	1.615	0.1	**10.0**	3.248	**60.0**	200	1.066
SMB-cryst	2.316	0.635	0.814	0.593	0.1	**10.0**	2.294	**60.0**	188	0.686
SMB-cryst-rac	2.019	0.951	1.071	0.951	0.05	**10.0**	2.544	**60.0**	200	0.665

Appendix C

Dynamic crystallizer model

In this Appendix, a dynamic version of the simple crystallizer model in the Eqs.(2.8) - (2.10) is introduced. Let ψ be the void fraction of the crystallizer, i.e. the volumetric fraction of the liquid phase. Further, let δ be the fraction of crystals of the enantiomer 1 of the solid phase of the crystallizer. If we assume that ψ and δ in the product removal are the same as inside the crystallizer and - as before - the densities of the solid and the liquid are constant and identical, a simple dynamic model can be formulated in the following form:

Total material balance of the liquid phase

$$\frac{d(\psi V)}{dt} = \dot{Q}_{evap} - \psi \dot{Q}_{out} - \sum_{1}^{2} k_i \left[X_{i,ml} - X_i^*\right] \tag{C.1}$$

Component material balances of both solutes in the liquid phase

$$\frac{d(\psi V X_{i,ml})}{dt} = \dot{Q}_{evap}\, X_{i,evap} - \psi \dot{Q}_{out} X_{i,ml} - k_i \left[X_{i,ml} - X_i^*\right] \tag{C.2}$$

Component material balance of enantiomer 1 in the solid phase

$$\frac{d((1-\psi)V\delta)}{dt} = k_1 \left[X_{1,ml} - X_1^*\right] - \delta(1-\psi)\dot{Q}_{out} \tag{C.3}$$

Total material balance for equal and constant densities of the solid and the liquid phase can be written as

$$\dot{Q}_{out} = \dot{Q}_{evap} \tag{C.4}$$

This arises from the equal density assumption whereby they cancel off.

The effect of finite crystallizer dynamics on the open loop behavior is illustrated in Figure C.1 for a capacity of 0.1 (red), 1 (blue) and 10 (black) volume units of

the crystallizer for a +17.5 % increase of the external feed concentration. For very small volumes, similar patterns of behavior as predicted with the quasi-static model are observed. In particular, instability in the form of self sustained oscillations is obtained. As can be expected, the oscillations are being damped away with increasing volume of the crystallizer. However, formation of undesired crystals, which is the major problem in this disturbance scenario remains independent of the volume of the crystallizer. Irrespective of the volume, the control strategy proposed above can be used to solve this problem. This is illustrated in Figure C.2 for the three different cases of Figure C.1. The controller parameters for the closed loop process is given in Table C.1.

Table C.1: Controller parameters for an SMB-crystallization process with a dynamic crystallizer model

Parameters	Value
$K_c[min/ml]$	0.55
$\tau_I[min]$	120.0

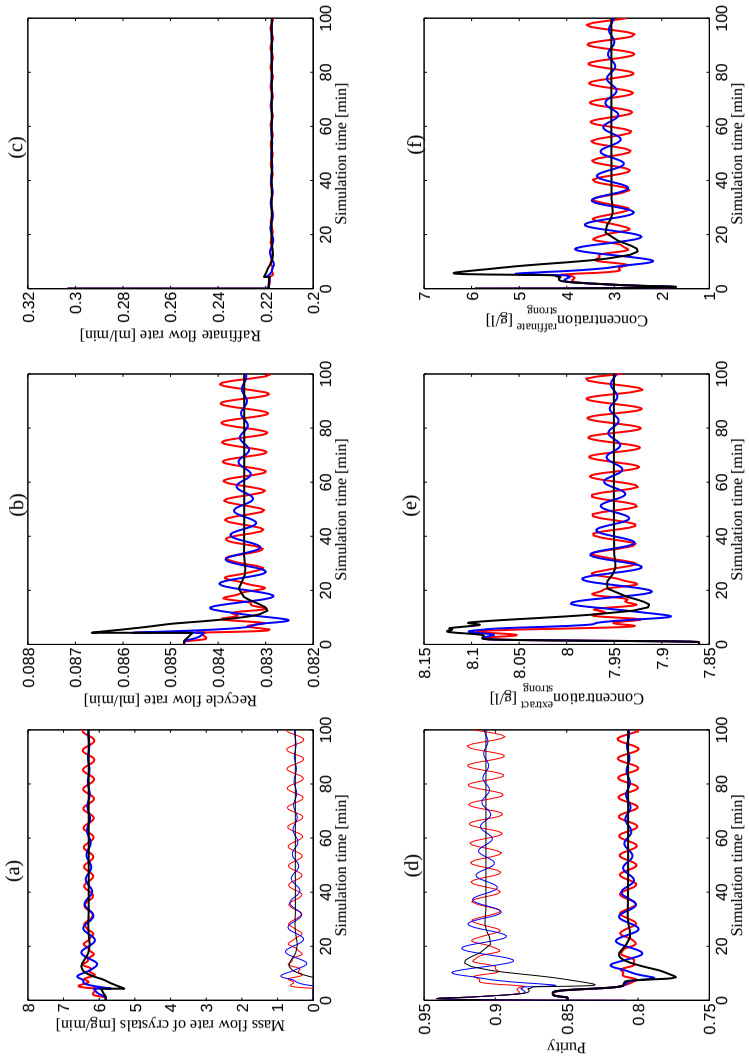

Figure C.1: Open loop dynamics for a step disturbance of +17.5% of the external feed concentration for a crystallizer at the extract with finite dynamics with a capacity of 0.1 (red), 1 (blue) and 10 (black) volume units. Meaning of thick and thin lines in diagrams (a) and (d) is as in Figure 3.3.

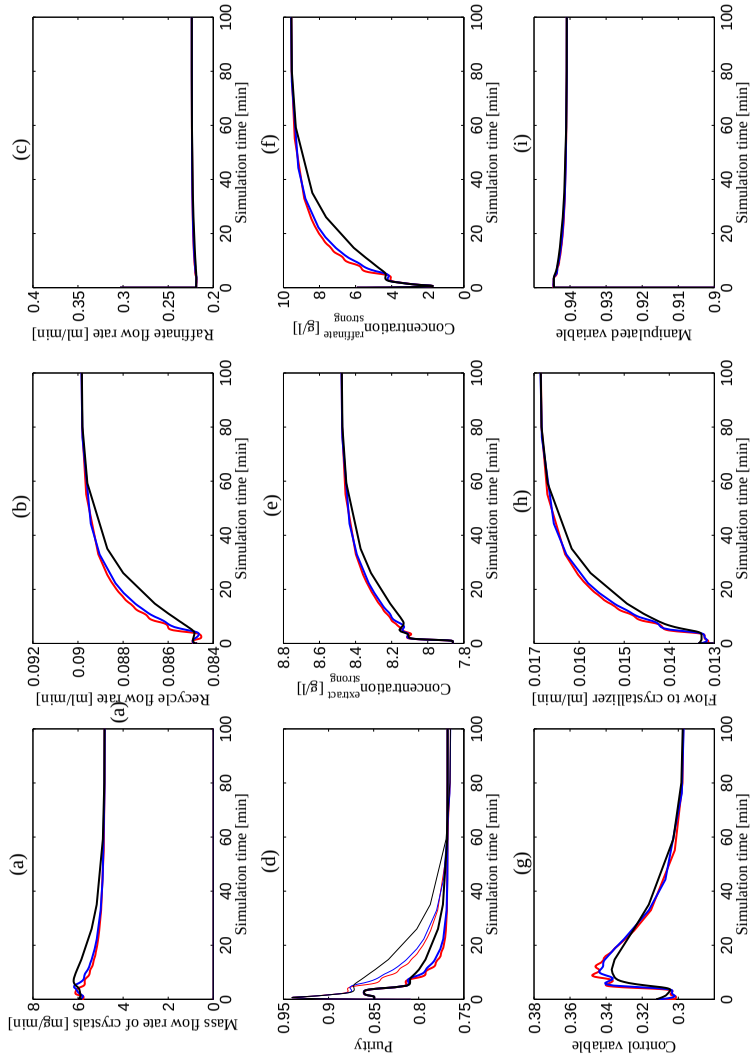

Figure C.2: Closed loop dynamics for a step disturbance of +17.5% of the external feed concentration for a crystallizer at the extract with finite dynamics with a capacity of 0.1 (red), 1 (blue) and 10 (black) volume units. Meaning of thick and thin lines in diagrams (a) and (d) is as in Figure 3.3.

Bibliography

[1] J. Jacques, A. Collet, and S. Wilen. *Enantiomers, Racemates and Resolutions*. Krieger, Malabar, 1994.

[2] B. Li and D. T. Haynie. *Encyclopedia of Chemical Processing*, Chapter "Chiral drug separation", page 451. Taylor and Francis, 2006.

[3] A. Rajendran, G. Paredes, and M. Mazzotti. Simulated moving bed chromatography for the separation of enantiomers. *J. Chromatogr. A*, 1216:709–738, 2009.

[4] M. Kaspereit. Separation of enantiomers by a process combination of chromatography and crystallization. Shaker, Aachen, 2006.

[5] M. Kaspereit, A. Seidel-Morgenstern, and A. Kienle. Design of simulated moving bed under reduced purity requirements. *J. Chromatogr. A*, 1162:2–13, 2007.

[6] H. Lorenz, P. Sheehan, and A. Seidel-Morgenstern. Coupling of simulated moving bed chromatography and fractional crystallisation for efficient enantioseparation. *J. Chromatogr. A*, 908:201–214, 2001.

[7] M. Kaspereit, K. Gedicke, V. Zahn, A. W. Mahoney, and A. Seidel-Morgenstern. Shortcut method for the evaluation and design of a hybrid process for enantioseparations. *J. Chromatogr. A*, 1092:43–54, 2005.

[8] H. Kaemmerer, M. J. Jones, H. Lorenz, and A. Seidel-Morgenstern. Selective crystallisation of a chiral compound-forming system – solvent screening, SLE determination and process design. *Fluid Phase Equilibria*, 296:192 – 205, 2010.

[9] H. Kaemmerer, R. Zinke, H. Lorenz, M. J. Jones, A. Seidel-Morgenstern, and M. Stein. Corrigendum to selective crystallisation of a chiral compound-forming system–solvent screening, SLE determination and process design by H. Kaemmerer et al. [*Fluid Phase Equilibria*. 296 (2010) 192–205]. *Fluid Phase Equilibria*, 307:110 – 112, 2011.

[10] T. Borren, J. Fricke, and H. Schmidt-Traub. *Integrated reaction and separation operations: Modelling and experimental validation*, chapter Reactive liquid chromatography, pages 191–239. Springer, Berlin, 2006.

[11] M. Kaspereit, J. García Palacios, T.F. Meixús, and A. Kienle. In Bertrand Braunschweig and Xavier Joulia, editors, *Computer-Aided Chemical Engineering, vol. 25 – 18th European Symposium on Computer Aided Process Engineering*, pages 97–102. 2008.

[12] M. Bechtold, S. Makart, M. Heinemann, and S. Panke. Integrated operation of continuous chromatography and biotransformations for the generic high yield production of fine chemicals. *Journal of Biotechnology*, 124:146 – 162, 2006.

[13] K. Petruevska-Seebach, K. Wrges, A. Seidel-Morgenstern, S. Ltz, and M. P. Elsner. Enzyme-assisted physicochemical enantioseparation processes – part ii: Solid-liquid equilibria, preferential crystallization, chromatography and racemization reaction. *Chem. Eng. Sci.*, 64:2473 – 2482, 2009.

[14] B. G. Lim, C.-B. Ching, R.B.H. Tan, and S.-C.Ng. Recovery of (-) -praziquantel from racemic mixtures by continuous chromatography and crystallisation. *Chem. Eng. Sci.*, 50:2289–2298, 1995.

[15] J. Blehaut and R.-M. Nicoud. Recent aspects in simulated moving bed. *Analusis Magazine*, 26:M60–M70, 1998.

[16] K. Gedicke, M. Kaspereit, W. Beckamnn, U. Budde, H. Lorenz, and A. Seidel-Morgenstern. Conceptual design and feasibility study of combining continuous chromatography and crystallization for stereoisomer separations. *Chem. Eng. Res. Des.*, 85:928–936, 2007.

[17] A. Rajendran. Equilibirum theory based design of simulated moving bed processes for reduced purity requirements: Linear isotherms. *J. Chromatogr. A*, 1185:216–222, 2008.

[18] M. Amanullah and M. Mazzotti. Optimization of a hybrid chromatography-crystallization process for the separation of tröger's base enantiomers. *J. Chromatogr. A*, 1107:36–45, 2006.

[19] J. García Palacios, M. Kaspereit, and A. Kienle. Conceptual design of integrated chromatographic processes for the production of single (stereo-)isomers. *Chem. Eng. Tech.*, 32:1392–1402, 2009.

[20] J. García Palacios, M. Kaspereit, and A. Kienle. Integrated simulated moving bed processes for the production of single enantiomers. *Chem. Eng. Tech.*, 34(5):688–698, 2011.

[21] J. García Palacios, B. Kramer, A. Kienle, and M. Kaspereit. Experimental validation of a new integrated simulated moving bed process for the production of single enantiomers. *J. Chromatogr. A*, 1218:2232–2239, 2011.

[22] K. Hashimoto, S. Adachi, H. Noujima, and Y. Ueda. A new process combining adsorption and enzyme reaction for producing higher-fructose syrup. *Biotechnology & Bioengineering*, 25:2371–2393, 1983.

[23] M. Bechtold, M. Füreder, and N. Wagner und S. Panke. Potenzial von prozessintegration mit adsorbern zur herstellung seltener monosaccharide eine modellbasierte untersuchung. *Chem. Ing. Tech.*, 82:65–75, 2010.

[24] M. Kaspereit, S. Swernath, and A. Kienle. Evaluation of competing process concepts for the production of pure enatiomers. *Org. Proc. Res. Dev.*, 16(2):353–363, 2012.

[25] J. Viswanathan and I. E. Grossmann. A combined penalty function and outer-approximation method for MINLP optimization. *Comp. Chem. Eng.*, 14:769–782, 1990.

[26] I. E. Grossmann, P. A. Aguirre, and M. Barttfeld. Optimal synthesis of complex distillation columns using rigorous models. *Comp. Chem. Eng.*, 29:1203–1215, 2005.

[27] J. Gangadwala and A. Kienle. MINLP optimization of butyl acetate synthesis. *Chem. Eng. and Proc.*, 46:107–118, 2007.

[28] J. Gangadwala, A. Kienle, Utz-Uwe Haus, D. Michaels, and R. Weismantel. Global bounds on optimal solutions for the production of 2,3-dimethylbutene-1. *Ind. Eng. Chem. Res.*, 45:2261–2271, 2006.

[29] T. F. Yee and Ignacio E. Grossmann. Simultaneous optimization models for heat integration-ii. heat exchanger network synthesis. *Comp. Chem. Eng.*, 14:1165–1184, 1990.

[30] E. Ahmetovia and I. E. Grossmann. Strategies for the global optimization of integrated process water networks. *Computer Aided Chemical Engineering*, 28:901–906, 2010.

[31] A. Lakshmanan and L. T. Biegler. Synthesis of optimal chemical reactor networks with simultaneous mass integration. *Ind. Eng. Chem. Res.*, 35:4523–4536, 1996.

[32] R. M. Lima and I. E. Grossmann. Optimal synthesis of p-xylene separation processes based on crystallization technology. *AIChE J.*, 55:354–373, 2009.

[33] Y. Kawajiri and L. T. Biegler. Nonlinear programming superstructure for optimal dynamic operations of simulated moving bed processes. *Ind. Eng. Chem. Res.*, 45:8503–8513, 2006.

[34] Y. Kawajiri and L. T. Biegler. Large scale optimization strategies for zone configuration of simulated moving beds. *Comp. Chem. Eng.*, 32:135–144, 2008.

[35] E. Kloppenburg and E. D. Gilles. Automatic control of the simulated moving bed process for c8 aromatics separation using asymptotically exact input/output linearization. *J. Proc. Cont.*, 9:41–50, 1999.

[36] Z. Zhang, M. Mazzotti, and M. Morbidelli. Powerfeed operation of aimulated moving bed units: changing flow rates during the switching interval. *J. Chromatogr. A*, 1006:87–99, 2003.

[37] O. Ludemann-Hombourger, G. Pigorini, R.-M. Nicoud, D. Ross, and G. Terfloth. Application of the "varicol" process to the separation of the isomers of the sb-553261 racemate. *J. Chromatogr. A*, 947:59–68, 2002.

[38] O. Ludemann-Hombourger, R.-M. Nicoud, and M. Bailly. The "varicol" process: a new multicolumn continuous chromatographic process. *Sep. Sci. and Tech.*, 35:1829–1862, 2000.

[39] S. Pushpavanam and A. Kienle. Nonlinear behavior of an ideal reactor separator network with mass recycle. *Chem. Eng. Sci.*, 56:2837–2849, 2001.

[40] K.P. Zeyer, S. Pushpavanam, and A. Kienle. Nonlinear behavior of reactor-separator networks: Influence of separator control structure. *Ind. Eng. Chem. Res.*, 42:3294–3303, 2003.

[41] W. L. Luyben. Snowball effects in reactor/separator processes with recycle. *Ind. Eng. Chem. Res.*, 33:299–305, 1994.

[42] C. Y. Chin and N.-H.L.Wang. Simulated moving bed equipment designs. *Sep. and Purification Reviews*, 33:77–155, 2004.

[43] C. Y. Chin, Y. Xie, Jr J. S. Alford, and N.-H.L.Wang. Analysis of zone and pump configurations in simulated moving bed purification of insulin. *AIChE J.*, 52:2447–2460, 2006.

[44] JuWeon Lee, Ching Ho Lee, and Yoon Mo Koo. Sensitivity analysis of amino acids in simulated moving bed chromatography. *BioTech and BioProc. Eng.*, 11:110–115, 2006.

[45] S. Natarajan and J. H. Lee. Repetitive model predictive control applied to a simulated moving bed chromatography system. *Comp. Chem. Eng.*, 24:1127–1133, 2000.

[46] A. Toumi and S. Engell. Optimization-based control of a reactive simulated moving bed process for glucose isomerization. *Chem. Eng. Sci.*, 59:3777–3792, 2004.

[47] G. Erdem, S. Abel, M. Morari, M. Mazzotti, M. Morbidelli, and J.H. Lee. Automatic control of simulated moving beds. *Ind. Eng. Chem. Res.*, 43:405–421, 2004.

[48] G. Erdem, S. Abel, M. Morari, M. Mazzotti, and M. Morbidelli. Automatic control of simulated moving beds - II: Nonlinear isotherm. *Ind. Eng. Chem. Res.*, 43:3895–3907, 2004.

[49] C. Grossmann, G. Erdem, M. Morari, M. Amanullah, M. Mazzotti, and M. Morbidelli. Cycle to cycle optimizing control of simulated moving bed plants. *AIChE J.*, 54:194–208, 2008.

[50] H. Schramm, S. Gruner, and A. Kienle. Optimal operation of simulated moving bed chromatographic processes by means of simple feedback control. *J. Chromatogr. A*, 1006:3–13, 2003.

[51] M. Fuetterer. An adaptive control concept for simulated moving bed plants in case of complete separation. *Chem. Eng. Tech.*, 31:1438–1444, 2008.

[52] M. Fuetterer. An adaptive control concept for simulated moving bed plants under reduced purity requirements. *Chem. Eng. Tech.*, 31:1816–1823, 2008.

[53] F. Charton and R. M. Nicoud. Complete design of a simulated moving bed. *J. Chromatogr. A*, 702:97–112, 1995.

[54] H. Kniep, G. Mann, C. Vogel, and A. Seidel-Morgenstern. Separation of enantiomers through simulated moving bed chromatography. *Chem. Eng. Tech.*, 23:853–857, 2000.

[55] H. Lorenz, D. Sapoundjiev, and A. Seidel-Morgenstern. Solubility equilibria in chiral systems and their importance for enantioseparation. *Eng. Life. Sci.*, 3:132–136, 2003.

[56] A. Brooke, D. Kendrick, A. Meeraus, and R. Raman. *GAMS A User‘s Guide*. GAMS Development corporation, Washington D.C., 1996.

[57] GAMS Development corporation, Washington D.C. *GAMS The Solver Manuals*, 2006.

[58] J. v. Langermann, M. Kaspereit, M. Shakeri, H. Lorenz, M. Hedberg, M. J. Jones, K. Larson, B. Herschend, R. Arnell, E. Temmel J.E. Backvall A. Kienle, and A. Seidel-Morgenstern. Design of an integrated process of chromatography, crystallization and racemization for the resolution of 2',6'-pipecoloxylidide (PPX). *Org. Proc. Res. Dev.*, 16:343–352, 2012.

[59] A. Jupke, A. Epping, and H. Schmidt-Traub. Optimal design of batch and simulated moving bed chromatographic separation processes. *J. Chromatogr. A*, 944:93–117, 2002.

[60] G. R. Kocis and I. E. Grossmann. Relaxation strategy for the structural optimization of process flow sheets. *Ind. Eng. Chem. Res.*, 26:1869–1880, 1987.

[61] M. Mangold, A. Kienle, E.D. Gilles, and K.D. Mohl. Nonlinear computation in DIVA-methods and applications. *Chem. Eng. Sci.*, 55:441–454, 2000.

[62] H. Schramm, M. Kaspereit, A. Kienle, and A. Seidel-Morgenstern. Simulated moving bed process with cyclic modulation of the feed concentration. *J. Chromatogr. A*, 1006:77–86, 2003.

[63] M. Golubitsky and D. G. Schaeffer. *Singularities and Groups in Bifurcation Theory*, volume 1. Springer, New York, 1985.

[64] J. A. Romagnoli and A. Palazoglu. *Introduction to Process Control*. CRC, Taylor and Francis, Oxford, 2006.

[65] S. Sommer, P. Müller, and A. Kienle. Iterative feedback tuning of PID controllers for reactive distillation processes: A comparison with relay feedback tuning. *Ind. Eng. Chem. Res.*, 50:9821–9828, 2011.

[66] W. L. Luyben, B. D. Tyreus, and M. L. Luyben. *Plantwide Process Control*. McGraw Hill, New York, 1998.

[67] M. P. Elsner, D. F. Menendez, E. A. Muslera, and A. Seidel-Morgenstern. Experimental study and simplified mathematical description of preferential crystallization. *Chirality*, 17:S183–S195, 2005.

[68] J. Viswanathan and I. E. Grossmann. An alternate MINLP model for finding the number of trays for a specified separation objective. *Comp. Chem. Eng.*, 17:949–955, 1993.